COLOUR VISION ASSESSMENT: FUNDAMENTAL STUDIES AND CLINICAL SIGNIFICANCE

Evgenia Konstantakopoulou

Doctor of Philosophy

City University London
Applied Vision Research Centre
Department of Optometry and Visual Science

January 2012

CONTENTS

LIST OF FIGURES

LIST OF TABLES

ACKNOWLEDGEMENTS

I am grateful to my supervisor, Professor John Barbur, for trusting me with this work and for the number of opportunities and support I was given throughout the last three years. I can only hope that our frequent disagreements on statistical issues will leave him with pleasant memories and pride, as I am afraid he was always right.

This work would not have been possible without the support from City University, through my three year doctoral studentship, for which I will always be thankful.

Dr Rodriguez-Carmona was a vital part of this work; her support, patience and encouragement were vital for me both professionally and personally. Marisa's boys, Adrian and Samuel, were the topic of daily discussions and although they will never understand their place in my acknowledgements, they deserve it.

I am grateful to all the participants, who passionately engaged in my studies and particularly to Judith Morris and Jeff Roberts for their input in recruitment.

Ioanna, Alex T., Harry, Vassilis, Martha, George, Mylena and Sofia have made my London experience unforgettable and Alessandro and Wei have supported me in every possible way during my presence at City. The birth of my little niece, Maya, has marked these three years and I can only hope I will make up for the lost time.

My examiners, Professor Jack Werner and Professor David Foster, made the examination a unique, enlightening and inspiring experience.

The biggest thank you goes to my parents and my brother for making me who I am and to Alex for making me happy!

DECLARATION

I grant powers of discretion to the University Librarian to allow this thesis to be copied in whole or in part without further reference to me. This permission covers only single copies made for study purposes, subject to normal conditions of acknowledgement.

ABSTRACT

When assessing colour vision clinically little value is given to the aetiologies that underlie inter-individual differences between normal trichromats. Retinal diseases have been associated with an impairment of colour vision and can cause a reduction in chromatic sensitivity that precedes the clinical manifestation of retinal changes. Ageing is a risk factor for the development of retinal diseases and can cause gradual deterioration in colour vision. The purpose of the first part of this thesis was to obtain additional information about the health of the retina by measuring the rate of loss of chromatic sensitivity with decreasing light level. The health of the retina (HR) index was introduced to identify and separate the effects of age from pre-clinical indications of retinal disease. Chromatic sensitivity was measured in 60 subjects (mean age 47.6 years, ranging from 16 to 79 years) at four light levels using the Colour Assessment and Diagnosis (CAD) test; measurement of pre-receptoral absorption by the crystalline lens and the macular pigment (MP) and the size of the pupil allowed an estimation of retinal illuminance. For normal subjects the HR index is largely independent of age (R^2 ~ 0.2), but ~11% of clinically normal, asymptomatic, older subjects exhibit impaired chromatic sensitivity. Lower light level does not preferentially affect chromatic sensitivity in older normal subjects and red-green (RG) chromatic sensitivity deteriorates at the same rate as yellow-blue (YB). The HR index provides a single number that captures how light level affects chromatic sensitivity irrespective of age and could be used to screen for pre-clinical signs of retinal disease.

The second part of this thesis focuses on female carriers of congenital RG colour vision deficiencies. Female carriers of colour vision deficiency have been studied extensively, but agreement still lacks regarding the processing of colour signals. The tetrachromatic theory has been suggested as an alternative to the integration of signals into the existing pathways and the ratio of the long- (L) to medium- (M) wavelength sensitive cones has also been examined. Chromatic sensitivity was measured at four light levels in 36 carriers of congenital RG colour deficiency and 26 normal trichromatic males using the CAD test; the retinal illuminance was estimated as described above. The Ishihara and American Optical pseudoisochromatic plates and the Nagel anomaloscope were also employed. When referenced to the male trichromats, carriers of DA needed ~25% increase in RG thresholds at all light levels. At low light levels carriers of protanomaly (PA) needed 28% less colour signal strength, whilst carriers of D required ~60% larger thresholds. Results suggest that in carriers of anomalous trichromacy the hybrid pigment is pooled with the spectrally closest normal pigment. Consequently, the reduced chromatic sensitivity of carriers of DA can be explained by the large separation between L' and L or M. The pooling of M' with M in carriers of PA leads to the increased chromatic sensitivity of PA carriers at lower light levels and is consistent with the subsequent stronger inhibition of the rods, whilst variation in the L:M ratio and hence the absolute M-cone density may be the principal factor underlying the poorer chromatic sensitivity of D carriers in the low photopic range.

This study highlights the importance of accurate measurements and interpretation of inter-subject variability in chromatic sensitivity. Deviations from the 'normal' can reveal information of clinical and fundamental significance and, if studied systematically, may elucidate previously unexplained aspects of colour processing.

SYMBOLS AND ABBREVIATIONS

°	Degrees
“	Inches
A	Area under the curve
AMD	Age-related Macular Degeneration
AO-HRR	American Optical – Hardy, Rand and Rittler
ARM	Age Related Maculopathy
BSCVA	Best Spectacle Corrected Visual Acuity
CAD	Colour Assessment and Diagnosis Test
cD	Carriers of Deuteranopia
cd·m^{-2}	Candelas per square metre
cDA	Carriers of Deuteranomaly
CIE	Commission Internationale d’ Eclairage
cP	Carriers of Protanopia
cPA	Carriers of Protanomaly
CRT	Cathode Ray Tube
D	Deuteranopia
d	Delta (difference)
DA	Deuteranomalous trichromatism (or deuteranomaly)
dLGN	Dorsal Lateral Geniculate Nucleus
E	Retinal illuminance
e	Eccentricity
FAZ	Foveal Avascular Zone
HFP	Heterochromatic Flicker Photometry
HR index	Health of the Retina index
Hz	Hertz
IOP	Intraocular Pressure
IR	Infrared
K layer	Koniocellular layer
L	Luminance
L cone	Long wavelength sensitive cone
L’ pigment	Hybrid cone pigment expressed in deuteranomaly
LC	Luminance Contrast
LogMAR	Logarithm of the Minimum Angle of Resolution
LW	Long Wavelength
m	Metres
M cone	Medium wavelength sensitive cone
M layer	Magnocellular layer
M’ pigment	Hybrid cone pigment expressed in protanomaly
MAP	Macular Assessment Profile
mm	Millimetres
MP	Macular Pigment
MPOD	Macular Pigment Optical Density
ms	Milli-seconds
mW	Milli-watts
n	Number
nm	Nanometres
OD	Optical Density
OS	Outer Segment
P	Protanopia
p	P value
P	Pupil
P layer	Parvocellular layer
PA	Protanomalous trichromatism (or protanomaly)
R^2	Square of the correlation coefficient
RG	Red-Green
RLM	Random Luminance Modulation
rmse	Root mean square error
RNFL	Retinal Nerve Fibre Layer
RPE	Retinal Pigment Epithelium
s	Seconds
S cone	Short wavelength sensitive cone
SD	Standard Deviation
SNO	Standard Normal Observer
SNU	Standard Normal Units
sr	Steradians
SW	Short Wavelength
T	Transmittance
Td	Trolands
UV	Ultraviolet
V(λ)	Spectral responsivity function
V1	Visual cortex
YB	Yellow-Blue
λ	Wavelength
µm	Micro metres
Σ	Sigma (sum)

THESIS SYNOPSIS

The studies described in this thesis were designed to investigate the aetiologies underlying the variability of colour vision in two distinct groups. The first study investigated the effects of age on chromatic sensitivity and the role pre-receptoral filters play in the reduction of chromatic sensitivity with age; the second study looked into the processing of colour signals in female carriers of congenital colour vision deficiency.

Chapter 1 presents an overview of the visual system, with emphasis on chromatic processing. This summary of the visual system starts from a brief anatomical description of the eye, focusing on the retina and the photoreceptors. Post-receptoral processing is discussed, followed by a description of the post-retinal visual pathways towards the lateral geniculate nucleus and the primary visual cortex.

Chapter 2 introduces normal colour vision; the fundamentals of colour perception are presented, along with genetics and variability among normal trichromats. Congenital and acquired colour vision deficiencies are also discussed. Carriers of congenital colour vision deficiency are introduced and the effects of X inactivation are examined in relation to the cone mosaic and the performance on various colour vision tests.

Chapter 3 describes the methods used to investigate colour vision in the two subject groups. The recruitment process and the inclusion criteria are described. In this study the Colour Assessment and Diagnosis (CAD) test was used for the measurement of chromatic sensitivity and the Macular Assessment Profile (MAP) test for the measurement of macular pigment and lens optical density. Measurement of pupil diameter at four light levels enabled an estimation of retinal illuminance. In addition,

the Nagel anomaloscope and the pseudoisochromatic plates were employed to investigate the processing of colour signals in carriers of congenital colour vision deficiencies. An overview of the statistical analysis is also presented in this chapter.

The results of the aforementioned studies are presented in Chapter 4. The effects of ageing on the pre-receptoral filters of the eye are described, as well as their effect on retinal illuminance. The Health of the Retina (HR) index is introduced, which captures the loss of chromatic sensitivity with decreasing retinal illuminance. Using the HR index the limits of variability are derived for a wide age range. The results on the carriers of congenital colour vision deficiency are also presented in this chapter, in relation to chromatic sensitivity, chromatic discrimination and performance on the pseudoisochromatic plates, in comparison to a control group.

Chapter 5 discusses the findings of the studies carried out. The results are compared to the literature and the advantages and disadvantages of the procedures employed are discussed. Explanations are sought for the findings, in relation to the HR index and the identification of outliers among normal, clinically healthy individuals. Hypotheses are put forward for the neural processing of colour signals in each group of carriers and these are discussed in relation to the literature.

Chapter 6 summarises the key findings of the aforementioned studies. The implications of these findings are discussed in view of the plasticity of the visual system, the ageing population and the need for identifying early signs of ocular disease.

1 THE VISUAL SYSTEM

1.1 ANATOMY OF THE HUMAN EYE

The eye is located in the orbit, surrounded by fatty tissue, and is divided in three main layers (Figure 1-1):

- The external layer, composed of the sclera and the cornea
- The intermediate layer, composed of the uvea (iris, ciliary body and choroid)
- The inner layer, i.e. the retina

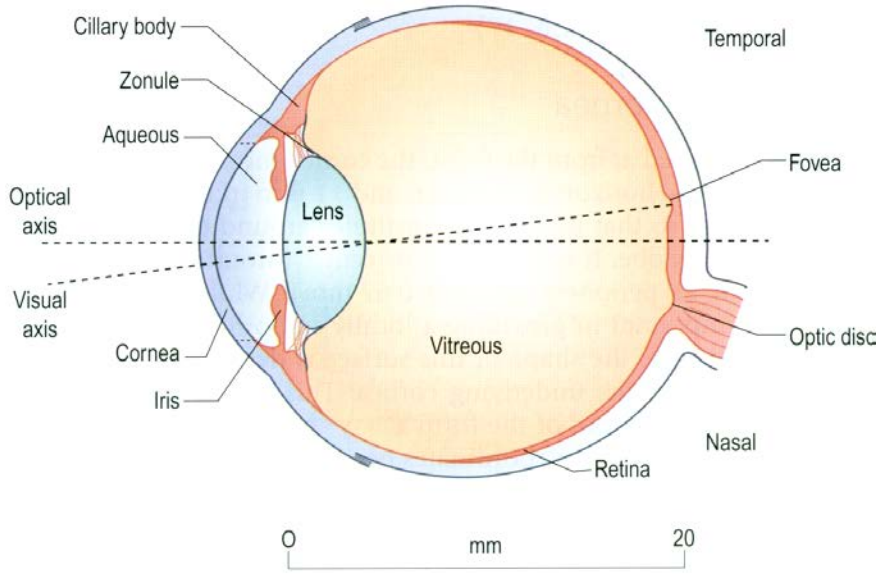

Figure 1-1: Anatomy of the human eye (Charman, 2009).

The cornea is the transparent, avascular most anterior structure of the eye. It covers approximately 1/6th of the eye surface and is the eye's first refractive structure. The cornea is approximately 530 µm thick, ranging from approximately 450 µm to 650 µm

in healthy normal eyes (Doughty and Zaman, 2000) and is arranged in 5 layers: the epithelium, Bowmann's layer, the stroma, Descemet's membrane and the endothelium. After birth and until approximately 2 years of age the cornea continues to grow and reaches a final size and shape. Ageing causes subtle changes in the cornea that have an almost negligible effect on its optical properties: epithelial basement membrane thickening, keratocyte density decline, increasing stiffness of the stroma, Descemet's membrane thickening. The cornea transmits most of the visible and infrared (IR) light (300-2500 nm), with maximum transmittance between 500-1300 nm. A decreasing amount of light transmission in human corneas of increasing age has been reported in vitro (Lerman, 1984), but this has not been confirmed by other studies (Boettner and Wolter, 1962; Beems and Van Best, 1990).

The sclera is a nearly spherical, white, opaque, avascular, rigid structure composed of connective tissue that covers the 5/6^{ths} of the eye surface. The main function of the sclera is to provide a tough external framework and to give the eye its shape, which prevents deformation of the retinal image. The sclera also forms an expansive-resistant structure to adapt to the intra-ocular pressure (IOP) forces, promotes aqueous outflow and is an attachment site for extra-ocular muscles. Finally, the sclera indirectly determines the refractive error, as it determines the absolute size of the eyeball.

The uvea is the middle, vascular layer of the eyeball. It consists of the iris and the ciliary body anteriorly and the choroid posteriorly. The iris is the pigmented circular structure behind the cornea; it is a circular muscle with a central round aperture called the pupil. The iris is pigmented, in order not to allow light through its structure. Some light does, however, penetrate the iris and scatters towards the retina. The iris is attached to the anterior part of ciliary body. The ciliary body is a triangular structure

that includes the ciliary muscle. The ciliary body is composed of three muscle fibre groups; the anterior zonular fibres form the ciliary processes, the suspensatory elements of the crystalline lens that surround the lens equator. Contraction of the ciliary muscle pulls the anterior choroid forward, thus promoting aqueous outflow, moves the apex of the ciliary processes towards the lens equator and releases the lens zonules, thus allowing accommodation.

Posterior to the ciliary body lies the choroid, the vascular layer between the sclera and the retina. The choroid is the main oxygen and nutrient supplier to the outer retina and the retinal pigment epithelium (RPE), through its choriocapillaries. The inner part of the choroid is called Bruch's membrane and is of major importance in age-related macular degeneration (AMD).

The retina is the innermost structure of the eye, where the initial neural processing takes place. The retina is a multilayered structure, comprising 10 layers (Figure 1-2): RPE, photoreceptors' inner and outer segment layers, outer limiting membrane, outer nuclear layer, outer plexiform layer, inner nuclear layer, inner plexiform layer, ganglion cell layer, nerve fibre layer and inner limiting membrane (Figure 1-2). The outer retina receives nutrients and oxygen from the choriocapillaries and the inner retina from the central retinal artery.

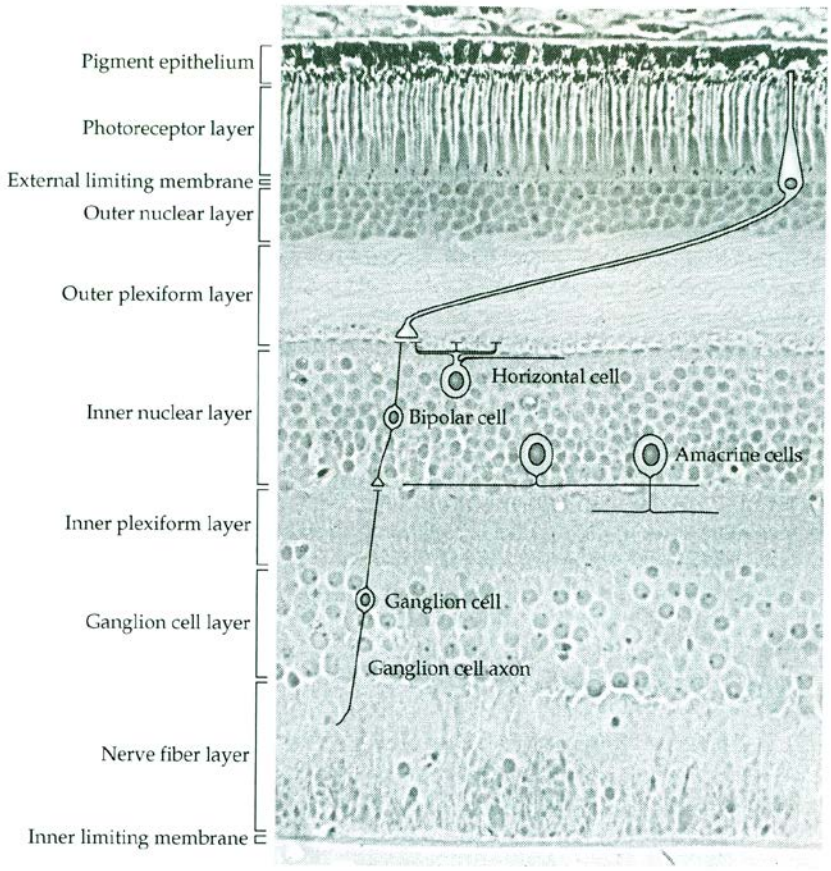

Figure 1-2: Light micrograph of a vertical section of a human central retina, along with the post-receptoral neurons (adapted from Oyster, 1999). The outermost layer of the retina is the RPE, followed by the photoreceptors' inner and outer segment layers, the outer limiting membrane, the outer nuclear layer, the outer plexiform layer, the inner nuclear layer, the inner plexiform layer, the ganglion cell layer, the nerve fibre layer and inner limiting membrane.

All retinal layers, apart from the RPE, have an active role in visual processing (described in section 1.3). The RPE is the outermost layer of the retina. The RPE does not actively participate in the encoding of visual information, but its main function relates to the phagocytosis of the outer photoreceptor segments. Additionally, its dark pigmentation reduces the amount of light scatter in the eye. The outermost part of the photoreceptors, the outer segment (OS), contains the photopigment necessary for the

absorption of light. The inner segments of the photoreceptors are separated from the nuclear layer by the external (outer) limiting membrane. The nuclei of the photoreceptors (rods and cones) lie in the outer nuclear layer and the nuclei of the second and third order neurons lie in the inner nuclear layer. The synapses between neurons are in the inner plexiform layer. In this layer synapses exist between bipolar cells, amacrine cells and horizontal cells and the ganglion cells. The ganglion cells form the innermost retinal layer, the ganglion cell layer, and their axons form the retinal nerve fibre layer (RNFL), which exits the eye through the optic nerve. The RNFL is separated from the vitreous by the inner limiting membrane.

The main structures of the retina are the optic disc, the macula lutea and the peripheral retina. The optic disc, the point where nerve fibres converge, exit the eyeball and transfer signals to the brain, is a circular structure, 1.5 mm in diameter, lying approximately 16^{o} from fixation. The optic nerve is also the main passage of the major retinal vessels to and from the retina. The macula lutea is a central area in the retina, approximately 5.5 mm in diameter that corresponds to the sharpest vision. The central depressed part of the macula is called the fovea (1.85 mm) and its most central part, the foveola, has a diameter of approximately 0.35 mm. The foveola is part of the foveal avascular zone (FAZ), which is however smaller than the fovea. The sharpest vision provided by the macula is a result of a dense cone mosaic and specialised wiring.

The macula has a characteristic yellowish colour, attributed to the pigment found in that region, the macular pigment (MP). The MP consists of two carotenoids, lutein and zeaxanthin (Bone et al., 1985; Handelman et al., 1988). Its maximum concentration is in the layer of the fibres of Henle (Snodderly et al., 1984a; Snodderly et al., 1984b; Trieschmann et al., 2008) and it is thought to have peak concentration in the centre of

the fovea (Snodderly et al., 1984a), although it may show a secondary peak (Berendschot and van Norren, 2006). The concentration of the MP decreases exponentially with eccentricity, but the peak value and the rate of decrease vary amongst individuals (Hammond et al., 1997). The extent to which the spatial distribution of the MP relates to its peak concentration in the fovea, other than as determined by the exponential decrease, remains uncertain (Hammond et al., 1997; Robson et al., 2003; Trieschmann et al., 2008).

The MP has band-pass spectral absorption characteristics and absorbs maximally blue light at ~ 454 nm (Snodderly et al., 1984b; Bone et al., 1992). Despite evidence on its effects on SW vision (Hammond et al., 1998; Werner et al., 2000) the extent to which the MP affects colour detection thresholds remains controversial (Rodriguez-Carmona et al., 2006; Barbur et al., 2010). Additionally, the effect of MP on hue discrimination may not be as significant as initially thought (Moreland and Dain, 1995; Davison et al., 2011). The MP does, however, reduce the amount of SW light reaching the retina, as it precedes the photoreceptors. The in-vivo assessment of MP can be carried out using motion photometry (Moreland, 2004), Raman spectroscopy (Bernstein et al., 1998), fundus reflectometry (van de Kraats et al., 2008), two-wavelength fundus autofluorescence (Wustemeyer et al., 2003; Egan et al., 2009) or steady-state visual evoked potentials (Robson and Parry, 2008).

The structures within the eye result in the formation of the anterior and posterior segments. The anterior segment is divided to the anterior chamber, the area between the posterior part of the cornea and the anterior part of the iris, and the posterior chamber, the area extending from the back of the iris to the lens. The aqueous humour circulates in the anterior and posterior chambers. The posterior segment is the large

area behind the crystalline lens and is filled with the vitreous gel, which is attached to the retina posteriorly and the ciliary body anteriorly.

The crystalline lens lies in the posterior chamber and is a transparent bi-convex crystalline structure, surrounded by the lens capsule, a thin transparent collagenous membrane. The crystalline lens is divided to the cortex and the nucleus. Water (~65%) and proteins (~34%) are the main constituents of the crystalline lens, with lipids, amino acids and glucose forming approximately 1% of its mass. The protein concentration of the lens is highest than any other body part and the proteins found in the lens are called crystallins. The lens has a number of metabolic activities, like glucose and protein metabolism, transportation of electrolytes, amino acids and glucose. The epithelial cells of the lens, lying just behind the lens capsule, differentiate to become lens fibre cells and the lens continues to change with age in terms of mass, thickness and curvature (Dubbelman and Van der Heijde, 2001; Dubbelman et al., 2001).

The absorption characteristics of the crystalline lens have been measured with a number of different techniques in the last half century. *Ex vivo* techniques using spectrophotometers were the first to be implemented for lens OD measurements (Boettner and Wolter, 1962; Weale, 1988; Gaillard et al., 2000; Dillon et al., 2004), but such measurements were often questioned given the post-mortem tissue changes that subsequently affect the validity of the measurements. As an alternative, *in vivo* techniques have been invented aiming at simplifying the measurements. Reflectance methods (Delori and Burns, 1996; Xu et al., 1997; Savage et al., 2001) have been used widely, but currently preferred techniques rely on visual psychophysical tests. The earliest visual psychophysical method for assessing lens density was by comparing the scotopic sensitivity of aphakes to normal phakic subjects and has yielded results comparable to *ex vivo* curves (van Norren and Vos, 1974). Due to the

significant time requirements necessary, this technique was superseded by photopic psychophysical techniques like flicker photometry and colour matching (Werner and Steele, 1988; Savage et al., 1993; Delori and Burns, 1996; Xu et al., 1997; Wooten et al., 2007).

The crystalline lens transmits light from the ultra-violet (UV) part of the spectrum to approximately 1900 nm in the IR. Its transparency is attributed to its thin epithelial cell layer, the permeable capsule, its avascularity and its pump mechanism. The lens starts transmitting at approximately 300 nm, but shows an increased absorption band around 320-390 nm (Boettner and Wolter, 1962; Weale, 1988; Gaillard et al., 2000) and its transmittance increases rapidly again beyond 390 nm. With increasing age the crystalline lens undergoes significant changes in terms of its optical properties, with more pronounced increases in the absorption of SW light (Werner, 1982; Pokorny et al., 1987; Sample et al., 1988; Weale, 1988; Gaillard et al., 2000; Savage et al., 2001; Berendschot et al., 2002). Age-related changes in the proteins of the lens also result in a progressive increase in the absorption maximum, which shifts towards lower wavelengths, followed by a smaller increase in the absorption of LW (Gaillard et al., 2000).

1.2 PHOTORECEPTORS

The human retina has two types of photoreceptors, lying inner to the RPE, the cones and the rods. The photoreceptors respond to light and transform the energy into electrical activity that is then transported to post-receptoral neurons. Their metabolic

activity is remarkably high, which explains their location closer to the rich choroidal blood supply.

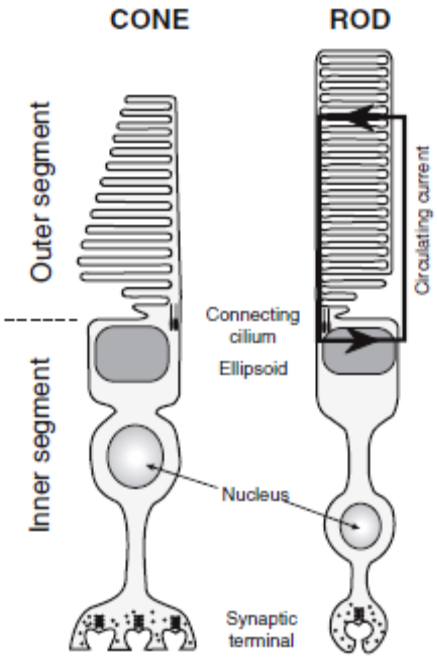

Figure 1-3: The main structural elements for rods and cones; the photopigment is located in the outer segment (OS). The inner segment contains cellular metabolic machinery. At the base of the cell the synaptic terminal connects to postsynaptic neurons. The black arrows show the path of the circulating electrical current for the rod (Burns and Lamb, 2004).

Rods and cones have four distinct structural regions: outer segment (OS), inner segment, cell body and synaptic terminal (Figure 1-3). The OS is filled with membrane discs that are free floating in rods, but attached to the outer segment in cones. Rods have cylindrical inner and outer segments (Figure 1-4); peripheral cones have a pyramidal shape (Figure 1-4), although the shape of foveal cones is very similar to rods. The discs in the OS carry the visual pigment in both the rods and the cones. The inner segment contains metabolic machinery for the provision of the necessary energy

for phototransduction. The OS is connected to the inner segment through the cilium and the synaptic terminal transmits the light signal to the post-receptoral neurons in the retina.

Figure 1-4: Scanning electron micrograph of the rods and cones of the primate retina (http://webvision.med.utah.edu/).

The photopigments contained in the OS differ between rods and cones. The photopigments consist of a protein molecule, the opsin, bound to a chromophore, the retinal. Rods contain rhodopsin, which absorbs maximally in the middle wavelength part of the spectrum. There are three cone classes, each of which is characterised by a different photopigment with different peak wavelength sensitivity (see section 2.1 and Figure 2-1). Cones can be sensitive to short, middle or long wavelength light and are named after their spectral sensitivities as short-, middle- or long-wavelength sensitive, or S, M and L, respectively. The amino acid sequence of the opsin is responsible for the spectral characteristics of the cone pigments.

When light is absorbed rhodopsin reaches an enzymatically active state, by transformation of the 11 *cis* retinal to all *trans* retinal (*cis-trans* isomerisation). The activated rhodopsin undergoes a number of processes, leading to the closure of ion

channels and a change in the electrical potential of the photoreceptor. As long as rhodopsin remains activated an amplified response will persist and will lead to the saturation of the receptor. The catalytic activity of rhodopsin is finally cut off by the *trans* transformation back to *cis* (Burns and Lamb, 2004). A similar process takes place during isomerisation of the pigments of the cones.

In the retina cones are outnumbered by rods, with approximately 92-110 million rods by comparison to 4-6.5 million cones (Osterberg, 1935; Curcio et al., 1990). The density and distribution of the rods and cones depends on the eccentricity from the fovea. The macula is considered a cone enriched area, where cones are thinner and densely packed. The tightly packed cones form a dense rod free cone mosaic, which peaks at the fovea (Curcio et al., 1990). The fovea is dominated by L and M cones; S-cones, unlike L and M cones, are fewer in number (4-8% of the total number of cones) and are not found in the centre of the fovea, over the area that falls within the rod free region, approximately 0.34^{o} in diameter (Curcio et al., 1991; Roorda et al., 2001). The S-cone peak density lies just outside the fovea between 0.1 - 0.3 mm eccentricity, and is greater than 2000 S cones/mm^2 (Curcio et al., 1991). The density of the cones drops rapidly as one moves towards the peripheral retina and extrafoveal cones tend to be larger than those in the fovea (Curcio et al., 1990). The density of the rods peaks at approximately 20^{o} from the foveola (Curcio et al., 1990) and declines gradually in the far periphery (Curcio et al., 1990).

Rods are specialised for low light vision, as they are more sensitive to light, partly as a result of greater convergence. Rods mediate vision exclusively at very low light levels, described as scotopic conditions. Cones are significantly less sensitive than rods, but have superior temporal properties and mediate colour vision under photopic conditions of illumination. In mesopic conditions rods interact with cones; there are two known

ways of rod-cone interactions, the gap junctions (or electrical synapses) and the convergence of rod signals through amacrine (A*II*) cells (Figure 1-5). Gap junctions are present in a number of vertebrate species and seem strong enough to transfer rod signals in the mesopic range. The convergence of rod signals through A*II* cells leads to a transportation of signals to bipolar cells transferring cone signals. A*II* cells may connect to OFF cone bipolar cells via sign inverting synapses and to ON bipolar cells via gap junctions (Buck, 2004).

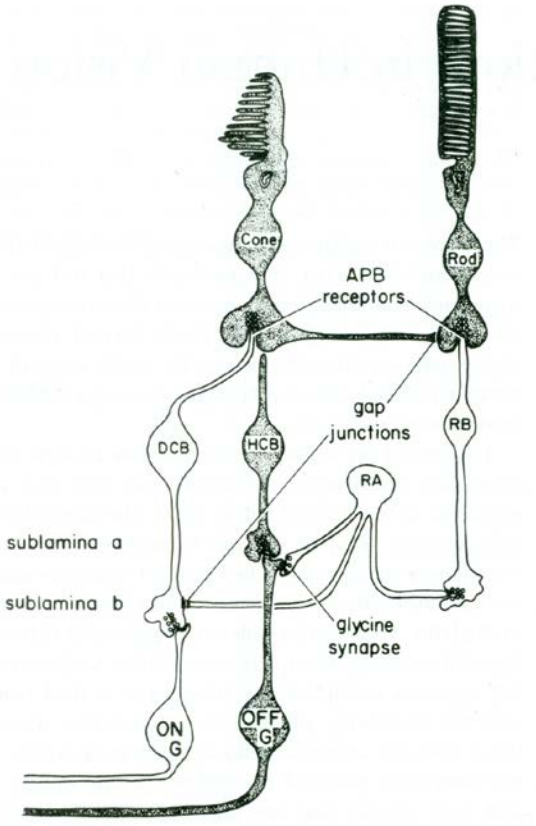

Figure 1-5: Diagram of the two known pathways for rod-cone interactions. Rod signals are transmitted to rod bipolars (RB), A*II* amacrine (RA) and depolarising and hyperpolarising cone bipolars (DCB and HCB, respectively). Rod signals also interact with cones via gap junctions (Buck, 2004).

1.3 POST- RECEPTORAL RETINAL PATHWAYS

The post-receptoral layers of the retina are shown in Figure 1-6. There are two main organisational patterns in terms of signal transportation, known as vertical and lateral arrangements. The first post-receptoral synapses take place between the cone and the bipolar cell. The bipolar cell synapses with a ganglion cell, which then transmits the signal towards its axon. This arrangement is the basis of fine spatial detail; the wiring of the photoreceptor towards the second order neurons plays a significant role in the level of sensitivity that can be achieved and variations exist throughout the retina. Rods show a large convergence, with signals from approximately 120 rods converging to one ganglion cell. Rods' sensitivity can be partly attributed to their greater convergence; the inputs of many rods converge into ganglion cells, thus increasing the likelihood of a response. Cones can combine the signals from approximately 6 cones towards one ganglion cell, but in the fovea there is a one-to-one wiring, i.e. one cone sends signals to one ganglion cell.

The signals being transmitted through the vertical pathway, however, can be influenced by the neighbouring photoreceptors. This is possible, as signals can also travel through the lateral pathway, which is present in two retinal levels. In the outer retina, the horizontal cells can influence the signals travelling directly from the photoreceptors to the bipolar cells. An intrusion of amacrine cells can exist in the inner retina, between bipolar and ganglion cells, transmitting signals from other bipolar, ganglion or amacrine cells. Rods are believed to have rod-specific bipolar and amacrine cells (Figure 1-5).

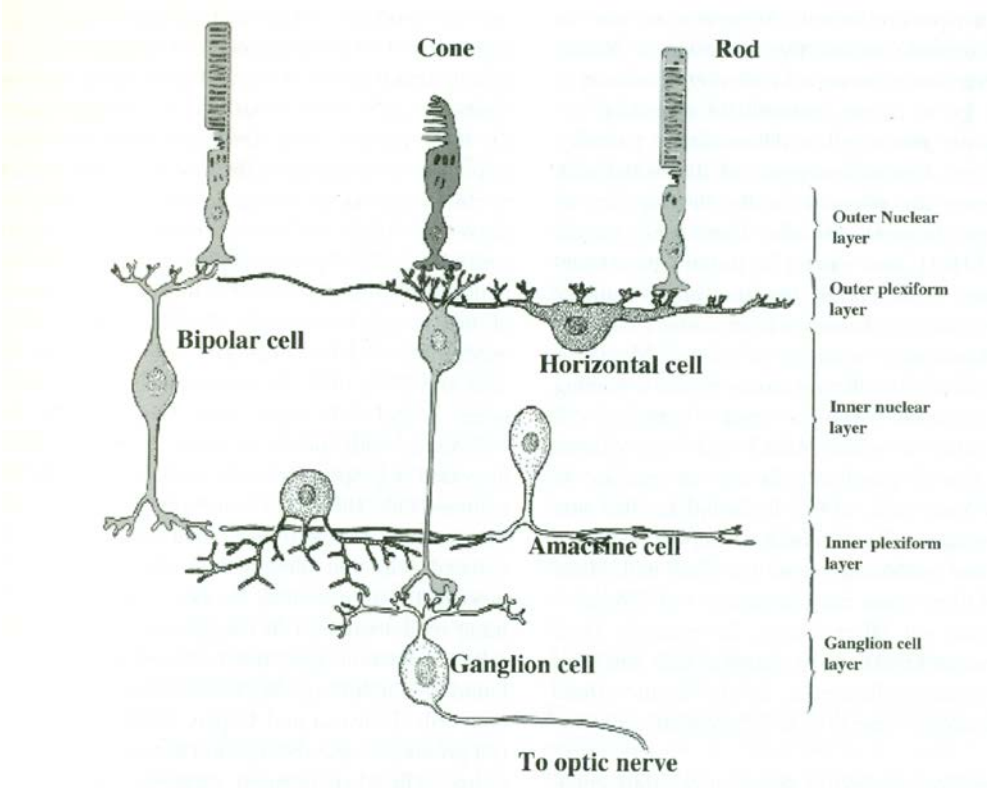

Figure 1-6: The post-receptoral retinal neurons and the retinal layers in which they are located (Barnstable, 2004).

An important feature of the neural processing is the duality of polarisation. Neurons can hyper- or hypo-polarise and this is equally important for luminance and colour processing. Signals converging to a ganglion cell carry information from specific areas of the retina, known as receptive fields. Receptive fields are circular and have a centre-surround organisation. ON-centre ganglion cells are excited at the centre and inhibited in the periphery, while OFF-centre ganglion cells are inhibited in the centre and excited in the periphery.

Luminance information is extracted by spatial opponency, by comparing luminance contrast differences. Colour opponency also exists and it is mediated by colour opponent ganglion cells. Colour opponent ganglion cells exhibit an excitatory response

in some wavelengths and an inhibitory response in other wavelengths in a centre-surround manner. Types 1 and 2 ganglion cells are colour opponent and show antagonistic responses to M and L and to S and L+M, respectively (Figure 1-7). Antagonistic ganglion cells may then give an output of +L/-M, -L/+M or +S-(L+M); recent evidence also suggests the presence of S-cone OFF ganglion cells (Klug et al., 2003). Luminance opponent ganglion cells (type 3) show an excitatory response across a wide range of wavelengths and combine inputs from both M and L.

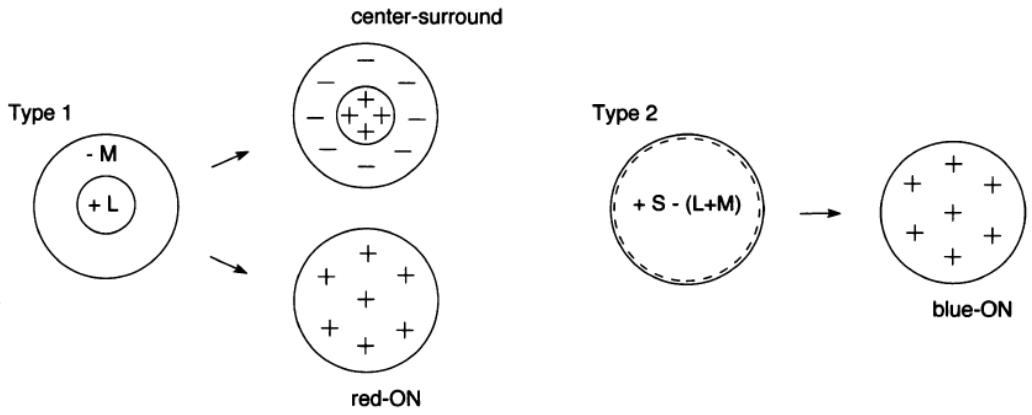

Figure 1-7: Schematic representation of the receptive fields of the colour opponent type 1 and type 2 ganglion cells (adapted from Dacey, 1996). In type 1 ganglion cells inputs from L and M cones are segregated to the centre and the surround of the receptive field; type 1 ganglion cells also show a centre-surround antagonism to luminance changes. Type 2 cells receive antagonistic input from S vs. L and M cones and do not show a centre-surround antagonism to luminance changes.

Post-receptoral processing can be attributed largely to two channels; the luminance and chromatic channels. The luminance channel is composed of signals from M and L cones and the colour channel is composed of signals from S, M and L. The colour processing channel is further separated into the red-green (RG) and yellow-blue (YB)

channels. These channels compare photoreceptor signals derived from L and M cones (RG) and L+M and S cones (YB).

1.4 POST- RETINAL MECHANISMS

Nerve fibres leaving the eye through the optic nerve reach the optic chiasm, where fibres from the nasal retina cross to the contra-lateral brain, whereas temporally originating fibres remain uncrossed. Nerve fibres continue through the optic tract to the dorsal lateral geniculate nucleus (dLGN).

The dLGN is a layered structure composed of six layers and a number of interlaminar regions (Kaas et al., 1978). The dLGN plays an important role in regulating the flow of visual information from the retina to the visual cortex. Each layer of the dLGN receives monocular input from the retina and each layer's maps are retinotopically aligned. Layers 1, 4 and 6 receive contralateral eye input and layers 2, 3 and 5 receive ipsilateral eye input. The dLGN contains three types of cell layers: layers made up of large cells (magnocellular layer or M), medium sized cells (pravocellular layer or P) and small cells in the interlaminar regions (koniocellular layer or K). M, P and K layers receive input primarily from unique classes of ganglion cell classes; therefore, input from type 1 and 2 ganglion cells are taken to P layers, whereas input from type 3 ganglion cells is taken to M layers (Leventhal et al., 1981). The K layers probably carry information that originates largely from S-cones (Dacey and Lee, 1994).

Cells from all six layers of the dLGN project to the primary visual cortex (V1), via the optic radiations. V1 has six principal layers and lies in the posterior part of the occipital cortex. The layers of V1 have been named by Brodmann (1909). Areas with the same stimulus responsivity (e.g. colour) are arranged in columns perpendicular to the

surface of the brain. V1 also shows well defined zones, known as blobs, and the areas between them are known as interblobs. V1 has been described as the area, where the information filtered and provided by the LGN is ultimately combined in a number of ways in order to extract information about the image features. Layers 4Ca and 4Cb are the major recipients of dLGN innervations, with the M layer projecting to 4Ca and the P layer projecting to 4Cb, whilst the K cells project to the blobs of V1. The signals in V1 are topographically arranged, like in the dLGN; the fovea, however, occupies a disproportionately large area on V1, which could partly explain its superior visual performance. V1 re-distributes signals to other anterior areas for further processing.

2 COLOUR VISION

2.1 NORMAL TRICHROMATIC COLOUR VISION

Normal colour vision is called trichromatic, as it relies on three different cone photopigments. There are three different cone types named after the photopigment they express. Photopigments can be maximally sensitive to short, middle or long wavelength light and subsequently cones are named as short-, middle- or long-wavelength sensitive, or S, M and L, respectively. A number of methodologies have been employed to determine the spectral sensitivities of the cone photopigments. Direct measurements involve densitometry and micro-spectroscopy. In cone densitometry light passes through the eye and the intensity of the retinal reflection is measured. Micro-spectroscopy involves the measurement of the spectral transmittance of a small beam of light passing through the OS of individual cones *in vitro*. Both these techniques have established the existence of the three types of cones and the rods (Rushton, 1966; Bowmaker and Dartnall, 1980).

The earliest sets of cone spectral sensitivities were established by König and Dieterici (1893); cone fundamentals were subsequently established by a number of studies (Stiles and Burch, 1959; Vos and Walraven, 1971; Smith and Pokorny, 1975; Stockman and Sharpe, 2000). The spectral sensitivities of the three cone classes are shown in Figure 2-1 along with the spectral sensitivity of the rods; S cones show maximum sensitivity at ~ 445 nm, rods at ~ 507 nm, M cones at ~ 540 nm and L cones at ~ 565 nm (Stockman and Sharpe, 2000). Recently a subgroup of ganglion cells containing the photosensitive pigment melanopsin was discovered; melanopsin shows

a maximum spectral absorption at ~ 484 nm and is believed to contribute to the control of the circadian rhythms (Berson et al., 2002).

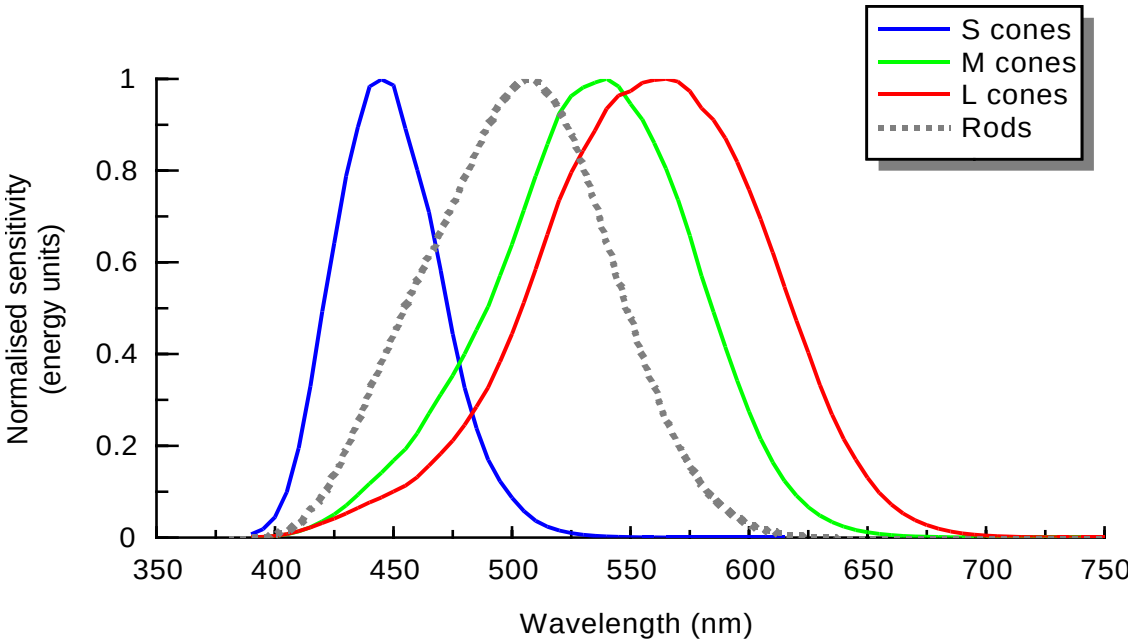

Figure 2-1: Fundamental cone and rod spectral sensitivities (Stockman and Sharpe, 2000). S cones show maximum sensitivity at ~445 nm, rods at ~507 nm, M cones at ~540 nm and L cones at ~ 565 nm (data obtained from http://www.cvrl.org/).

The spectral sensitivities reveal the probability that a specific photon will be absorbed by a cone. This means that the wavelength of a light can modify the probability of a given photon being absorbed by a receptor, but the receptor does not carry any information about the wavelength of the absorbed light; this is known as the *Principle of Univariance* (Rushton, 1972). Trichromacy relies on the existence of three classes of cones and the comparison of the signals between the three cone signals. Colour processing starts at receptoral level, where cones absorb light and send an input to the post-receptoral neurons.

Colour processing is associated with two main channels that emerge from opponent processing. Colour opponency was initially suggested by Hering in 1874 (Hering,

1964) and involves the comparison of signals between different cone inputs. The RG channel utilises differences between the inputs of L and M cones, whilst the YB channel compares signals derived from the M and L cones to the signals originating from the S cones (Figure 2-2 and Figure 1-7). The overlapping sensitivities of the three cone photopigments allow an astonishing number of combinations of excitation levels, which in turn leads to the perception of a large number of different colours.

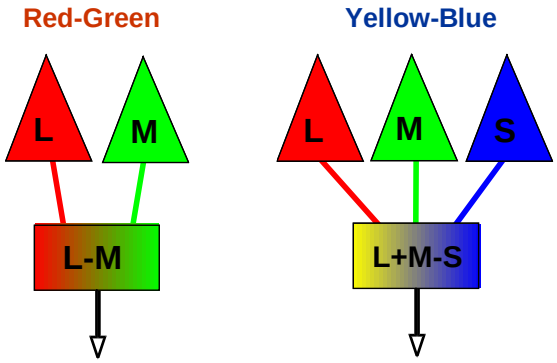

Figure 2-2: Simplified schematic representation of the polarity sensitive channels mediating RG and YB discrimination. The RG channel compares signals from the M and L cones, whereas the YB channel compares the S cone signals to the combined M and L signals.

2.1.1 Genetics and variability of normal colour vision

The genes that specify the human M and L cone pigments have been localised at Xq28 on the X chromosome (Nathans et al., 1986). The S cone opsin has been located on the autosome chromosome 7 at location 7q32 (Nathans et al., 1986). The L and M genes originated from a gene duplication during primate evolution and are ~98% homologous (Neitz et al., 1999).

The L and M ospins have 6 exons each, of which exon 5 is the most important for colour vision and exons 2, 3 and 4 have a smaller effect. Exon 5 encodes for amino acid dimorphisms that are responsible for the majority of differences between the various L and M pigments and it essentially separates pigments into L or M (Neitz and Neitz, 2011). Amino acid dimorphisms encoded in exons 2, 3 and 4 produce spectral subtypes both in normal and colour defective vision (Winderickx et al., 1993; Neitz et al., 1995a). Amino acid differences have been shown to be responsible for the spectral shifts in the L and M pigments; colour vision behaviour has therefore been attributed to the expressed ospins (Neitz et al., 1995b; Neitz et al., 1996).

There is significant variability in the amino acid sequences of the L and M pigments, which results in the variability of spectral sensitivity amongst 'normal' subjects. This means that all people with normal colour vision do not share the exact same L and M pigments. There is more variability for the L cone pigments; a longer and a shorter version of the L pigment sensitivities form the most common variations, with spectral sensitivities approximately 4 nm apart (Neitz and Jacobs, 1986).

The X chromosome can contain more than one gene coding for L and M cone pigments (Neitz and Neitz, 1995). The presence of more than one gene encoding for L and M pigments caused significant interest and a number of studies investigated how many and which genes are expressed. It has been long believed that only two pigment genes from each array are finally expressed (Winderickx et al., 1992), since expression of specific genes was absent in some individuals. More recent data, however, suggested that occasionally more than two pigments with long wavelength (LW) sensitivities can be expressed in individuals with normal colour vision (Sjoberg et al., 1998). Consequently, both males and females can express genes coding for more

than two distinct L and M cone pigments (Neitz and Jacobs, 1990; Sjoberg et al., 1998).

Apart from spectral differences, inter-individual variability can occur in the optical density (OD) of the cone photopigments. The differences in the effective OD of the cones are thought to originate from amino acid variations in exon 2 and are thought to primarily affect the efficiency of the quantal catch (Neitz et al., 1999), whilst changes in the cone OS size can also affect the effective OD. Variation in pigment OD can also cause differences in absorption spectra, by differences in self-screening. Differences in OD can provide an advantage for some colour deficient observers, as will be discussed in sections 2.2.1 and 5.2.

Individual differences in colour vision might be mediated by the spatial organisation of the cone photoreceptor mosaic. As mentioned in section 1.2, S cones are rather sparse in the retina and absent from the central 0.34^{o} of the fovea. On average L cones dominate the retinas of normal trichromatic individuals, with fewer M cones and even fewer S cones (Figure 2-3). A number of techniques have been used to enable imaging/examination of the cone mosaic and evaluating the relative numbers of L, M and S cones. Retinal densitometry and adaptive optics are the latest technique, but immunohistochemistry has been used in post-mortem eyes (Bumsted and Hendrickson, 1999; Roorda et al., 2001; Hofer et al., 2005). The average percentage of S cones at 1^{o} eccentricity from the fovea has been estimated as approximately 6% (Hofer et al., 2005). Estimating the L:M cone ratio has been less straightforward and varies significantly amongst normal trichromats. The average L:M cone ratio is ~ 2:1 (Cicerone and Nerger, 1989; Carroll et al., 2000; Kremers et al., 2000), ranging from 0.4:1 to 16.5:1 (Brainard et al., 2000; Carroll et al., 2002; Hofer et al., 2005), although highly skewed ratios are relatively rare (Carroll et al., 2002). Knoblauch and co-

workers have suggested a model for the development of the retinal cone mosaic based on the stochastic differentiation of a cone between becoming L or M (Knoblauch et al., 2006). Expression of an L or M gene protects that gene from silencing and increases the probability that it will be reproduced in the next cycle. The protection form silencing may explain the slight clumpiness occasionally observed in the human cone mosaic (Hofer et al., 2005). The effect of highly skewed L:M cone ratios on colour vision remains poorly understood and highly debated, but some studies show a small indirect effect on the cone opponency and subsequently on chromatic sensitivity (Gunther and Dobkins, 2002). This effect will be discussed further in section 5.2.

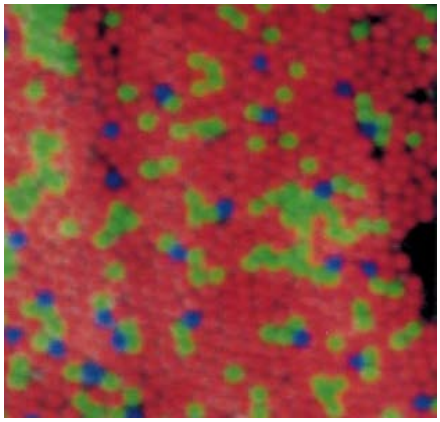

Figure 2-3: Pseudocolour image of the cone mosaic of a normal trichromatic subject. Blue, green and red colours represent S, M and L cones, respectively (Roorda and Williams, 1999).

Apart from receptoral inter-individual differences, variation in the pre-receptoral filtering of light can affect colour vision in normal trichromatic individuals. The crystalline lens and the MP selectively absorb SW light (see section 1.1), while the pupil diameter can indirectly affect chromatic sensitivity by reducing the amount of light reaching the retina. These topics will be discussed further in section 2.3.2, 4.1 and 5.1.

2.2 CONGENITAL COLOUR VISION DEFICIENCIES

Approximately 8% of the male population and 0.4% of females are colour deficient (Birch, 2001). Congenital colour vision deficiencies arise from the absence of the 'normal' S, M or L cones. Colour vision deficiencies are primarily divided into three categories, relating to the lack or abnormal functions of the contributing pigment; protan deficiencies occur when there is no contribution from the L cones, deutan deficiencies when the M cones do not contribute to vision and tritan deficiencies when there is no S cone contribution to vision. Further classification exists on the number of present photopigments; anomalous trichromacies are characterised by the presence of three cone pigments, where one is spectrally shifted with respect to the 'normal', whilst dichromacies refer to deficiencies where one cone class is missing and colour vision is reduced to two dimensions.

Table 2-1 shows the incidence of the various types of congenital colour vision deficiencies. Deuteranomalous trichromatism is the most common congenital deficiency in males, followed by deuteranopia and protan deficiencies. Congenital tritan colour vision deficiencies are rare compared to congenital RG defects. Tritanomaly and tritanopia are usually clustered together in the generic term 'tritan deficiencies' due to their very low incidence. Congenital colour vision deficiencies do not affect other visual functions, are binocular, symmetrical and stable throughout life.

Type of deficiency	Males (%)	Females (%)
Protanopia (P)	~1.01	~0.02
Protanomalous trichromatism (PA)	~1.08	~0.03
Deuteranopia (D)	~1.27	~0.01
Deuteranomalous trichromatism (DA)	~4.63	~0.36
Tritan deficiencies	0.2% to 0.01% *	
Total	~7.99%	~0.42%

Table 2-1: Incidence of congenital colour vision deficiencies (adapted from Wright, 1952; Went and Pronk, 1985; Sharpe et al., 1999; Birch, 2001) (*variable results among studies).

2.2.1 Anomalous trichromacies

Anomalous trichromacies are characterised by the presence of three cone pigments, one of which is 'abnormal'. The abnormal (hybrid) pigment replaces the function of a normal pigment, but has a different spectral sensitivity; replacement of the L pigment by a hybrid pigment (M') is called protanomalous trichromatism or protanomaly (PA). Replacement of the M pigment by an abnormal pigment (L') is called deuteranomalous trichromatism or deuteranomaly (DA). Generally, the severity of anomalous trichromacies depends on the similarity of the pigments serving colour vision (Neitz et al., 1996).

Protanomalous trichromatism is characterised by smaller spectral separations between M and M', compared to the separation between L and L' in DA (Neitz and Neitz, 2011), because the amino acid substitutions have a smaller effect on the spectral sensitivity of M cone pigments relative to L pigments. Therefore, as a group, protanomalous trichromats show poorer colour discrimination than deuteranomalous trichromats.

Interestingly, protanomalous colour vision may also arise from mutations that do not shift the peak spectral sensitivity of the M cone pigments, but produce M pigments of identical spectral sensitivity and different OD (Neitz et al., 1999). The difference in OD gives these subjects advantages compared to single cone dichromats (protanopes), but bleaching of the pigments can minimise the difference in OD leading to dichromatic vision.

2.2.2 Dichromacies

Dichromacy is characterised by the absence of one cone pigment. Subsequently, dichromats' colour vision depends on only two cone pigments. There are three types of dichromacy, depending on the missing photopigment; protanopes lack the L cones, deuteranopes lack the M cones and tritanopes lack the S cones. Most dichromats result from the presence of a single X cone pigment; deuteranopes are 'single gene dichromats' that only have an L gene on the X-chromosome, whilst protanopes either have a single M opsin gene, or have multiple genes in which the first two encode opsins that produce M pigments identical in spectra (Nathans et al., 1986; Neitz et al., 1999; Jagla et al., 2002).

In recent years deleterious combinations of amino acids have been discovered, which can be produced as a consequence of intermixing of L and M opsin genes. One such combination at the exon 3 encoded amino acid position is Leucine 153, Isoleucine 171, Alanine 174, Valine 178 and Alanine 180, which is commonly abbreviated as 'LIAVA' (Carroll et al., 2004). The LIAVA combination leads to the absence of cone function when associated to an L or an M opsin gene. Males whose L opsin contains

the LIAVA combination are protanopes, whilst males whose M opsin contains this combination are deuteranopes. Dichromacies can also be caused by mutations that code for an opsin, which fails to finally produce a functional photopigment (Bollinger et al., 2001; Carroll et al., 2009). The most common such mutation is named C203R and results from the replacement of the cysteine residue with the amino acid arginine at position 203.

2.2.3 Inheritance

Red-green congenital colour vision deficiencies are inherited in an X-linked manner. The genetic location of the genes coding for L and M pigments on the X chromosome renders these genes to express dominantly in males and recessively in females. A male inheriting one copy of a gene coding for an ‘abnormal’ L or M pigment would be colour deficient, whereas a female inheriting the same gene would have normal or near normal colour vision (also discussed in section 2.4.3) and would be a heterozygous carrier of that gene. Figure 2-4 shows an example of inheritance of RG deficiency. The X linked inheritance pattern dictates that the offspring of a female carrier will inherit the exact same type and severity of colour deficiency. This may only be disrupted if two different abnormal genes are combined in a female (see also section 2.4.1).

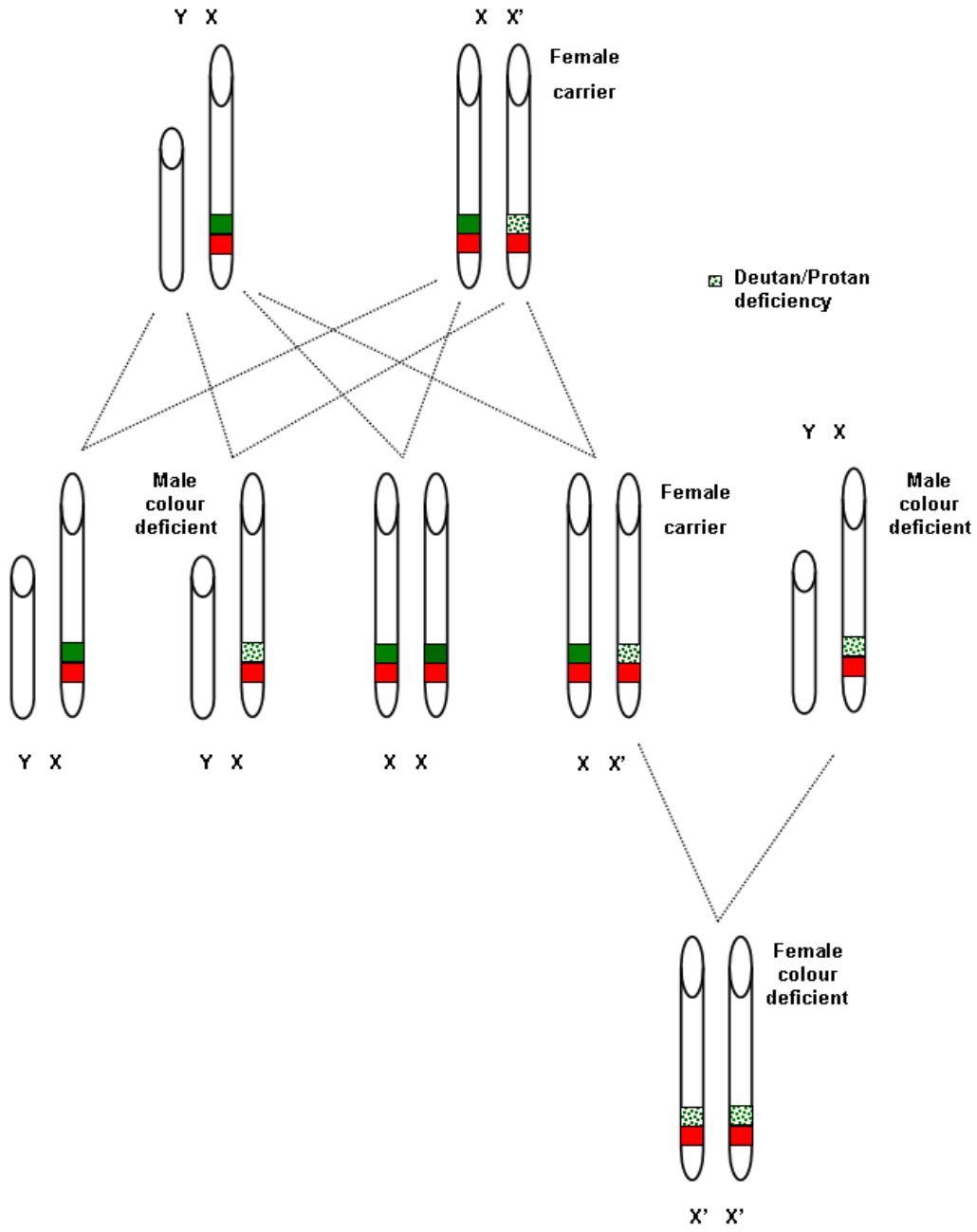

Figure 2-4: Inheritance pattern of RG colour deficiencies. Red and green squares indicate the L and M cone pigments. The dotted green square indicates a deutan (or protan) deficiency. Each male offspring of a woman carrying the colour vision deficiency has 50% chances of inheriting the deficiency. Each female offspring has 50% chances of inheriting the same gene and being a carrier of this deficiency. The female offspring of a female carrier and a colour deficient male may be colour deficient.

The S cone opsin has been located on the autosome chromosome 7 (Nathans et al., 1986); therefore, mutations in the S opsin gene cause tritan defects that are inherited in a dominant manner. In autosomal dominant inheritance, the offsprings of each affected individual will inherit and may express the deficiency. Tritan defects show very variable penetrance and members of the same family may carry the same mutation but express it variably (Baraas et al., 2007). Variable gene expression underlies the large differences in the incidence of tritan defects among studies (Table 2-1).

2.3 ACQUIRED COLOUR VISION DEFECTS

Acquired colour vision deficiencies are fundamentally different from congenital deficiencies; they may be either monocular or binocular and may also be asymmetrical. Acquired deficiencies are usually progressive and other visual functions, like visual acuity and visual fields, might be affected. The most important aetiologies underlying acquired colour vision loss are disease related. Ageing can also produce a gradual worsening of colour vision.

The first classification of acquired colour vision defects was done by Köllner (1912). A classification of acquired colour vision defects was later attempted by Verriest (1963) and a modern categorisation is shown in Table 2-2. Acquired deficiencies were categorised as Type 1, 2 or 3 and have been associated with ocular pathologies. Acquired deficiencies often present in atypical forms and the description of Table 2-2 is, therefore, not exhaustive.

Type of acquired deficiency	Characteristics	Association
Type 1	Protan-like deficiency	Progressive cone dystrophies, Chloroquine toxicity
Type 2	Deutan-like deficiency, with a secondary reduction in SW sensitivity	Optic neuropathies, Ethambutol toxicity
Type 3	Tritan-like defects	Rod dystrophies, peripheral retinal lesions, macular pathologies

Table 2-2: Classification of acquired colour deficiency; Type 1 deficiency results in a protan-like defect and Type 2 in a deutan-like defect. Tritan-like deficiencies have been classed as Type 3 (Birch, 2001).

2.3.1 Ocular and systemic disease

Colour vision is significantly affected by a number of ocular and systemic diseases. Multiple sclerosis, vitamin deficiencies, alcohol and tobacco abuse, thyroid ophtalmopathy, exposure to chemical solvents, medication, optic neuritis, diabetic retinopathy, AMD and glaucoma have been shown to affect colour vision (Russell et al., 1991; Pacheco-Cutillas et al., 1999; Lawrenson et al., 2002; Attarchi et al., 2010; O'Neill-Biba et al., 2010). Ocular diseases can affect colour vision before their clinical manifestation; age related maculopathy (ARM) and diabetes mellitus have been repeatedly shown to affect colour vision in the absence of any clinical signs (Applegate et al., 1987; Hardy et al., 1992; Feitosa-Santana et al., 2010) and colour vision loss has been characterised as the first indication of progressive cone-rod dystrophies (Mantyjarvi, 1990).

The fact that established retinal diseases affect colour vision is expected, as lesions of the very sensitive receptoral and post-receptoral structures can disrupt the processing of the signals. It is however of great interest that subtle clinically undetectable changes in the retina and/or optic nerve may alter visual function before the detection of reliable clinical signs of ocular disease. This has been shown before for glaucoma, where clinically detectable sensitivity loss in the visual field becomes evident only after approximately 20-50% of the ganglion cells have apoptosed (Harwerth et al., 1999). These findings justify the need for careful examination of colour vision in the absence of clinical signs of ocular or systemic disease, especially in the elderly.

2.3.2 Ageing

For a long time researchers have been investigating the severity and patterns of colour vision loss with increasing age; Lakowski (1962) and Verriest (1963) were one of the first to report an age-related deterioration of colour vision, with a greater impact on SW and a tritan-like colour vision defect. Given the changes in the optics of the eye, researchers have primarily attributed the age related deterioration of colour vision to lens yellowing and senile pupil miosis (Winn et al., 1994). Marked deterioration of colour vision has been demonstrated when the expected reduction in retinal illuminance for older subjects was simulated in younger subjects. It was then concluded that because of lens yellowing and senile pupil miosis “the overall reduction of retinal illuminance can shift the vision into the mesopic range, which is itself characterised by a tritan-like colour vision defect“ (Verriest, 1963). Indeed, it has been shown that the retinal illuminance of a 60 year old subject is approximately 1/3 of that

of a 20 year old subject (cited by Werner et al., 1990) and that there is a marked SW sensitivity loss in the mesopic range (Walkey et al., 2001). However, the commonly occurring AMD had already been identified as a possible underlying aetiology for the senile loss of colour vision.

A number of studies have investigated the effects of age on various aspects of colour vision, primarily hue discrimination (Verriest et al., 1982; Knoblauch et al., 1987; Kinnear and Sahraie, 2002; Beirne et al., 2008). Interestingly, the interpretation of the results of these studies varied significantly; some studies attributed the age-related deterioration of hue discrimination to the reduction of retinal illuminance (Knoblauch et al., 1987), whereas others failed to reproduce age related losses by simulating lens yellowing (Beirne et al., 2008). This indicated that neural mechanisms could not be ruled out. Chromatic sensitivity and wavelength discrimination have also shown an age related deterioration, either particularly at SW (Knoblauch et al., 1987; Haegerstrom-Portnoy, 1988; Johnson and Marshall, 1995; Shinomori et al., 2001) or uniformly for S, M and L sensitive mechanisms (Knoblauch et al., 2001).

Further evidence became available from studies investigating the sensitivities of isolated cone mechanisms. It was then evident that not only S cones, but also L and M cones, lose sensitivity with age (Elsner et al., 1988; Haegerstrom-Portnoy, 1988; Johnson et al., 1988; Werner and Steele, 1988; Schefrin et al., 1992), implicating receptoral and/or post-receptoral sites. If solely pre-receptoral filters were responsible for the age-related loss of chromatic sensitivity, S cones should show sensitivity losses when measured on a corneal level, but not on a retinal level, i.e. after controlling for the absorption of light by pre-receptoral filters. S cone sensitivity losses, however, differed when measured on a corneal or a retinal level, indicating that an additional neural mechanism did contribute to the age related chromatic sensitivity loss.

Additionally, since the lens and MP do not significantly absorb middle and LW light, reduction of the M and L cone sensitivities should be the result of some neural aetiology.

It is now agreed that age-related colour vision loss is a result of pre-receptoral filters and neural ageing, but it remains difficult to separate between age-related loss and disease. Of particular significance are the reasons that might underlie receptoral and/or post-receptoral sites of colour vision loss. An age-related reduction in ganglion cells has been reported in healthy ageing (Gao and Hollyfield, 1992; Curcio and Drucker, 1993) and in glaucoma (Harwerth et al., 1999), before the clinical manifestation of visual field defects. Rod and cone photoreceptor densities reduce with increasing age (Keunen et al., 1987; Gao and Hollyfield, 1992; Curcio et al., 1993; Panda-Jonas et al., 1995), with rod dysfunction and loss shown for ARM and healthy ageing (Curcio et al., 2000; Owsley et al., 2001), whilst other changes in the efficiency and integrity of cones have been well documented in healthy ageing (Marshall, 1978; Schefrin et al., 1992). The RPE and Bruch's membrane, two structures of outmost importance in AMD, undergo constant changes with ageing (Bird, 1992; Starita et al., 1996; Curcio et al., 2001). Post-retinal, age-related changes have been associated with age-related pathological conditions (Gupta et al., 2009), but are also present in healthy ageing (Ahmad and Spear, 1993).

Ageing is a continuous process, preceded by development and in many cases followed by disease (Knoblauch et al., 2001). Similarly, retinal diseases like AMD are considered an accelerated form of ageing, whilst others, even though clearly pathological, are more likely to occur at older individuals (e.g. glaucoma). Separating healthy, non pathological, age-related colour vision loss from developing retinal

diseases is, therefore, a challenge of major clinical importance to the ageing population.

2.4 CARRIERS OF COLOUR VISION DEFICIENCIES

2.4.1 X inactivation

The genes that specify M and L wavelength sensitive cone pigments are on the X chromosome (Nathans et al., 1986) and express dominantly in males. Mothers and daughters of colour deficient males are obligate carriers of one copy of the RG colour deficient gene and are known as heterozygous carriers (see Figure 2-4); one of their X chromosomes is carrying the 'normal' gene, whereas the other chromosome carries the gene coding for RG deficiency.

Because women carry two X chromosomes, there are two copies of the genes coding for cone opsins. To balance the expression of X linked genes, one of the X chromosomes is silenced by what is known as X-chromosome inactivation or Lyonisation (Lyon, 1961; Lyon, 1972; Lyon, 2002). X-chromosome inactivation occurs very early during female mammalian development and aims at dosage compensation with males, who have only a single X chromosome. The choice of which X chromosome is inactivated in each cell is random in somatic tissue, but once silencing has taken place for one chromosome, the inactivation remains stable and every descendant cell follows the same inactivation pattern as its precursor cell. Therefore, females express two populations of cells that differ in the X chromosome that is active (paternal or maternal). The X inactivation pattern is believed to be random and,

therefore, X originating cells must be derived from each chromosome by 50% chance, i.e. each female should express half maternal and half paternal genes. Thus, an equal number of cells in a tissue will have active maternal or paternal X chromosome and the other X chromosome will be silenced.

Evidence, however, exists for skewed X inactivation patterns, where most cells express genes preferentially from a single chromosome. Approximately 9% of females have skewed X inactivation, where one X chromosome is inactivated preferentially with respect to the other (Amos-Landgraf et al., 2006). Such an example has been demonstrated in relation to colour vision deficiencies in two female monozygotic twin daughters of a deuteranomalous father (Jorgensen et al., 1992); one of the twins exhibited deuteranomalous colour vision, whereas the other twin daughter had normal colour vision. The colour deficient daughter showed a predominantly paternal expression, whereas the daughter with normal colour vision showed mainly maternal expression, as identified by genetic testing. The incidence of skewed X inactivation might increase with age (Cotter et al., 1995; Busque et al., 1996; El Kassar et al., 1998; Sharp et al., 2000; Bittel et al., 2008), whilst skewed, non-random X inactivation has also been observed in a wide range of neoplastic tissues (Brown, 1999).

It is generally accepted that approximately 15% of the female population carry a gene coding for colour vision deficiency. The percentage of women who carry two defective genes (L and M) has not been studied extensively. If these women carry two copies of a gene coding for the same colour vision deficiency they would manifest colour deficiency themselves. However, if the two arrays express opposing types of defects, one for protan and one for deutan defects, the female should have near normal colour vision, as the defects would complement each other (Tait and Carroll, 2009).

2.4.2 Cone mosaic

The implications of random X-inactivation for the cone mosaic and the photopigments generated are highly dependant on the type of the colour deficiency carried. Congenital RG dichromacies are characterised by the absence of either M or L cones in the retina, i.e. the absence of M cones in deuteranopia (D) and the absence of L cones in protanopia (P). In carriers of dichromacy therefore, the normal X chromosome codes for both M and L cones but the 'deficient' chromosome codes for only one type of cone (M in carriers of P and L in carriers of D). X inactivation therefore shifts the L:M cone ratio towards higher values in carriers of D and towards lower values in carriers of P. The L:M cone ratio has been shown to vary significantly amongst normal trichromats (Brainard et al., 2000; Carroll et al., 2002; Hofer et al., 2005) and skewed ratios are present among the normal population (Carroll et al., 2002), but carriers of dichromacies can have ratios that often extend beyond the normal variability (Miyahara et al., 1998; Gunther and Dobkins, 2002; Hofer et al., 2005). Highly skewed L:M cone ratios may have a small indirect effect on the cone opponency and subsequently on chromatic sensitivity (Gunther and Dobkins, 2002; Lee, 2004). The large variation in the size of the RG anomaloscope matching range in normal trichromats has also been attributed to selective amplification of cone signals and noise at low light levels in subjects with skewed L:M ratio (Barbur et al., 2008).

In anomalous trichromacy the peak spectral responsivity of either the M or L pigment is shifted to a different wavelength. Deuteranomalous trichromats rely on two L sensitive pigments (L and L') and protanomalous trichromats have two M sensitive pigments (M and M'). As a result, a female carrier of anomalous trichromacy can express four spectrally distinct photopigments (Nagy et al., 1981) and can therefore

exhibit a unique cone mosaic. The spatial arrangement of the 'deficient' and normal cones in the retina of carriers of anomalous trichromacies is not yet clear. The presence of patches of 'normal' and 'colour deficient' cones, known as mosaicism (Born et al., 1976; Cohn et al., 1989) has been demonstrated, as has the random arrangement of the four types of cones (Roorda et al., 2001; Hofer et al., 2005).

A difference in the spatial arrangement of the cones could, in theory, have an effect on the processing of the signals originating from the four different pigments; mosaicism implies that signals from the hybrid M' would have to be exclusively pooled with the L cone responses in carriers of PA (Sun and Shevell, 2008). A random cone arrangement would not dictate a processing pattern based on spatial arrangement and would allow the pooling of signals based on their spectral similarities (Sun and Shevell, 2008). That would imply that chromatically opponent ganglion cells would recognise M' and M as essentially 'typical M cones' and would sum the chromatic signals as L-(M+M') in carriers of PA (since there is a smaller separation between M and M', see section 2.2.1). In carriers of DA, where the separation between L and L' is larger, the L' could be recognised as a 'typical L cone' if it was spectrally closer to the L cone pigment, leading to a colour signal of L+L'-M; if L' lay closer to M, the ganglion cell signal would be L-(M+L').

2.4.3 Effects on colour vision

Heterozygous carriers of colour vision deficiencies have traditionally been assessed without subgroup analyses for each carried deficiency; reduced chromatic sensitivity, errors in pseudoisochromatic plates, reduced hue discrimination, enlarged matching ranges and displaced midpoints in anomaloscope testing and reduced sensitivity to

some wavelengths have been the most common reports for female carriers of colour vision deficiency (Pickford, 1949; Crone, 1959; Krill and Schneiderman, 1964; Verriest, 1972; Cohn et al., 1989; Jordan and Mollon, 1993; Hood et al., 2006).

The luminosity function of carriers of protan deficiency differs from that of normal subjects (Crone, 1959) and shows reduced sensitivity to LW lights (Yasuma et al., 1984; Miyahara et al., 1998). As a result of reduced sensitivity to LW, protan carriers may need more red light to match monochromatic yellow from a mixture of red and green light on the Nagel anomaloscope (Schmidt, 1955), a finding that has, however, been contradicted by other reports (Waaler, 1927; Wieland, 1933; Jordan and Mollon, 1993). The chromatic sensitivity of protan carriers is comparable to normal trichromatic males (Hood et al., 2006), as is their hue discrimination according to some studies (Jordan and Mollon, 1993); results on the width of the matching ranges have been controversial (Jordan and Mollon, 1993; Jordan et al., 2010). Deutan carriers generally show worse colour vision than protan carriers and normal trichromats. Carriers of deutan deficiency (DA and D) have shown reduced chromatic sensitivity (Hood et al., 2006), hue discrimination (Verriest, 1972; Lang and Good, 2001) and more errors on the Ishihara plates (Waaler, 1927; Crone, 1959; Jordan and Mollon, 1993) when compared to normal trichromats.

The processing of colour signals in carriers of congenital colour vision deficiency remains of great interest. The fourth photopigment that is expressed in carriers of anomalous trichromacy could have a significant effect on the way the colour signals are processed. So far carriers of congenital colour vision deficiency have been examined as a group and only few studies have separated the analysis for deutan and protan carriers. The fundamentally different underlying cone mosaics, however, require a more detailed analysis; carriers of anomalous trichromacy should be

examined separately from carriers of dichromacy. The studies carried out so far remain inconclusive as to how the signals from the additional pigment contribute to colour vision; the presence of a fourth, separate post-receptoral channel for the processing of the hybrid pigment has been proposed as an alternative to the integration of the four pigments in the three existing channels (Jordan and Mollon, 1993). Recent studies indicate that the shifts in the Rayleigh match midpoints can provide insight into the pooling of the hybrid pigment's signals in carriers of anomalous trichromacy (Sun and Shevell, 2008).

2.5 AIMS AND OBJECTIVES

The aim of this thesis was to investigate the variability of normal colour vision in relation to ageing and heterozygote carriers of congenital colour vision deficiencies. More specifically this thesis aims to:

- Investigate the effects of age on pre-receptoral filters of the eye, i.e. the crystalline lens and the macular pigment
- Control for the effects of pre-receptoral filters on chromatic sensitivity and investigate the effects of ageing on chromatic sensitivity with respect to the retina
- Investigate the chromatic sensitivity of female carriers of congenital colour vision deficiency
- Investigate the processing of colour signals in female carriers of congenital colour vision deficiency

3 METHODS

This chapter describes the recruitment process and the tests used for the investigation of chromatic sensitivity, macular pigment and lens optical density, pupil diameter, retinal illuminance and chromatic discrimination.

3.1 SUBJECTS

Subjects were recruited from the City University Optometry Clinics, the City University Colour Vision Clinics and via local advertisements. All tests used in this study had been approved by the City University Research and Ethics Committee and adhered to the principles of the Declaration of Helsinki. Each subject was provided with an information sheet prior to their agreement to participate and was required to grant informed consent before taking part. All subjects underwent a full ophthalmic assessment before taking part in the study, including measurement of corrected and/or uncorrected visual acuity, binocular vision assessment, refraction for 2.5 m and 0.7 m, pupil reactions, intra-ocular pressure measurement and indirect ophthalmoscopy. The inclusion criteria for the study required that all subjects:

- Were aged between 16 and 80 years of age
- Had healthy eyes with no history of ocular disease, surgery or laser treatment
- Had no ocular co-morbidity
- Had normal colour vision
- Were healthy and did not suffer from any diseases known to affect colour vision. Subjects were not excluded if they suffered from high blood pressure,

hypercholesterolemia and/or hyper/hypo-active thyroid that had no ocular manifestations and were properly controlled. The aforementioned conditions are very common in the population and exclusion of these would not represent the current status of the ageing population, e.g. ~18% of people in the UK are treated for high blood pressure (National Centre for Social Research and University College London Department of Epidemiology and Public Health, 2011), whilst approximately 52% of adults have a total cholesterol level of 5 mmol/L or above (National Centre for Social Research and University College London Department of Epidemiology and Public Health, 2008). However, none of the subjects included in this study were taking medication known to affect colour vision (Lawrenson et al., 2002).

Subjects were excluded from the study if:

- Their best spectacle corrected visual acuity (BSCVA) was worse than 0.3 LogMAR
- They were found to be congenitally colour deficient
- They were found to have any ocular abnormalities or suspicion of ocular diseases, including congenital crystalline lens opacities. Subjects with age related crystalline lens opacities (cortical cataract, nuclear sclerosis and/or sub-capsular cataract) were not excluded from this study
- They suffered from any disease known to affect colour vision (e.g. diabetes mellitus, multiple sclerosis) (Dain et al., 1990; Russell et al., 1991; Feitosa-Santana et al., 2010; O'Neill-Biba et al., 2010)

All female subjects were questioned about any known colour deficient male relatives and were categorised accordingly. The above inclusion/exclusion criteria were

designed to enable the investigation of differences in chromatic sensitivity that could most probably be attributed to the objectives of this study rather than other, potentially confounding factors.

3.2 CHROMATIC SENSITVITY

Chromatic sensitivity was measured using the Colour Assessment and Diagnosis (CAD) test. The CAD test measures chromatic sensitivity along 16 directions in the Commission Internationale d' Eclairage (CIE) 1931 chromaticity chart, using multiple randomly interleaved staircases with variable step sizes and a four-alternative forced-choice procedure.

The stimulus is generated with 30 bit resolution in the centre of a large uniform background field on a visual display (LaCIE Electron Blue, 20" CRT monitor). The stimulus consists of a square array of 15 x 15 achromatic checkers, subtending a horizontal visual angle of approximately 3.3^o x 3.3^o at a viewing distance of 2.5 m. The background chromaticity is set as the MacAdam 'white' in the 1931 CIE-x,y chromaticity coordinates x=0.305 and y=0.323. The luminance of each checker scintillates every 40 to 80 ms, with equal probability, within a range defined as a percentage of the standard luminance; the CAD test employs a range of ± 45%. The variation of the checks is such that the average luminance over the stimulus is constant and equal to that of the background, thus providing a steady state of light adaptation independently of any chromatic displacement. This random luminance modulation (RLM) is applied spatially and temporally, creating achromatic dynamic luminance contrast (LC) noise that masks the detection of luminance contrast signals

and isolates the use of chromatic signals (Barbur and Ruddock, 1980; Barbur et al., 1981; Barbur et al., 1994; Rodriguez-Carmona et al., 2005). The 45% noise has been selected, as it ensures that the colour detection thresholds of all dichromats tested during the development of the CAD test reach the limits of the phosphors of the display (Rodriguez-Carmona, 2006).

A smaller, coloured test stimulus, which comprises 5 x 5 checkers (subtending a visual angle ~ 0.8^o at a viewing distance of 2.5 m) is buried in the larger array of LC checkers. The chromaticity of the test stimulus can be any of the 16 predefined directions in the CIE 1931 (x,y) chromaticity chart (56^o, 60^o, 64^o, 68^o, 140^o, 145^o, 170^o, 175^o, 236^o, 240^o, 244^o, 248^o, 320^o, 325^o, 350^o, 355^o) (Figure 3-1). The test stimulus moves diagonally at a speed of ~4^o/s from one corner of the square towards the opposite and the subject's task is to indicate the direction of the movement of the coloured stimulus, by pressing one of the four buttons arranged appropriately on a response box. If no coloured stimulus is seen the subject is asked to guess by pressing randomly one of the four buttons. The chance probability of a correct response is 1 in 16 (Barbur, 2004), as the correct direction has to be reported twice in succession before the colour signal of the stimulus is decreased according to the interleaved staircase procedure. The initial step size is 0.025 units, reducing exponentially to a final 0.001 units. The test is terminated after 11 reversals and the mean of the last 6 reversals is taken as a threshold estimate for the colour direction.

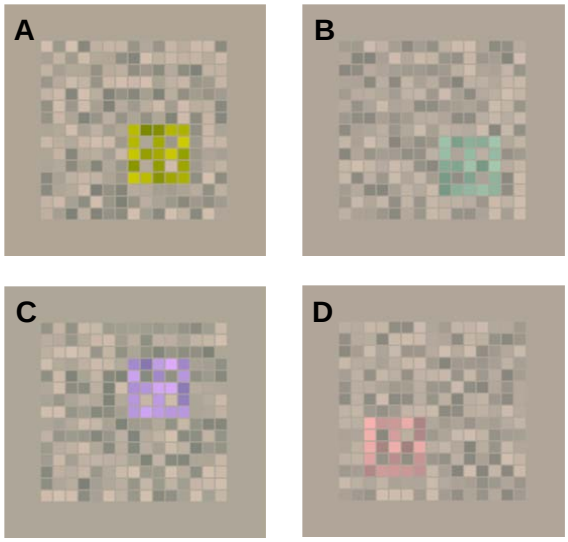

Figure 3-1: CAD test stimuli at 4 directions (A: 64°, B: 145°, C: 248°, D: 325°)

The CAD test algorithm used in this study averages the chromatic signals measured at the 16 chromaticity directions to compute the mean red-green (RG) (140°, 145°, 170°, 175°, 320°, 325°, 350°, 355°) and yellow-blue (YB) (56°, 60°, 64°, 68°, 236°, 240°, 244°, 248°) thresholds. The CAD test produces a numeric threshold for RG and YB chromatic sensitivity that is expressed in 'standard normal units' (SNU). The colour signal strength for the average normal trichromatic observer is taken as 1 SNU (Rodriguez-Carmona et al., 2005). Therefore, a RG threshold of 2 SNU would indicate that a subject requires twice the RG colour signal strength that would be sufficient for the average normal observer. A threshold <1.0 SNU means that the subject requires less colour signal and subsequently has better chromatic sensitivity compared to the average normal trichromatic observer.

Figure 3-2 shows a plot of the CAD test results for an observer with normal colour vision; the results are plotted on a CIE 1931 (x,y) chromaticity chart. Although the CIE (x,y) chart is nonlinear, the measured RG and YB thresholds can be predicted accurately for any state of chromatic adaptation and over a large range of luminances,

based on the cone excitation signals produced by the adapting background field (Jennings and Barbur, 2010). When colour thresholds are measured as chromatic displacements away from background chromaticity, the cone contrasts generated are approximately linearly proportional to these thresholds (Rodriguez-Carmona et al., 2012).

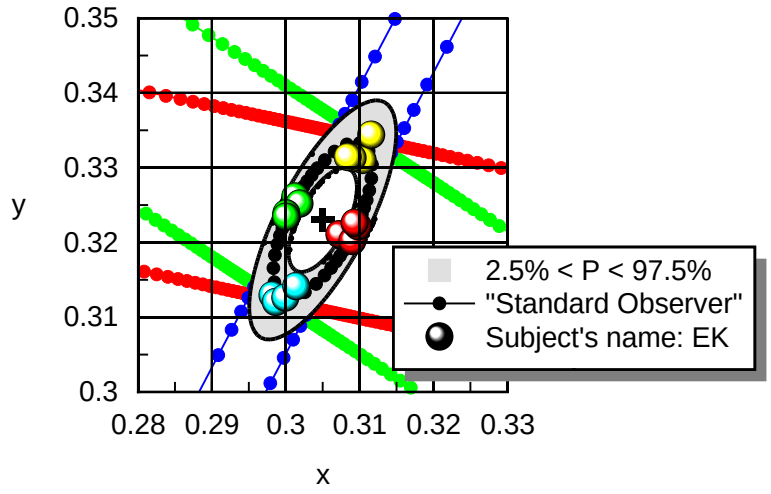

Figure 3-2: CAD plot for subject EK (RG threshold=1.02, YB threshold=0.98).

The subjects viewed the display through a hood from a distance of 2.5 m and adapted to the uniform background field for one to three minutes before the onset of the test. The CAD test was carried out monocularly for screen background luminances of 2.6, 7.8, 26 and 65 $cd \cdot m^{-2}$.

3.2.1 CRT monitor calibration

The CRT monitor was calibrated regularly, to ensure the correct luminance of monitor's guns. An automated luminance calibration programme determined the

relationship between the bit values set on the driver card for the red, green and blue guns and the resulting screen luminance. The programme contains values for the CIE standard observer (Wyszecki and Stiles, 1982).

The luminance calibration programme was used in conjunction with an LMT 1003 luminance meter to calibrate automatically the luminance characteristics of the monitor. This involved measurement of the luminance versus applied voltage relationship for each gun. Measurements were acquired every 2 voltage steps of the 1024 steps of the 10-bit graphics card. The spectral output of each gun was measured using a Gamma Scientific Telespectroradiometer (Model 2030-31) and provided the chromaticity coordinates of each phosphor. Radiance data were acquired at 5 nm intervals between 380-780 nm. The spectral radiance distribution and the luminance versus gun voltage of the guns of the monitors are shown in Figure 3-3A and Figure 3-3B. The system was turned on ~20-30 minutes before testing.

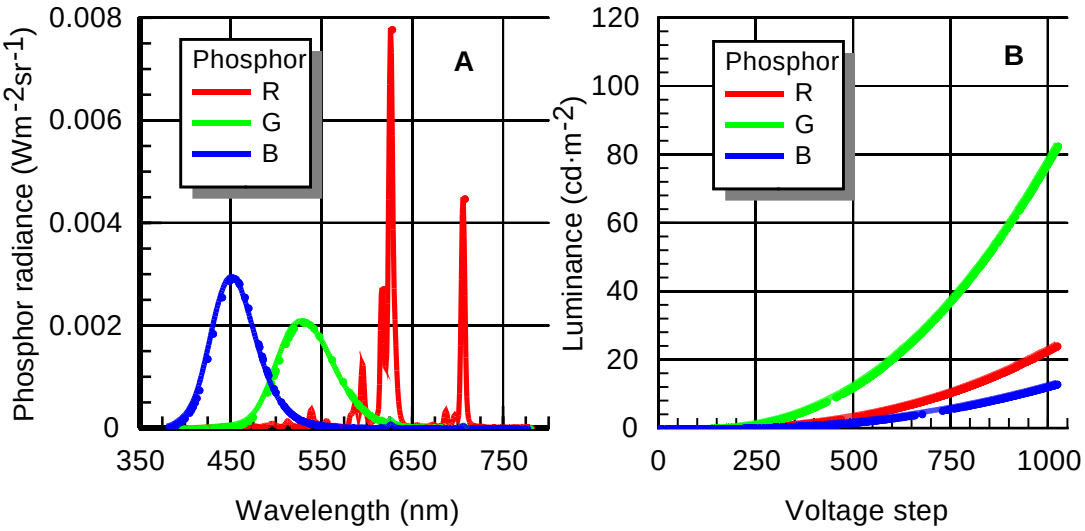

Figure 3-3: Absolute spectral radiance measurement for the red (R), green (G) and blue (B) phosphors of the CRT display (A) and luminance versus gun voltage calibration for the R, G and B phosphors (B).

3.3 MACULAR PIGMENT

The Macular Assessment Profile (MAP) test is a heterochromatic flicker photometry (HFP) technique, where a notch filter is utilised to separate the outputs of the three phosphors into two separate components. The test beam is composed of SW light and is absorbed by the crystalline lens and the MP and the reference beam is composed of LW light and is not absorbed by the lens and the MP (the absorption of SW by the crystalline lens will be discussed in 3.4) (Barbur et al., 2010). The technique is implemented on a 17", CRT monitor (Eizo T566) driven at a frame rate of 140 Hz. The spectral transmittance of the custom designed filter is shown in Figure 3-4A. The unfiltered spectral output of the three phosphors of the display is shown in Figure 3-4B and the wavelength radiance distributions of the filtered test and reference beams employed in the MAP test are shown in Figure 3-4C. The background as seen through the notch filter has a luminance of approximately 54 $cd \cdot m^{-2}$ and this is made up of 24 (red), 24 (green) and 6 (blue) $cd \cdot m^{-2}$. The red and the green phosphor guns each contribute a mean luminance of 16 $cd \cdot m^{-2}$ to the reference beam. The blue phosphor contributes only a steady 2 $cd \cdot m^{-2}$ and this value remains unchanged throughout the test. This arrangement ensures that during the test, the stimulus appears darker than the background and is always seen by the subject. The test beam is derived only from the filtered blue phosphor and peaks at ~ 450 nm with a half maximum spectral width of ± 28 nm (Figure 3-4C).

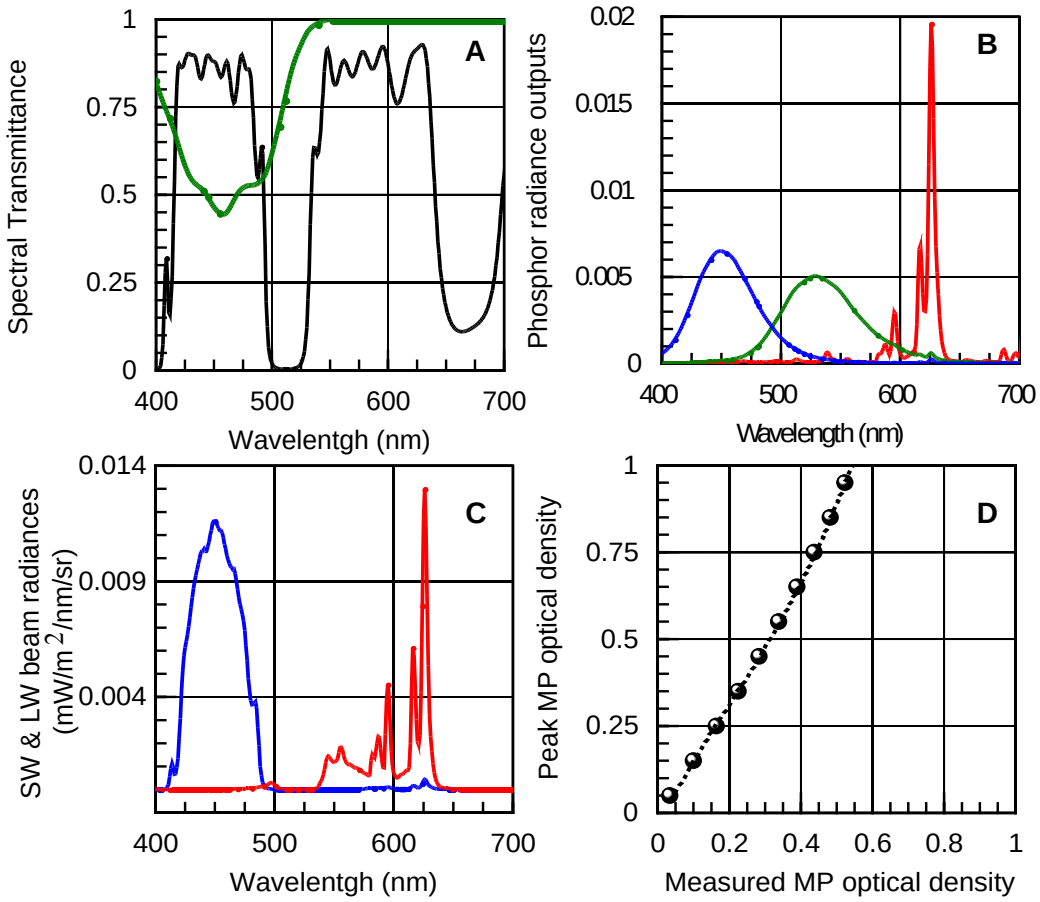

Figure 3-4: Example of an optical 'notch' filter design. A: The spectral transmittance function of the 'notch' filter employed in the MAP test (black curve) and the spectral transmittance characteristics of the average MP of the eye (green curve), i.e. λ_{peak} = 454 nm, OD_{peak} = 0.35 (Stockman and Sharpe, 2000). B: Unfiltered typical wavelength radiance distributions of the red, green and blue phosphors of the CRT monitor. C: Filtered spectral wavelength radiance distributions of the two beams employed in the MAP test. D: Output of photometric model that predicts the relationship between the measured MPOD and the corresponding peak MPOD. The prediction assumes a detector response equivalent to the photopic V(λ) function of the eye corrected for absorption by the mean MPOD (Stockman and Sharpe, 2000).

The reference beam is modulated sinusoidally at ~ 17 Hz in counterphase to the test beam (Figure 3-5) and the modulation depth is constant at 12.7%. The luminance modulation of the reference beam is achieved with 18% modulation of the red

phosphor component and only 9% modulation of the green phosphor luminance. The addition of the green phosphor component to the reference beam ensures that both L and M cones contribute significantly to the detection of both the reference and the test beams. This means that, when the flicker null point is achieved, the modulation amplitude of single cone signals is reduced, as opposed to relying on cancelling relatively large counter-phased M and L cone signals through the luminance channel. Broadening the spectral width of the reference beam through the additional modulation of the green phosphor may also have a further advantage, since the effects of possible differences in the relative numbers of L and M cones at the fovea and in the periphery will be minimised.

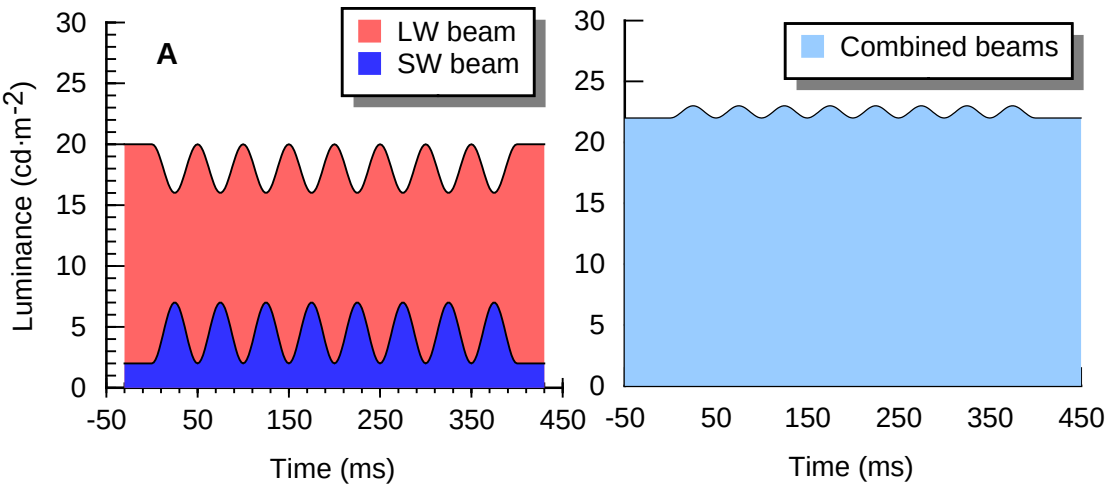

Figure 3-5: Temporal profiles of the luminances of the MAP test beams. The LW and SW beams are modulated sinusoidally in counter phase (A) and combine to the residual modulation profile of the flickering stimulus (B).

The MAP test measures MPOD at 0^{o}, 0.8^{o}, 1.8^{o}, 2.8^{o}, 3.8^{o}, 6.8^{o} and 7.8^{o}. The stimulus is always generated around the centre of the display, but the orientation of the rectangular band and the fixation dot and guides can move appropriately to test any

selected meridian. The stimulus is a small disc of angular subtense 0.36° at the fovea and a sector annulus at more eccentric locations (Figure 3-6). The stimulus dimensions change non-linearly with eccentricity (Appendix A). At distant eccentricities the small dot and guides serve as fixation. For stimulus eccentricities less than 3^o, a mirror symmetric, non-flickering stimulus is also generated on the other side as shown in Figure 3-6B; this arrangement minimises the subject's tendency to saccade to the side of the flickering stimulus.

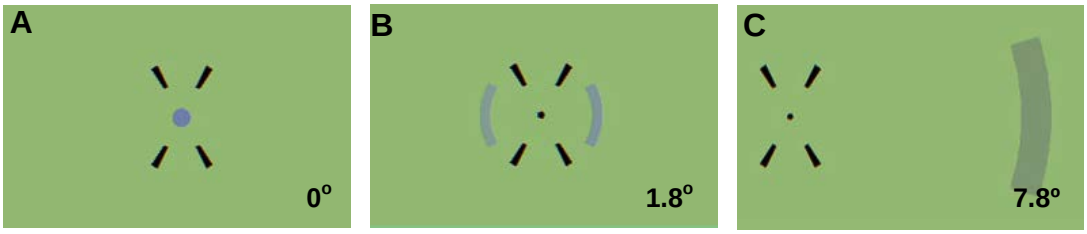

Figure 3-6: Screen dumps of the stimulus employed in the MAP test. Examples are shown at the fovea (A) and at eccentricities of 1.8° (B) and 7.8° (C) on the horizontal meridian.

The small test stimulus diameter employed at the fovea in the MAP test (~0.36^o) minimises errors that arise in systems employing larger stimuli. The advantage of the small stimulus relies on the reduction in spatial averaging, which produces a more accurate estimate of peak MPOD; this is only possible because of light adaptation, which increases the subject's sensitivity to flicker. This is also consistent with other reports, which suggest that smaller foveal stimuli tend to give larger maximum MPOD values (Hammond et al., 1997; Barbur et al., 2010) compared to larger stimuli of approximately 1^o (Hammond and Caruso-Avery, 2000; Beatty et al., 2001; Ciulla and Hammond, 2004). The MAP test data are in good agreement with MPOD measurements made with the Moreland anomaloscope (Barbur et al., 2010); the latter

employs a larger stimulus at the fovea and consequently the foveal measurement is taken to reflect the MPOD value at an eccentricity of 0.32^{o} (Moreland et al., 2001).

When the stimulus is presented to the eye the SW test beam starts with zero modulation and as a result the subject perceives strong flicker caused entirely by the reference beam. The subject increases the mean luminance of the SW test beam (by increasing the modulation amplitude) in discrete steps to slowly reduce and finally to null out the perception of flicker. As the mean luminance of the SW beam increases a point is reached when the perception of rapid flicker disappears, only to reappear after further increase of the SW beam luminance and to be perceived as 'bright' flicker, when the flicker signal generated by the SW beam dominates. A double reversal procedure is followed to first measure the low flicker threshold, when the stimulus appears darker than the background, and then the high flicker threshold, when the null flicker point is approached from above (i.e., the test beam luminance is higher than that required for no flicker perception and the stimulus appears more 'bluish' and brighter than the background). Four randomly interleaved measurements are taken for each spatial location and the average of the two thresholds is taken as the flicker null point. Figure 3-7 shows the graphical output of the MAP test.

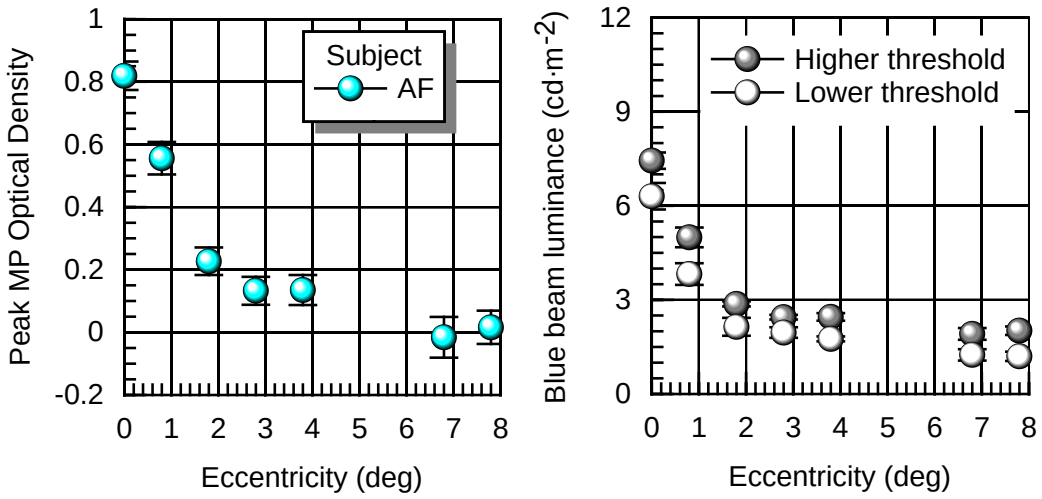

Figure 3-7: MAP test output. A: Typical spatial profile showing the exponential decrease in MPOD with stimulus eccentricity after correction for peak absorption density. This subject has a peak MPOD of 0.82. B: Lower and higher thresholds of the SW beam, which represent the luminance needed to cancel the perception of flicker, when approaching the threshold from below and above the flicker-null midpoint.

The MPOD was calculated as

$$\mathrm{MPOD} = \log_{10}\frac{L_i}{L_o}.$$

Equation 3-1

L_i is the mean luminance of the modulated SW test beam at location, *i*, and L_o is the average test beam luminance for the last two most peripheral locations tested (i.e., 6.8^o & 7.8^o).

When the test beam is spectrally broader than the peak absorption wavelength of the MP, as in the case of the MAP test, the peak MPOD is underestimated and the error involved is a non-linear function of MP density. Figure 3-4D shows the relationship between the measured MP density and the peak density for the filter employed in the

MAP test. The relationship between the predicted peak and measured MP values is based on the photometric model described in Appendix B. The model makes use of the relative spectral distributions of the reference and test beams, the spectral extinction function of the MP and the spectral luminous efficiency function V(λ) of the eye, with the MP for the standard observer removed. The MAP test results can be used without correction for peak density; however, the need to compare results with other studies, particularly those that employ spectrally narrow beams or estimates based on spectral analysis of light reflected from the retina (Wustemeyer et al., 2003; Robson et al., 2005; van de Kraats et al., 2006), justifies the use of the photometric conversion model. The MPOD data shown in Figure 3-7A have been converted to show the peak MPOD. The test was performed monocularly at a viewing distance of 0.7 m, for the eye with the best BSCVA. MP measurements were taken for the horizontal meridian (Figure 3-6).

3.4 LENS OPTICAL DENSITY

In the MAP test, the modulation of the LW reference beam remains unchanged (i.e., 12.7%) at each eccentricity. This modulation generates a supra-threshold flicker signal. The amplitude of this signal and hence the strength of the flicker generated depends on a number of factors including pre-receptoral absorption of light, the size of the pupil and the sensitivity of the retina and the visual pathways. All these factors remain unchanged and affect in an identical way the signal generated when the SW test beam is modulated in counter-phase to the reference beam, except for changes in the spectral absorption properties of the lens and the MP. The MPOD at the two

largest eccentricities employed in the MAP test (i.e., 6.8^o & 7.8^o) is likely to be extremely small (Berendschot and van Norren, 2006) and therefore negligible. The lens does, however, absorb the SW blue beam more than the LW reference beam. A subject with large absorption of blue light by the lens is therefore likely to require an increased amount of blue light to null out the flicker generated at every eccentricity, but the increase in the far periphery will not be contaminated by absorption by the MP. The luminance of the SW test beam needed to cancel out the effectiveness of the LW reference beam at the two most extreme peripheral locations in the MAP test also reflects the absorption of blue light by the lens. The absorption of SW light by the crystalline lens increases rapidly with age, but lenses of young subjects still absorb some blue light (van de Kraats and van Norren, 2007). The average lens transmittance of blue light (T_{AVG}) over the wavelength range that describes a SW beam is given by:

$$T_{AVG} = \frac{\int_{390}^{700} T_L(\lambda) SW(\lambda) d\lambda}{\int_{390}^{700} SW(\lambda) d\lambda},$$

Equation 3-2

where $T_L(\lambda)$ is the spectral transmittance of the lens and $SW(\lambda)$ is the wavelength radiance distribution of the test beam. The exact value of T_{AVG} cannot be computed, but any changes in the subject's average lens OD with respect to young subjects can be calculated. Pilot experiments involving 34 subjects < 22 years of age yielded a median value, $L_o \pm$ SD, for the mean luminance of the SW test beam (Appendix C). The relative optical density of the lens for any subject can be defined with respect to the young subject group:

$$OD = \log_{10} \frac{L_p}{L_o},$$

Equation 3-3

where L_p represents the subject's mean luminance in the periphery and L_o represents the median value for the young subjects group (i.e., the 34 subjects < 22 years old) at the same locations. This definition delineates OD changes with respect to the young subjects' group. A negative value for optical density means that the subject's lens absorption of blue light is less than the mean value for the young subject group.

3.4.1 Predictions based on the Van de Kraats and van Norren model (2007)

van de Kraats and van Nooren (2007) modelled the effects of age on the optical density of human ocular media from 300 to 700 nm, taking into account all pre-receptoral structures (cornea, aqueous humour, lens and vitreous). The spectral density of the human ocular media was described as:

$$D_{media(\lambda)} = d_{RL(age)} \cdot M_{RL(\lambda)} + d_{TP(age)} \cdot M_{TP(\lambda)} + d_{LY(age)} \cdot M_{LY(\lambda)} + d_{LOUV(age)} \cdot M_{LOUV(\lambda)} + d_{LO(age)} \cdot M_{LO(\lambda)} + d_{neutral}$$

Equation 3-4

The subscript 'RL' stands for 'Rayleigh loss', 'TP' for 'tryptophan', 'LY' for 'lens young', 'LOUV' for 'lens old ultra-violet', and 'LO' for 'lens old'. 'Mi' are templates describing the spectral shape of each component and 'di' are the density coefficients. In order to examine how well the MAP test measures approximate the lens OD with respect to the

model described by van de Kraats and van Norren, Equation 3-4 was adapted with respect to the absorption by the crystalline lens only. The spectrally neutral losses were excluded and this approach led to:

$$D_{media(\lambda)} = d_{TP(age)} \cdot M_{TP(\lambda)} + d_{LY(age)} \cdot M_{LY(\lambda)} + d_{LOUV(age)} \cdot M_{LOUV(\lambda)} + d_{LO(age)} \cdot M_{LO(\lambda)}$$

Equation 3-5

Equation 3-5 was then applied to 390-700nm and to 10-80 years of age. The OD and transmittance (T) derived are shown in Figure 3-8.

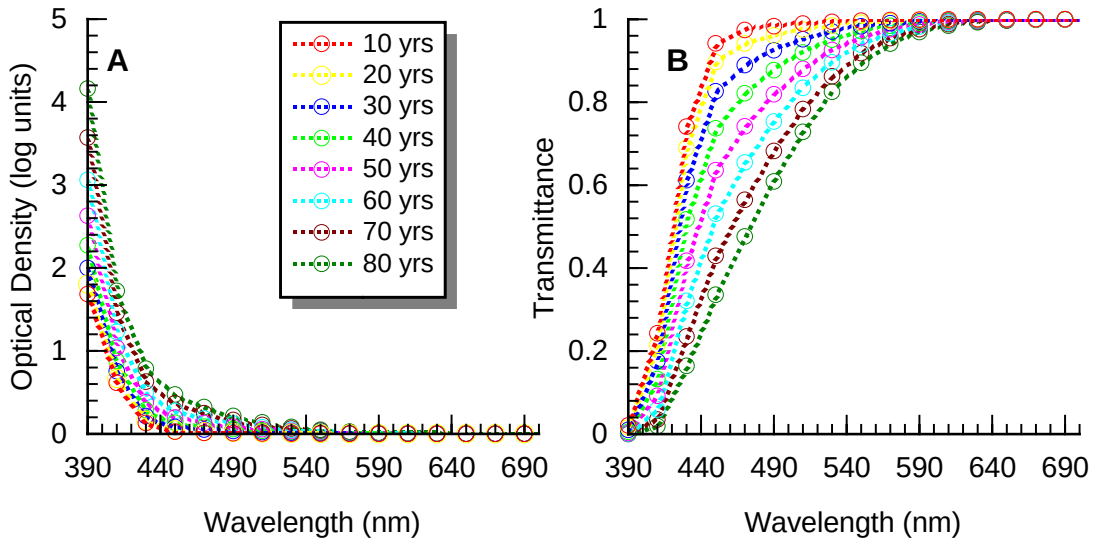

Figure 3-8: Optical density (A) and transmittance (B) of the crystalline lens, adapted from van de Kraats and van Norren (2007).

Following Equation 3-2 the radiance of the SW beam of the MAP test (Figure 3-1) was utilised to estimate the expected transmittance of the crystalline lens for the SW beam of the MAP test. This yielded an age-related increase in the OD of the crystalline lens, which was then referenced to the average young observer (Figure 3-9). A polynomial

model was fitted to the data derived (R^2=0.99, p<0.001). These data will be compared to the measured lens OD for the population of this study using the MAP test in 4.1.1.2. These calculations were made to validate the MAP test as a technique for measuring lens OD and not to promote the use of average age-corrected values; individual variation of the lens OD will be discussed in sections 4.1.1.2 and 5.1.

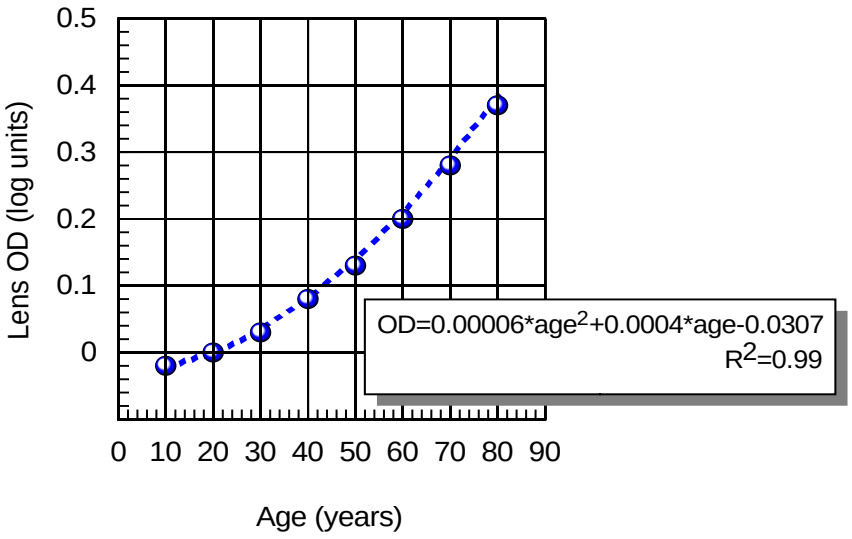

Figure 3-9: Lens OD based on the van de Kraats and van Norren model, adjusted for the SW beam used in the MAP test.

3.5 PUPIL DIAMETER

Pupil diameter was measured using the P_SCAN 100 system (Alexandridis et al., 1991). The system uses infrared video imaging techniques to measure the size of the pupil and to compute its centre coordinates (Barbur et al., 1987). A pulsed infra-red illumination system is used to illuminate the iris for 4 ms within each image frame, to eliminate pupil image smear caused by eye movements. The subject views a uniform

display, similar to that employed in the CAD test. The system is focused as the patient fixates the centre of the screen and a number of pupil measurements are averaged. All measurements were taken monocularly with the subject viewing a uniform background of 2.6, 7.8, 26 and 65 $cd \cdot m^{-2}$, under conditions identical to those employed for the CAD test.

3.6 RETINAL ILLUMINANCE

Retinal illuminance (E) was computed from a knowledge of screen luminance, pupil size and the combined transmittance of the lens and the macular pigment (average MPOD over the central 2.8^{o}) for SW light. Retinal illuminance in relation to RG chromatic sensitivity was calculated by taking into account only the area of the pupil (P) and the luminance of the screen (L), i.e.,

$$E = L \cdot P$$

Equation 3-6

When assessing retinal illuminance in relation to YB chromatic sensitivity the combined transmittance of the subject's lens and the macular pigment (T_C) was also included in the calculation, i.e.,

$$E = L \cdot P \cdot T_c$$

Equation 3-7

3.7 ISHIHARA PSEUDOISOCHROMATIC PLATES

The Ishihara test is one of the most widely accepted colour vision screening tests, with the 38-plate edition recommended for clinical use (Birch and McKeever, 1993). The first 25 plates contain single or double-digit numerals and the remaining 13 plates are designed for the examination of non-verbal subjects. The first 25 plates represent different designs, as shown in Table 3-1.

Plates	Design
1	Demonstration
2-9	Transformation
10-17	Vanishing
18-21	Hidden digit
22-25	Classification

Table 3-1: Design of the Ishihara plates.

For this study the 38 plate edition was used, but only the 21 transformation, vanishing and hidden digit plates were administered. The first plate demonstrates the visual task of the test. The 8 transformation plates contain two numerals; one that is recognisable by the colour normal observer and one with a specific chromatic and lightness contrast that can be read by the colour deficient observer; these numerals can be seen as a different digit by colour deficient observers. Vanishing designs contain numerals that, although seen properly by the normal observer, are not visible to colour deficient subjects. Figure 3-10 shows the demonstration, a transformation and a vanishing design plate.

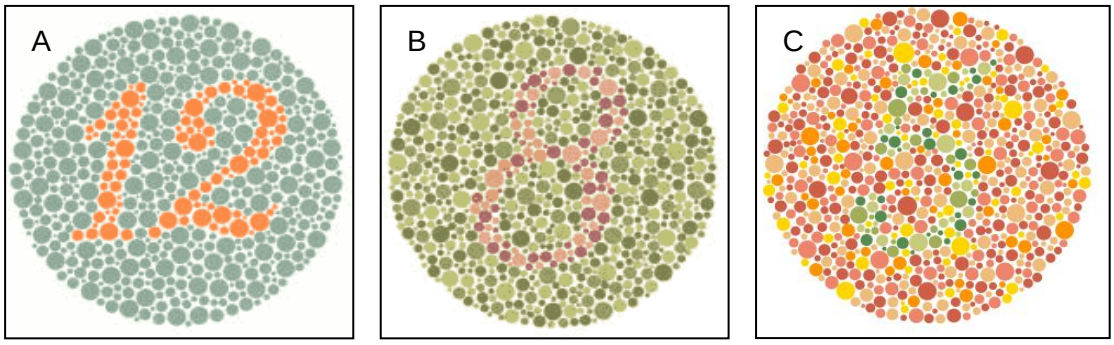

Figure 3-10: The Ishihara pseudoisochromatic plate test; demonstration (A), transformation (B) and vanishing (C) designs. The colours of the plates may not be reproduced accurately, as the printed colour and illuminant might vary.

Some researchers distinguish between 'errors' and 'misreadings' when administering the Ishihara test. An error is considered when a number other than the correct one is seen on the transformation plates, or when no number is seen on the vanishing designs, whilst a misreading occurs when an observer fills in the partial loops of a number (Birch, 2001) (Appendix D). For this study no differentiation was made between errors and misreadings. The Ishihara plates were not designed for identifying tritan deficiency and cannot detect congenital or acquired tritan deficiencies.

The test was performed in a dark room and the Ishihara book was placed on a specially designed tray, at 45^{o} angle below a Macbeth Easel lamp, with a colour temperature of ~6700K (Kollmorgan Corp. Waltham, Massachusetts). The illuminance level as measured in the plane of the plate was 280 lm/m^{2}. The examiner turned the pages and allowed the subjects to view each page for approximately 4 s. The test was performed monocularly, at approximately 0.7 m viewing distance.

3.8 THE AMERICAN OPTICAL – HARDY, RAND AND RITTLER TEST

The American Optical – Hardy, Rand and Rittler (AO-HRR) pseudoisochromatic plates were first printed in 1954 (Hardy et al., 1954) and are very often used in conjunction with the Ishihara plates. The test consists of 20 test plates, preceded by 4 demonstration plates. The test has 6 plates for screening, 10 plates for grading the severity of protan and deutan defects and 4 plates for grading tritan defects. The plates have geometrical shapes (circle, triangle and cross) in vanishing designs, printed in neutral colours on a background matrix of grey dots (Figure 3-11). The saturation of the colours increases in successive plates to produce designs with progressively larger colour differences (Hardy et al., 1954). The 2nd edition of the AO-HRR plates was used and the test was administered in reverse order (Birch, 2001). The test was performed in conditions identical to those described in section 3.7.

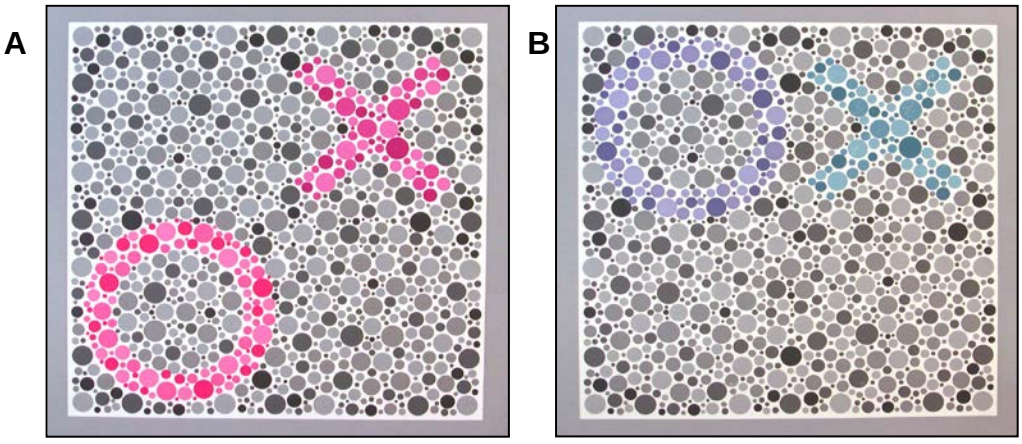

Figure 3-11: The American Optical - Hardy, Rand and Rittler pseudoisochromatic plate test; (A) plate used for the detection of severe protan and deutan deficiency and (B) for tritan deficiency. The colours of the plates may not be reproduced accurately, as the printed colour and illuminant might vary.

3.9 NAGEL ANOMALOSCOPE

The Nagel anomaloscope (Nagel Type I, Schmidt and Haensch GmbH and Co., Berlin, Germany) is a Maxwellian view instrument in which two halves of a 3^{o} circular bipartite field are illuminated by monochromatic yellow (589 nm, lower half-filed) and a mixture of red and green light (670 nm and 546 nm, upper half-field). Two control wheels are used to adjust the red-green mixture ratio and the luminance of the yellow field. The red-green mixture wheel can be adjusted from 0 (pure green light) to 73 (pure red light), while the luminance of the mixture is kept constant (Figure 3-12).

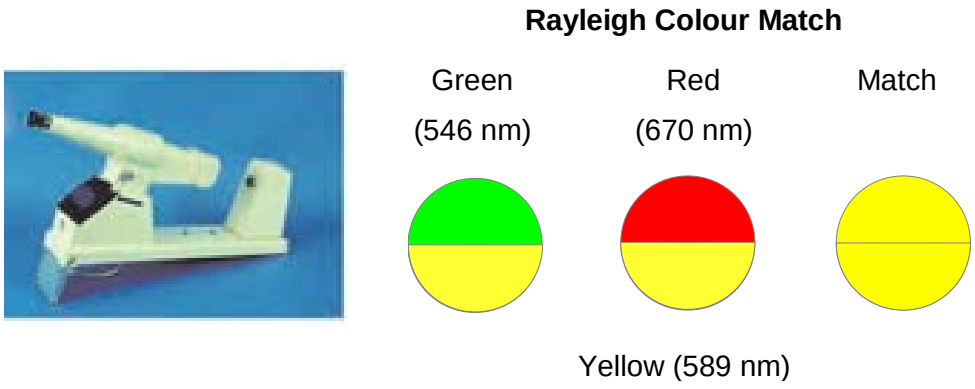

Figure 3-12: Illustration of the Nagel anomaloscope (Nagel Type I, Schmidt and Haensch GmbH and Co., Berlin, Germany) and its bipartite field.

The limits of the matching range were determined first by allowing the observer to make four initial exact colour and luminance matches. Then the examiner set a predetermined RG mixture ratio (based on the mean of the observer's initial matches) and the observer had to adjust the intensity of the yellow hemi-field to achieve the best possible match. Using this procedure a number of red-green mixture ratios were investigated on either side of the mean, to establish the extreme ends of the range,

when the subject could no longer make a match. The range of the anomaloscope was identified as the number of scale units between the lower and higher limits of the observer's RG match and the midpoint as the middle value between the RG match limits. A low photopic ambient illumination was provided in the testing room by a distant tungsten-halogen lamp.

3.10 STATISTICAL ANALYSIS

For regression analysis and non-parametric testing the SPSS® statistical software was used (version 15.0, SPSS Inc., Chicago, Illinois), for non-linear function fitting the JMP® software (Version 4.0.5, SAS Institute Inc., Cary, NC) and for probability distributions MATLAB® (Version 7.0.1, The MathWorks Inc., Massachusetts).

4 RESULTS

4.1 THE EFFECTS OF AGEING ON CHROMATIC SENSITIVITY

4.1.1 Pre-receptoral filters

4.1.1.1 Subjects

A total of 162 subjects (105 females and 57 males) were recruited according to the inclusion criteria outlined in section 3.1 and were assessed with the MAP test, as described in section 3.3. The mean age of the subjects was 44.7 years, ranging from 16 to 79 years (Table 4-1).

Mean ± SD	Median	Range	Male : Female
44.7 ± 17.96	47.0	16 to 79	1:1.8[†]

Table 4-1: Demographics of the population (n=162) ([†] ratio).

4.1.1.2 The effects of ageing on the optical density of the crystalline lens

The effects of ageing on the OD of the crystalline lens, as measured by the MAP test, are shown in Figure 4-1. The lens OD increased significantly with increasing age, although a significant variability was evident for all ages. A significant number of subjects younger than 50 years of age had lens OD measures that indicated lower absorption than the average young observer. A lens clearer than that of the average young observer was not observed for subjects over 50 years of age, with the exception

of one 62 year old female. The increase in lens OD was best described by a polynomial model (R^2=0.52, p<0.001).

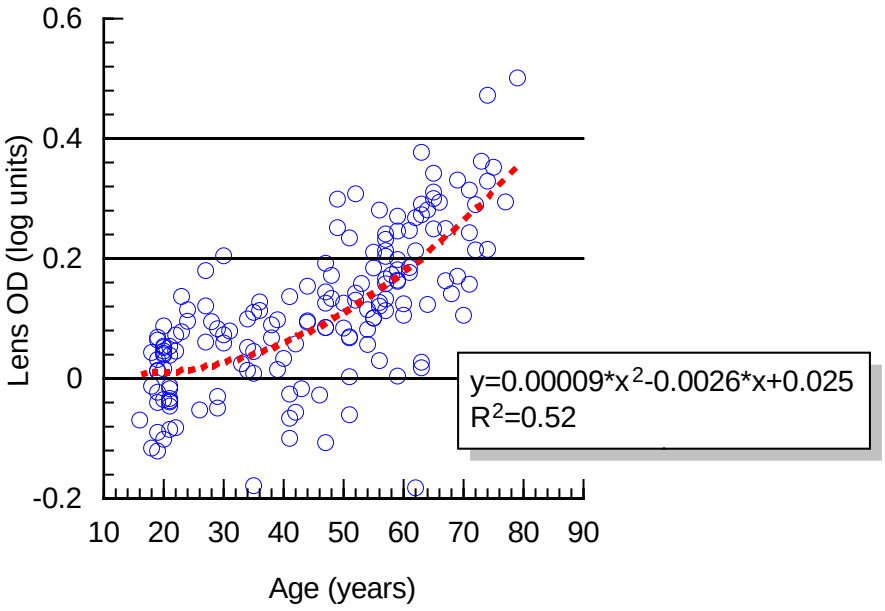

Figure 4-1: Lens OD measurements for 162 subjects and polynomial fit (R^2=0.52, p<0.001), as measured with the MAP test. The test beam of the MAP test peaks at 450 nm and has a half maximum width of ± 28 nm (Figure 3-4C).

Section 3.4.1 described the reconstruction of the van de Kraats and van Norren model (2007) for predicting the OD of the crystalline lens using the SW beam of the MAP test. The results predicted by the van de Kraats and van Norren model (2007) (see Figure 3-9) are compared to the measured lens OD values acquired with the MAP test (Figure 4-1). The fitted function for the 162 subjects seems to agree well with the predictions of the van de Kraats and van Norren model (R^2=0.99, p<0.001) (Figure 4-2) and the differences do not exceed 0.02 log units.

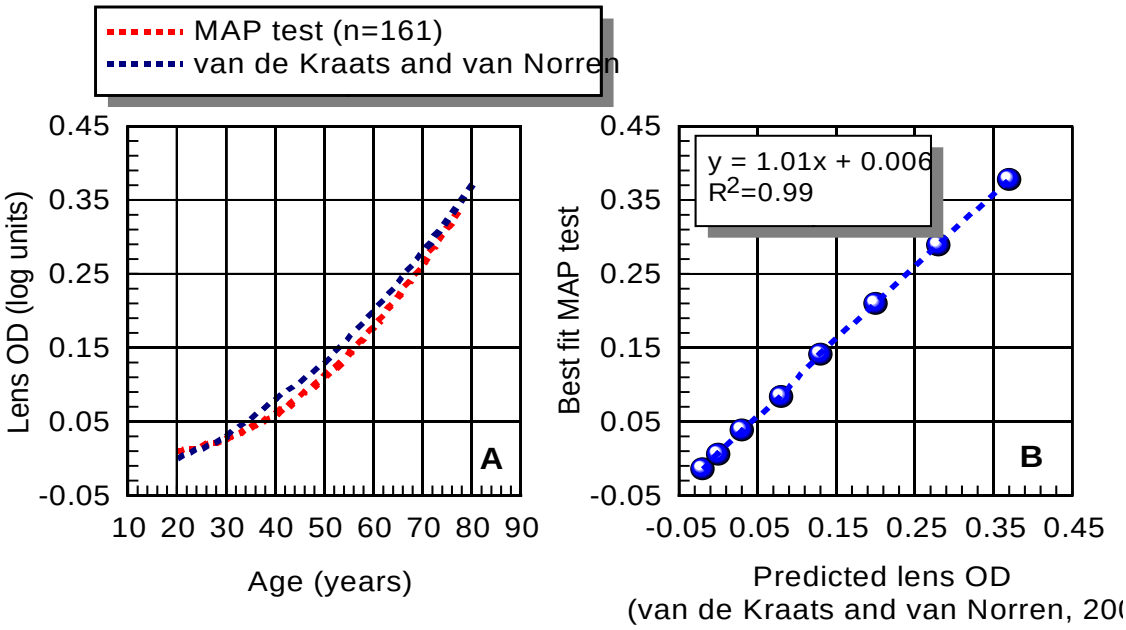

Figure 4-2: Comparison of the reconstructed van de Kraats and van Norren model (2007) and the MAP test (A) and linear correlation of the two approaches (B) (R^2=0.99, p<0.001).

4.1.1.3 The effects of ageing on the optical density of the macular pigment

The mean peak MPOD of the population was 0.5, ranging from 0.08 to 0.98 and the average MPOD over the central 2.8° was 0.28 (Table 4-2). The effects of age on peak MPOD and average MPOD over the central 2.8° are shown in Figure 4-3. There was a small significant decrease in peak MPOD (measurement at 0°, see section 3.3 and Figure 3-6A) with age (0.02 decrease of peak MPOD per decade, R^2=0.04, p=0.01), but the average MPOD over the central 2.8° remained unaffected by age (R^2=0.0004, p=0.81).

	Mean ± SD	Median	Range
Peak MPOD	0.5 ± 0.19	0.52	0.08 to 0.98
Average MPOD 2.8°	0.28 ± 0.11	0.28	0.05 to 0.58

Table 4-2: Mean ± SD, median and range of the peak MPOD and the average MPOD over the central 2.8° for the study population (n=162).

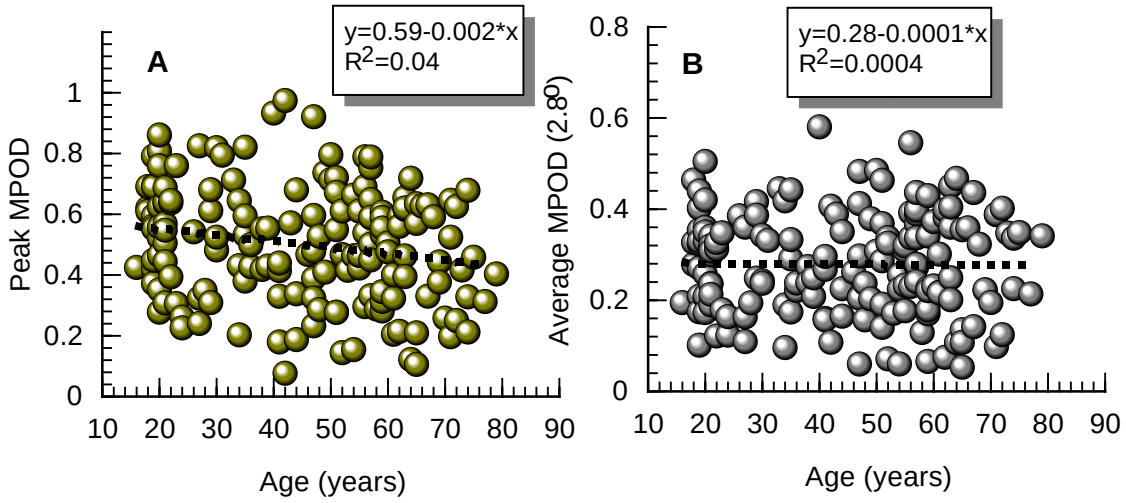

Figure 4-3: Effects of age on peak MPOD (A) (R^2=0.04, p=0.01) and average MPOD over the central 2.8° (B) (R^2=0.0004, p=0.81) (n=162).

4.1.2 The limits of normal colour vision

4.1.2.1 Subjects

A total of 60 subjects were recruited in an attempt to establish the effects of 'normal' ageing on chromatic sensitivity. The mean age of the population was 49.0 years, ranging from 16 to 79 years (Table 4-3). Chromatic sensitivity was measured using the

CAD test for 65, 26, 7.8 and 2.6 cd·m^{-2}; the average MPOD over the central 2.8^{o}, the lens OD and the pupil diameter were also measured. For 49 of the 60 subjects chromatic sensitivity was measured at all 4 light levels, whilst for 11 subjects measurements were performed at 3 light levels.

Mean ± SD	Median	Range	Male : Female
49.0 ± 19.0	55.0	16 to 79	1:1.4†

Table 4-3: Demographics of the population (n=60) († ratio).

4.1.2.2 The effects of age on retinal illuminance

Sections 4.1.1.2 and 4.1.1.3 described the age-related changes in the absorption characteristics of the pre-receptoral filters (the crystalline lens and the MPOD). All 60 subjects included in this study were part of the wider study on the effects of age on pre-receptoral filters and age affected their lens OD and MPOD in a similar manner.

Apart from the crystalline lens and the MP, the pupil constricts significantly with age. This has been attributed to a number of factors, among which are an age-related reduction of the sympathetic tone, a decrease in the activity of the pupil dilator muscle, a reduced inhibition of the parasympathetic impulses, vascular rigidity of the iris and collagen thickening (Schafer and Weale, 1970; Korczyn et al., 1976; Winn et al., 1994). Figure 4-4 shows the age related constriction in pupil diameter for 65, 26, 7.8 and 2.6 cd·m^{-2}. The pupil diameter was maximally affected by age at the lowest light level tested, i.e. 2.6 cd·m^{-2}, with a rate of 0.37 mm per decade.

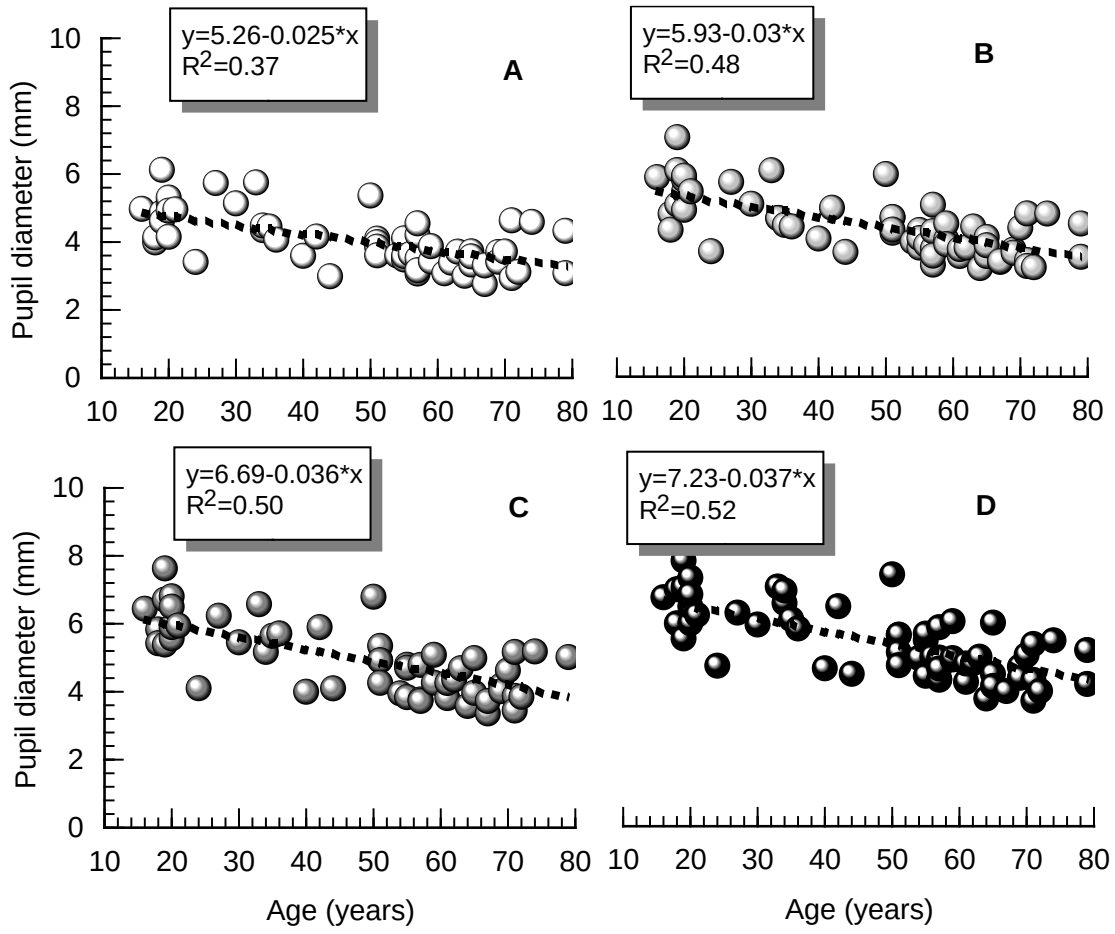

Figure 4-4: Pupil constriction as a function of age for 65 (A), 26 (B), 7.8 (C) and 2.6 cd·m^{-2} (D) (all p<0.001) (n=60).

Given the significant changes in the optics of the eye with age it is expected that the retinal illuminance (E) will be affected as one gets older. Figure 4-5 shows the reduction in retinal illuminance for RG chromatic sensitivity, as a function of age for 65, 26, 7.8 and 2.6 cd·m^{-2} and Figure 4-6 shows the reduction of retinal illuminance with respect to YB chromatic sensitivity, as a function of age for the same screen luminances. The retinal illuminance was significantly affected by age for all tested light levels (all p<0.001).

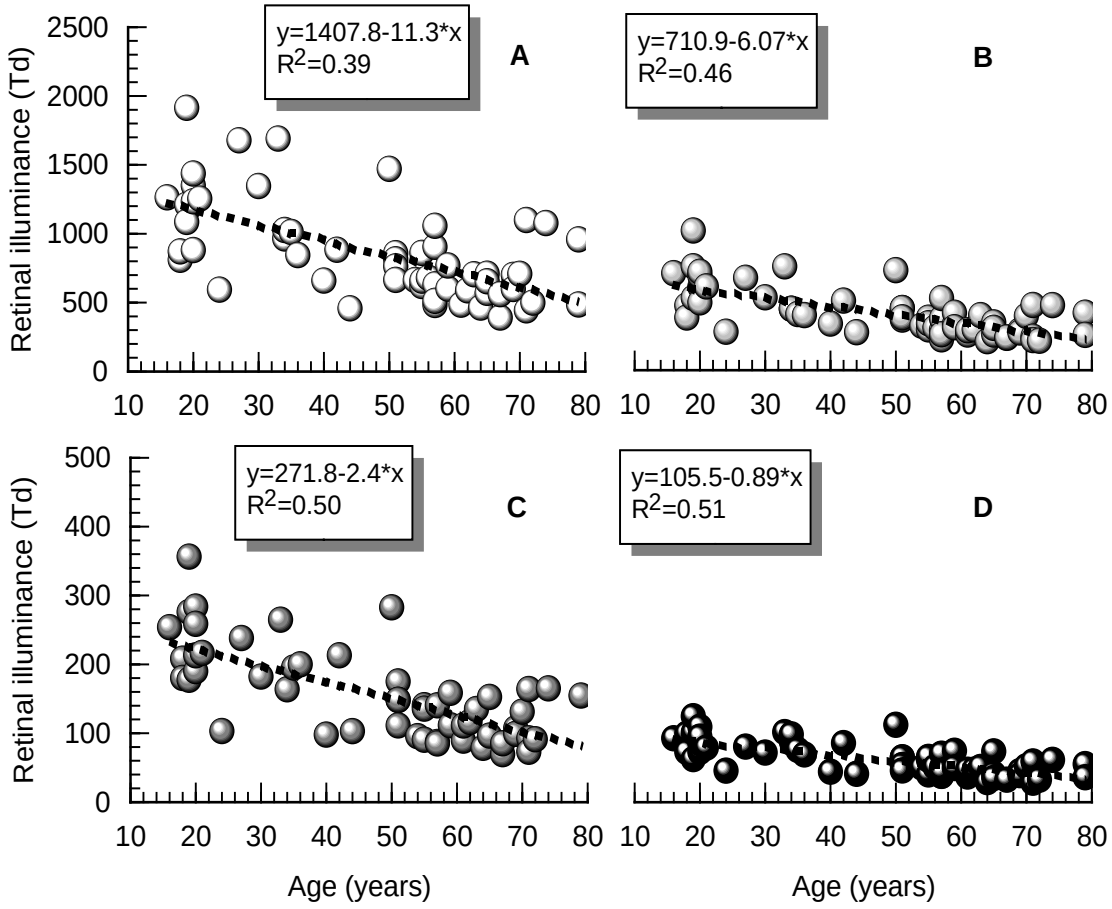

Figure 4-5: Reduction of retinal illuminance with increasing age for 65 (A), 26 (B), 7.8 (C) and 2.6 cd·m^{-2} (D) (all p<0.001) for RG chromatic sensitivity (n=60).

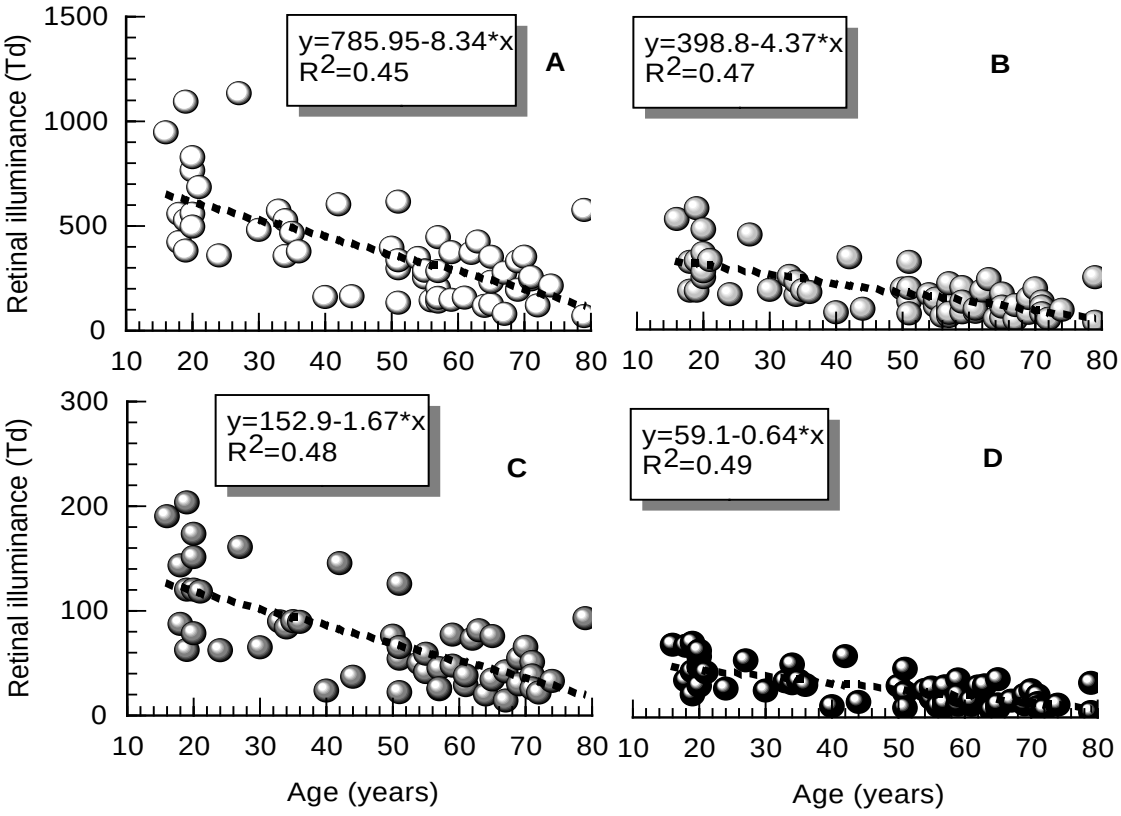

Figure 4-6: Reduction of retinal illuminance with increasing age for 65 (A), 26 (B), 7.8 (C) and 2.6 cd·m^{-2} (D) (all p<0.001) for YB chromatic sensitivity (n=60).

Given the significant decrease of retinal illuminance with increasing age, comparing chromatic sensitivity between different age groups without knowledge of retinal illuminance levels can prove misleading. Figure 4-7 shows the effects of age on the colour detection thresholds measured at 26 cd·m^{-2}, which is the default light level for screening with the CAD test (R^2=0.29, p<0.001 for RG detection thresholds and R^2=0.27, p<0.001 for YB detection thresholds). Given the large variability of the lens OD and the pupil diameter, as shown in Figure 4-1 and Figure 4-4, assuming an average reduction in retinal illuminance with increasing age would not be realistic.

Within the decade 50-59 years the retinal illuminance of the population for 26 cd·m^{-2} spanned a range of 260 Td. Subsequently the comparison of the measured colour detection thresholds of two or more subjects of even a very similar age must rely on the retinal illuminances of these subjects. These reductions in retinal illuminance with age are an important factor when deciding on the 'normality' of the colour detection thresholds and this becomes of outmost clinical importance for older populations. Section 4.1.2.3 will attempt to set normal limits in the ageing population, taking into account the reductions in retinal illuminance attributable to pre-receptoral filters and pupil constriction.

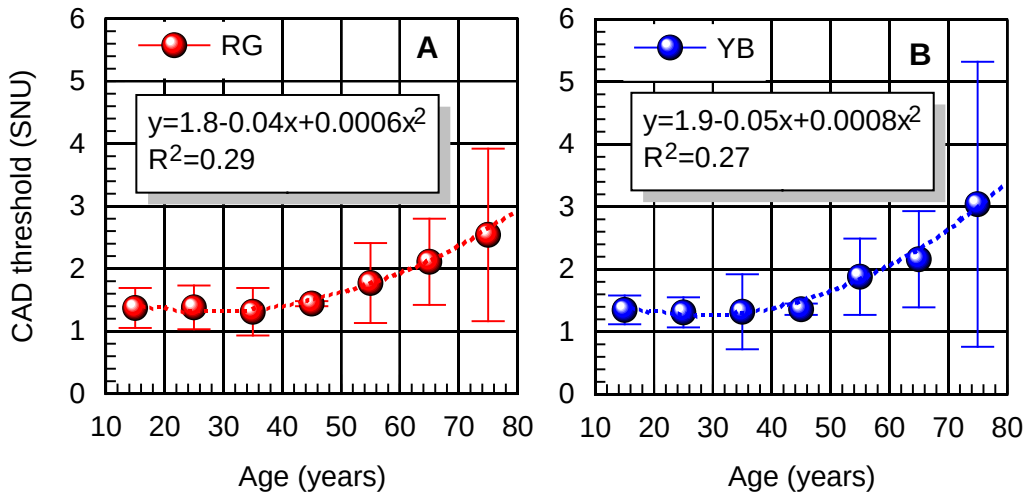

Figure 4-7: Effects of age on measured RG (A) and YB (B) thresholds (mean ± SD) at 26 cd·m^{-2}, without correction for retinal illuminance (R^2=0.29, p<0.001 and R^2=0.27, p<0.001, respectively) (coefficients represent the correlations for the raw data) (n=60).

4.1.2.3 The ‘Health of the Retina’ index

In order to define the normal limits in a population of a wide age range an attempt was made to reference every subject to a ‘standard normal observer’ (SNO) that would define the expected performance for a range of light levels.

The colour detection thresholds for the 60 participating subjects were plotted against the retinal illuminance for the corresponding screen luminances that were employed on the CAD test, as shown in Figure 4-8. An empirical non linear model was then fitted to describe the change of the colour detection thresholds with reducing retinal illuminance for the group. The threshold (T) versus retinal illuminance (E) was described by:

$$T = \kappa \cdot E^{-\alpha} + T_o$$

Equation 4-1

Parameters κ, α and T_o are subject specific; parameters κ and α described how rapidly the threshold increases with reducing retinal illuminance and T_o describes the asymptotic threshold (Barbur et al., 2006). Observation of Figure 4-8 reveals that the retinal illuminances for YB chromatic sensitivity spanned a limited range, attributed to SW light absorption by the lens and the MPOD.

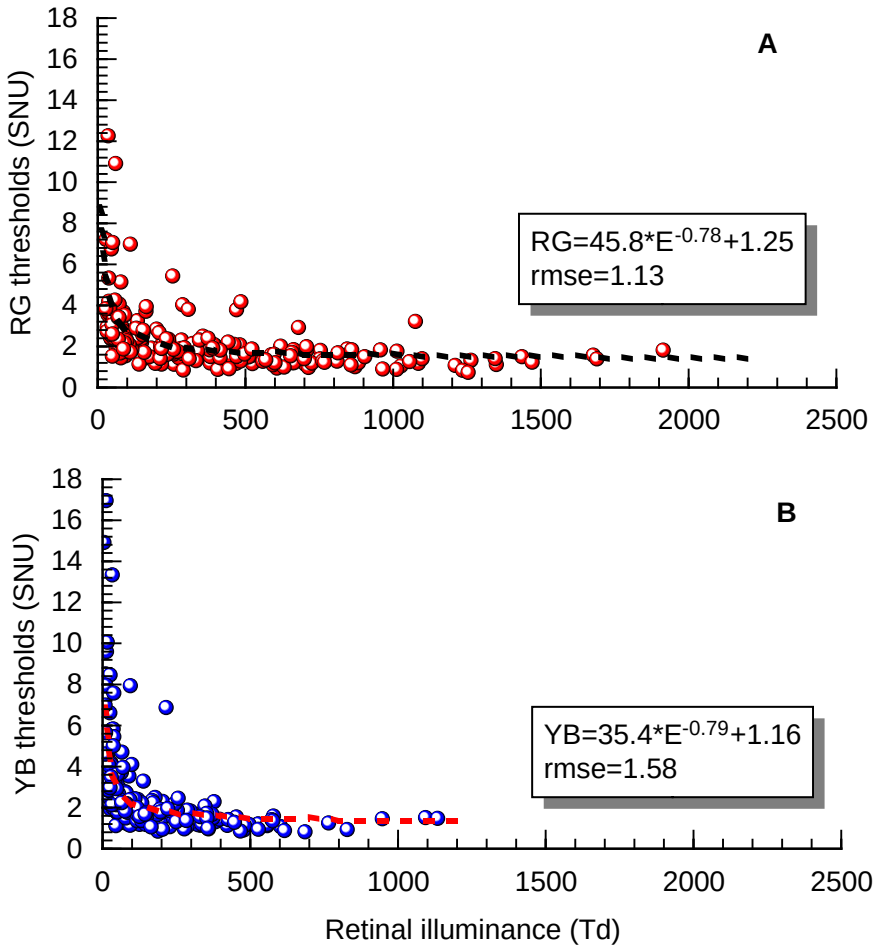

Figure 4-8: RG (A) and YB (B) detection thresholds' change as a function of retinal illuminance and fitted empirical models (n=60).

The areas under the curves (A) were then calculated, by integrating the thresholds for a given range of retinal illuminances for all the subjects participating in this study. In order to standardise the approach for RG and YB colour detection thresholds the areas under the curves were calculated for 25-900 Td for both RG and YB detection thresholds. The areas under the curves, calculated using Equation 4-2, are shown in Figure 4-9 and were treated as the standard normal observer (A_{SNO}), against which every single subject was compared to.

$$A_{SNO} = \int_{25}^{900} \kappa \cdot E^{-\alpha} + T_o = \left[\frac{\kappa}{(1-\alpha)} \cdot E^{(1-\alpha)} + T_o \cdot E \right]_{25}^{900}$$

Equation 4-2

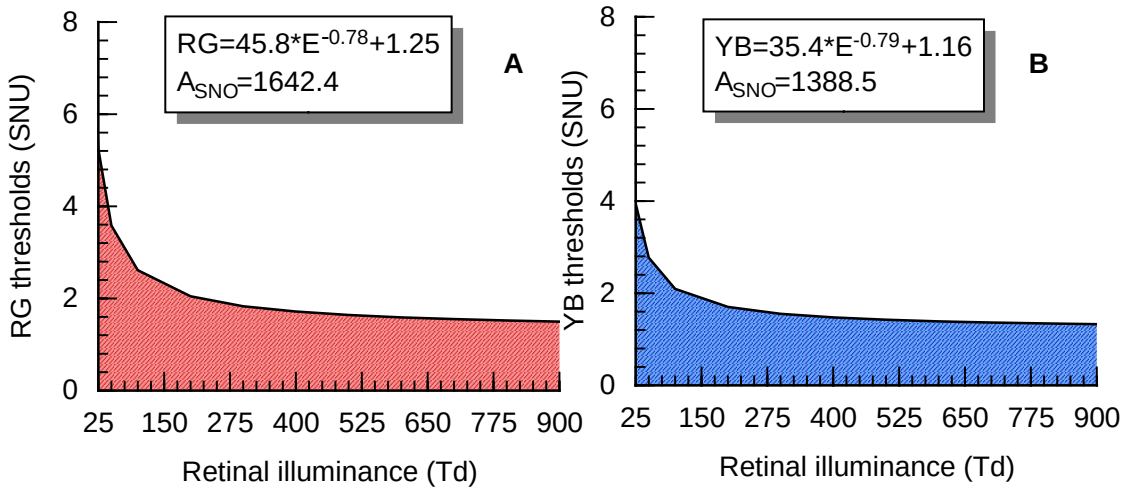

Figure 4-9: Areas under the curves for RG (A) and YB (B) colour detection thresholds (25-900 Td) for the 60 subject that defined the 'standard normal observer' (A_{SNO}).

Equation 4-1 was then applied to each recruited subject to describe the subject specific effect of retinal illuminance on RG and YB thresholds. The majority of the subjects over the age of 50 years had significantly reduced retinal illuminances compared to younger subjects. The nature of the model defines the various parameters based on the rate of change of the colour detection thresholds, which in turn depends on the retinal illuminances that the thresholds were measured at. A subject with low retinal illuminances would show a high rate of change of his/her colour detection thresholds, as shown in Figure 4-8. Parameter T_o can be largely affected as shown in Figure 4-10C. The fitted model for a 71 year old subject with low retinal illuminances unrealistically predicts an asymptotic threshold of -2.25 SNU. To avoid

this unrealistic prediction one additional point was added to the dataset for each subject, designed to reflect the optimum threshold expected for a high retinal illuminance. This point was selected to correspond to twice the subject's highest retinal illuminance and was fixed to 90% of the highest measured threshold. This chosen reduction in threshold is justified, since the doubling of the screen luminance from 26 $cd \cdot m^{-2}$ to 65 $cd \cdot m^{-2}$ causes a similar reduction in mean threshold for the group data. This additional point improved the fit for all subjects with reduced measured retinal illuminances, but caused negligible changes for subjects that achieved high retinal illuminances, where the asymptotic threshold was already very well approximated by the model (Figure 4-10 A and B). In the example of Figure 4-10 (C and D), where an extra point is added as described above, the fit is improved (rmse=0.23 versus 0.28) and a realistic asymptotic threshold is predicted (0.82 versus -2.25). Without this approach chromatic sensitivity could be overestimated in older subjects who happened to have reduced retinal illuminance.

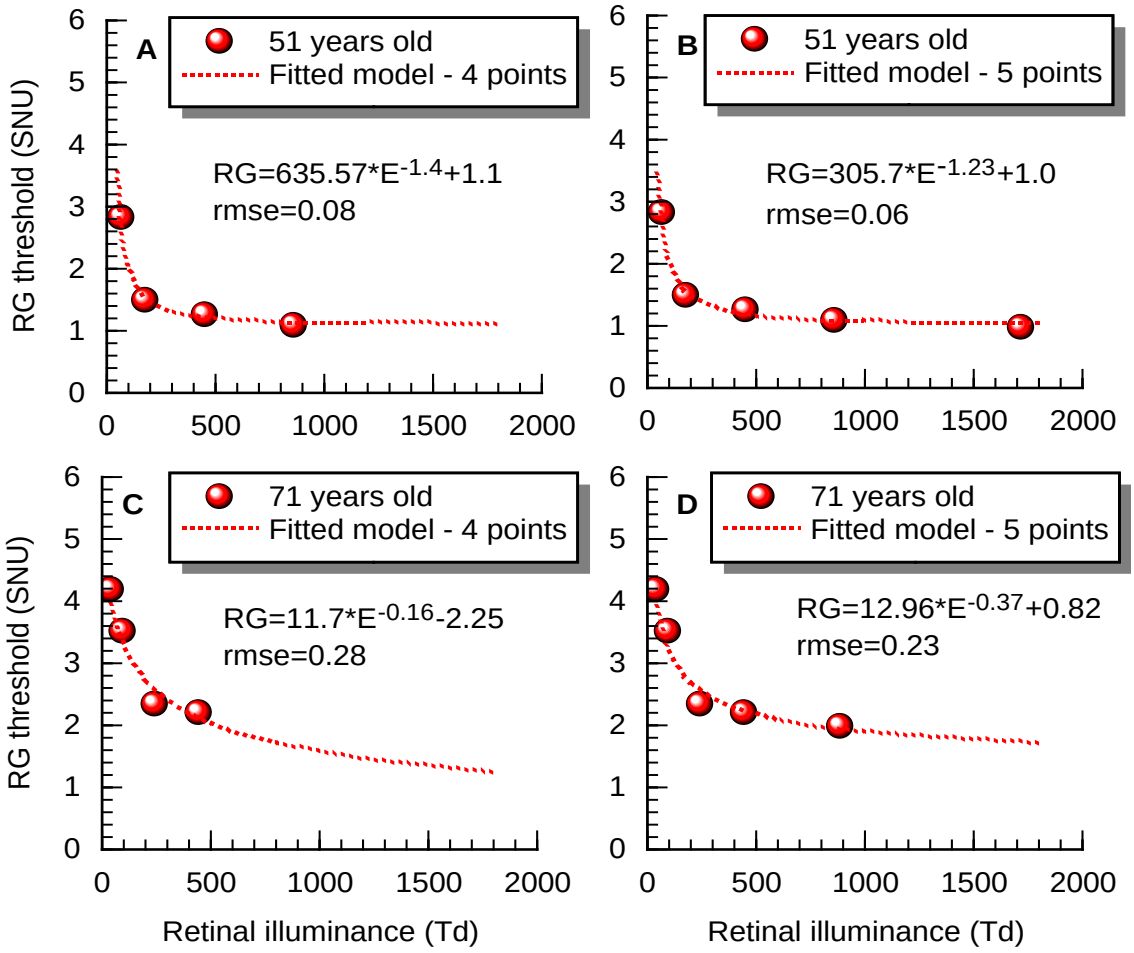

Figure 4-10: Measured RG thresholds and fitted models for two subjects (51 and 71 years old). A: Fitted model for a 51 year old subject without the addition of an 'extra' point. B: When adding the 'extra' point, the asymptotic threshold only changes by 0.1 SNU and the rmse remains unchanged. C: Fitted model for a 71 year old subject, with low retinal illuminances, without the addition of the 'extra' point. The asymptotic threshold is '-2.25'. D: The added data point improves the fit (rmse=0.23 versus 0.28) and estimates a realistic asymptotic threshold (0.82 versus -2.25).

Equation 4-2 was then used to compute the area under the curve for each of the 60 recruited subjects. The Health of the Retina (HR) index for a given subject was defined as the fractional change in the area under the curve for any subject (A_s) with respect to the area under the curve for the median observer (A_{SNO}):

$$HR_{index} = 1 - \frac{A_S}{A_{SNO}}$$

Equation 4-3

A positive HR index indicates a smaller area under the curve, hence lower thresholds than the SNO for the same range of retinal illuminances and better performance than the SNO (Figure 4-11 A and B). A negative HR index indicates a larger area under the curve for that subject compared to the SNO, thus higher thresholds and, consequently, reduced chromatic sensitivity (Figure 4-11 C and D).

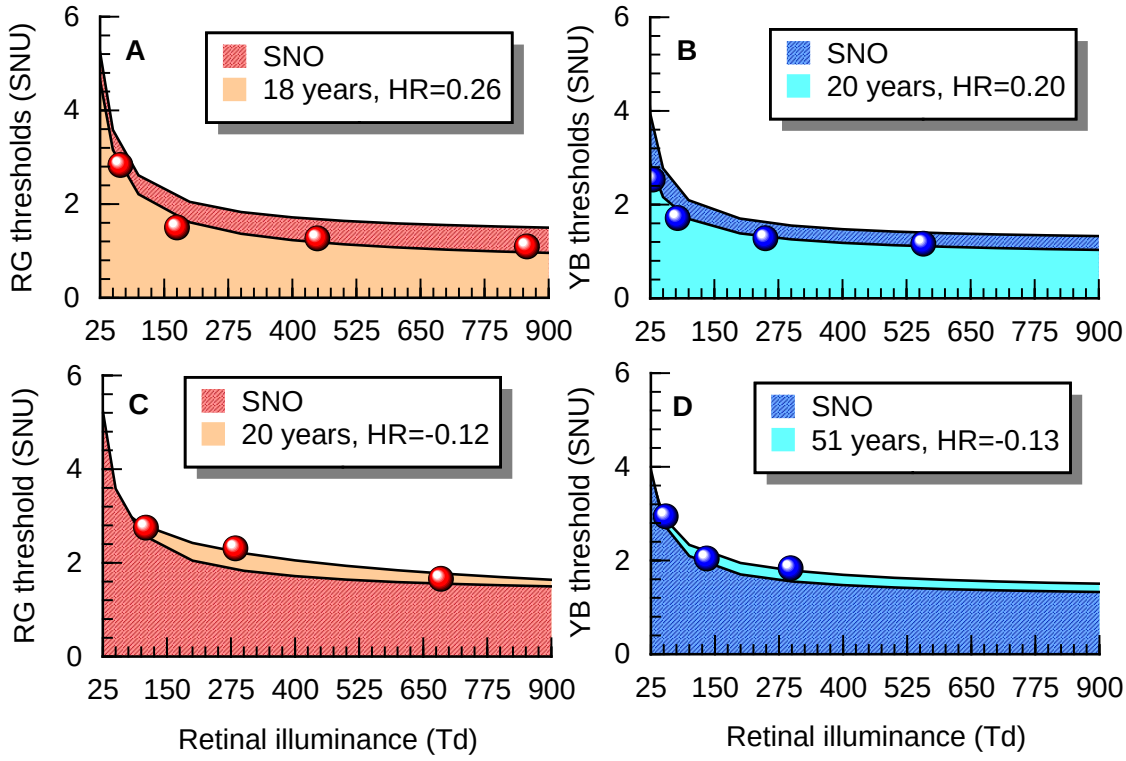

Figure 4-11: Examples of the 'areas under the curves' and the HR indices for RG and YB detection thresholds for 4 subjects with positive (A and B) and negative (C and D) HR indices.

The HR indices were computed for all subjects for RG and YB detection thresholds. The probability functions of the statistical distribution of the RG and YB HR indices of the population are shown in Figure 4-12. To set statistical limits the 95% cumulative probability (within 2.5th and 97.5th percentiles) was estimated and is shown in Table 4-4. Two subjects were lying outside the 95% limits for YB HR indices (61 and 74 years old with HR indices -1.33 and -3.16, respectively) and 1 subject for RG HR index (79 years old with HR index -1.7).

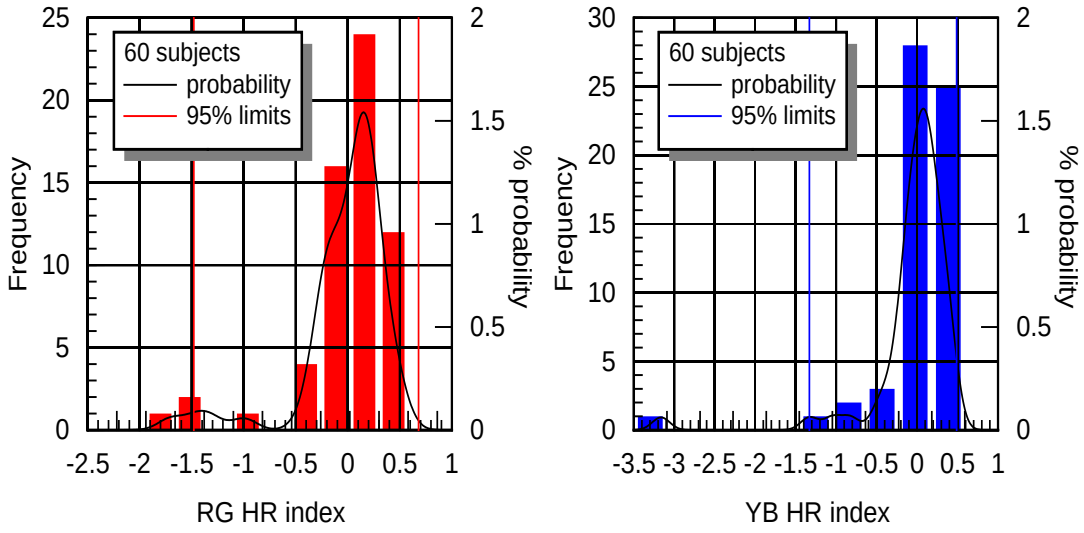

Figure 4-12: Histogram, probability functions and 95% limits of the distributions for RG (A) and YB (B) HR indices for 60 subjects (the bandwidth was set to 0.12 for the RG and 0.11 for the YB HR index probability functions and the kernel function was normal for both probability functions).

	RG HR index		YB HR index	
Cumulative probability	2.5%	97.5%	2.5%	97.5%
HR index	-1.48	0.68	-1.33	0.49

Table 4-4: The 95% limits for the RG and YB HR indices for 60 subjects.

Observation of Figure 4-12 reveals that the 3 outliers lie far from the main body of the distribution and are unlikely to be part of this population (discussed in section 5.1). These subjects were treated as outliers and excluded from further analysis. After excluding these 3 outliers the same analysis was repeated for the 57 remaining subjects using Equation 4-2 and Equation 4-3, which led to the probability functions shown in Figure 4-13 and the 95% limits shown in Table 4-5.

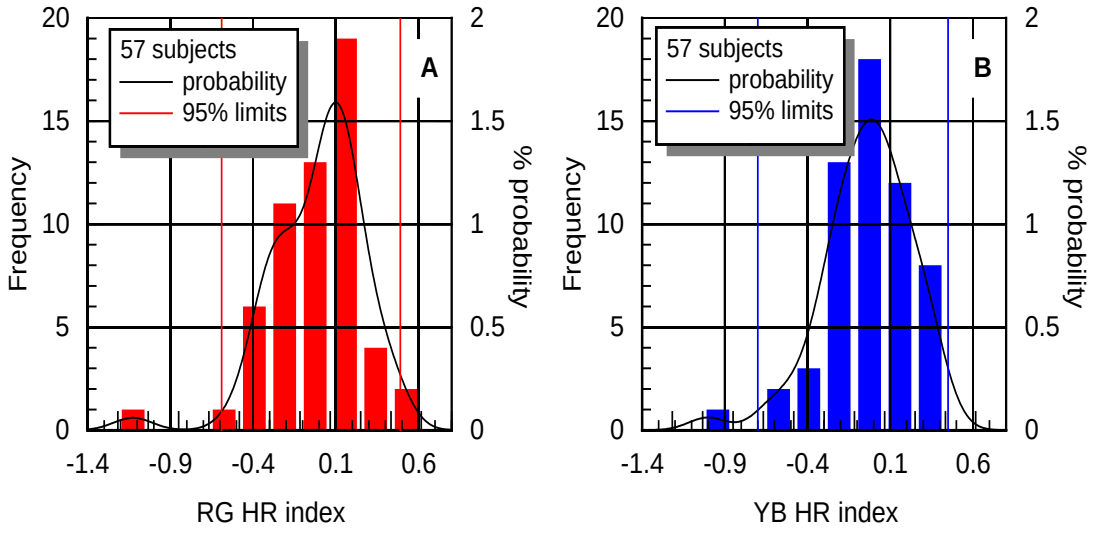

Figure 4-13: Histogram, probability functions and 95% limits of the distributions for RG (A) and YB (B) HR indices for 57 subjects (the bandwidth was set to 0.12 for the RG and 0.12 for the YB HR index probability functions and the kernel function was normal for both probability functions).

	RG HR index		YB HR index	
Cumulative probability	2.5%	97.5%	2.5%	97.5%
HR index	-0.59	0.49	-0.70	0.45

Table 4-5: The 95% limits for the RG and YB HR indices for 57 subjects.

Two more subjects were lying outside these limits, one for YB (57 year old male, HR=-1.0) and one for RG (56 year old female, HR=-1.13). Observation of Figure 4-13 reveals again that the 2 outliers lie separate to the main body of the distribution and are very likely part of a different distribution. These subjects were then excluded and the same analysis was repeated for 55 subjects.

The 5 subjects excluded following the procedures described above were also identified as outliers using Tukey's box-plot (see Appendix E). The final probability functions of the distributions of the RG and YB HR indices are shown in Figure 4-14 and the 95% limits in Table 4-6.

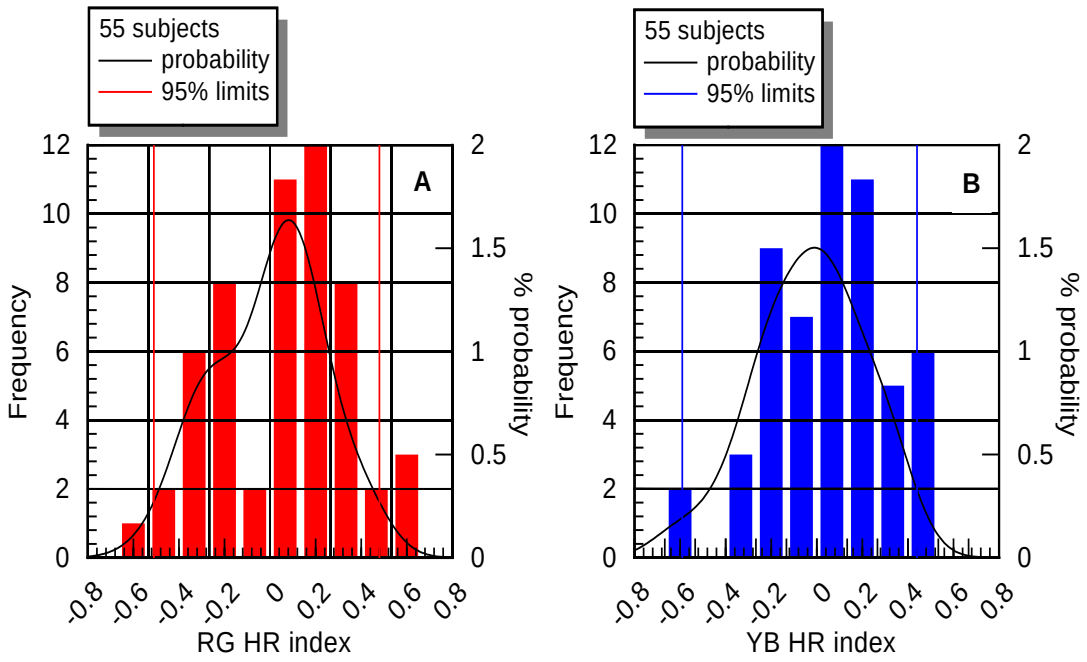

Figure 4-14: Histogram, probability functions and 95% limits of the distributions for RG (A) and YB (B) HR indices for 55 subjects (the bandwidth was set to 0.12 for the RG and 0.11 for the YB HR index probability functions and the kernel function was normal for both probability functions).

	RG HR index		YB HR index	
Cumulative probability	2.5%	97.5%	2.5%	97.5%
HR index	-0.51	0.48	-0.59	0.44

Table 4-6: The 95% limits for the RG and YB HR indices for 55 subjects.

Two subjects were identified to lie outside the 95% limits described in Table 4-6, one for YB (36 year old male, HR=-0.64) and one for RG (64 year old male, HR=-0.54). Figure 4-15 shows the final 95% limits for the RG and YB HR indices for the 60 initially recruited subjects. In total 7 outliers (11.7%) were identified; 3 subjects showed 'abnormal' RG and YB HR indices, whereas 2 subjects were outside normal limits for the RG HR index only and 2 subjects were outside normal limits for the YB HR index only. Details of the outlying subjects are shown in Table 4-7.

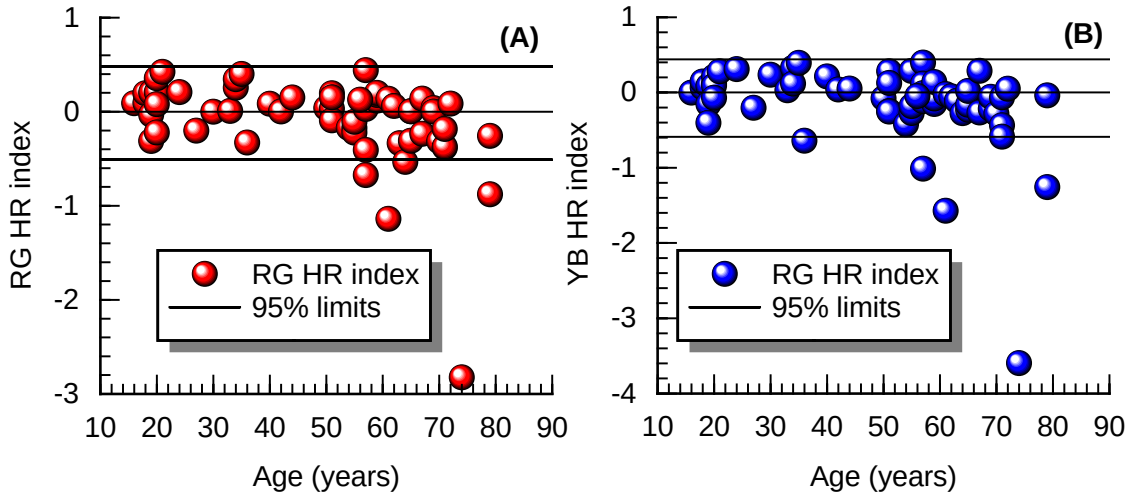

Figure 4-15: RG and YB HR indices and 95% limits (n= 60).

ID	Age	Gender	RG HR index	YB HR index
141	36	Male	-0.33	-0.64
53	56	Female	-1.17	-0.05
92	57	Male	-0.35	-1.01
186	61	Female	-1.68	-1.57
161	64	Male	-0.53	-0.28
194	74	Female	-1.52	-3.60
196	79	Female	-1.94	-1.26

Table 4-7: Details of the subjects with abnormal HR indices (n=7).

The HR indices of the 'normal' subjects varied from -0.41 to 0.44 for RG chromatic sensitivity and from -0.59 to 0.40 for YB chromatic sensitivity, for an age span of more than 6 decades. The RG and YB HR indices remained relatively unaffected by age (R^2=0.21, p=0.003 and R^2=0.17, p=0.009, respectively) (Figure 4-16).

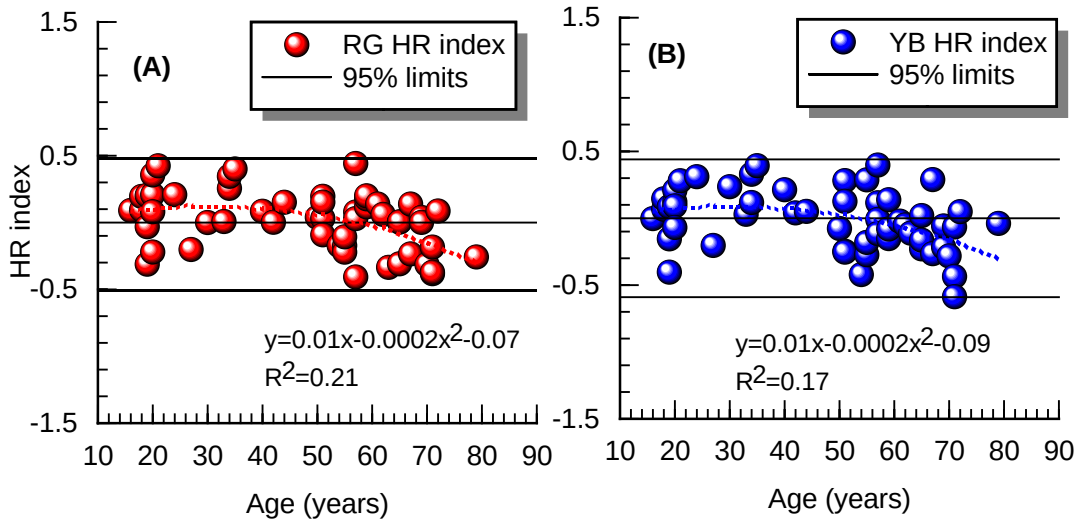

Figure 4-16: Effect of age on the RG (A) (R^2=0.21, p=0.003) and YB (B) (R^2=0.17, p=0.009) HR indices of the 'normal' subjects (n=53).

There was a significant correlation between the RG and YB HR indices for the subjects falling within normal limits (R^2=0.55, p<0.001) as shown in Figure 4-17, but less so for the 7 outlying subjects (R^2=0.23, p=0.3) (Figure 4-18).

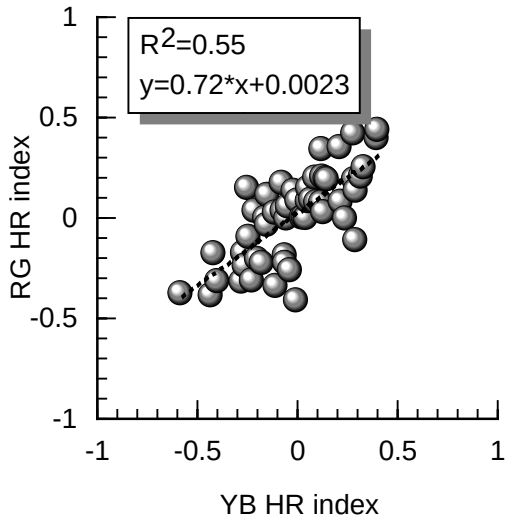

Figure 4-17: Correlation of YB and RG HR indices for 53 'normal' subjects (R^2=0.55, p<0.001).

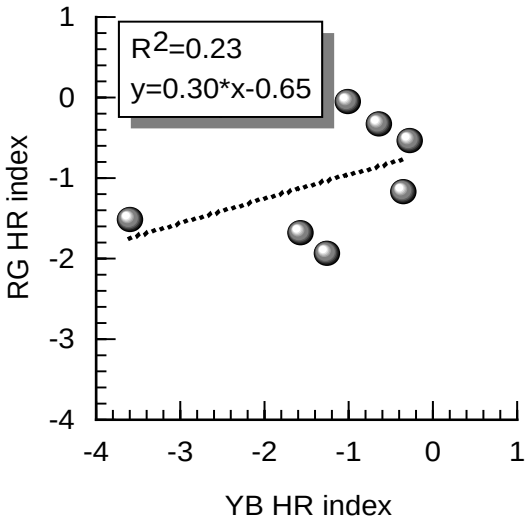

Figure 4-18: Correlation of RG and YB HR indices for the 7 subjects lying outside the normal limits (R^2=0.23, p=0.3) (n=7).

4.1.3 Effects of light level and age on chromatic sensitivity

The effect of age on chromatic sensitivity was investigated for the 53 subjects with normal colour vision, i.e. the subjects that fell within 'normal limits' for the RG and YB HR indices. To minimise the variability of the results the effects of age on the ratio of the colour detection thresholds for 900 Td and 50 Td were investigated. The aim was to examine if age affects the retina preferentially at high or low light levels. Figure 4-19 shows how age affects the RG and YB detection thresholds at 900 Td, with respect to

the thresholds at 50 Td. At the level of the retina, i.e. after controlling for retinal illuminance, there is no evident preferential effect of age on colour detection thresholds for specific light levels. On the contrary, when pre-retinal factors like the pupil and lens OD are not taken into account colour detection thresholds seem to be affected more by age at low light levels (Figure 4-20).

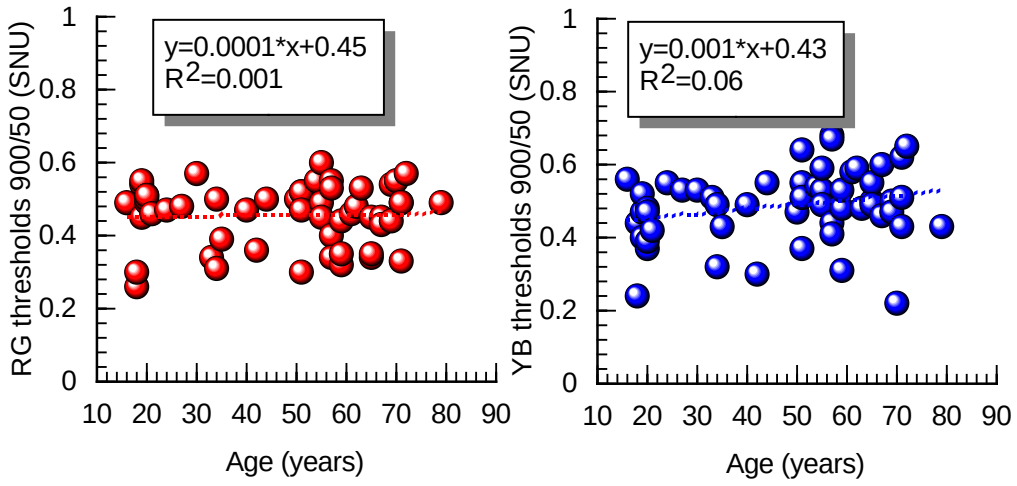

Figure 4-19: Effect of age on the ratio 900/50 Td for RG (A) and YB (B) thresholds (R^2=0.001 and R^2=0.06, p=0.8 and 0.08, respectively) (n=53).

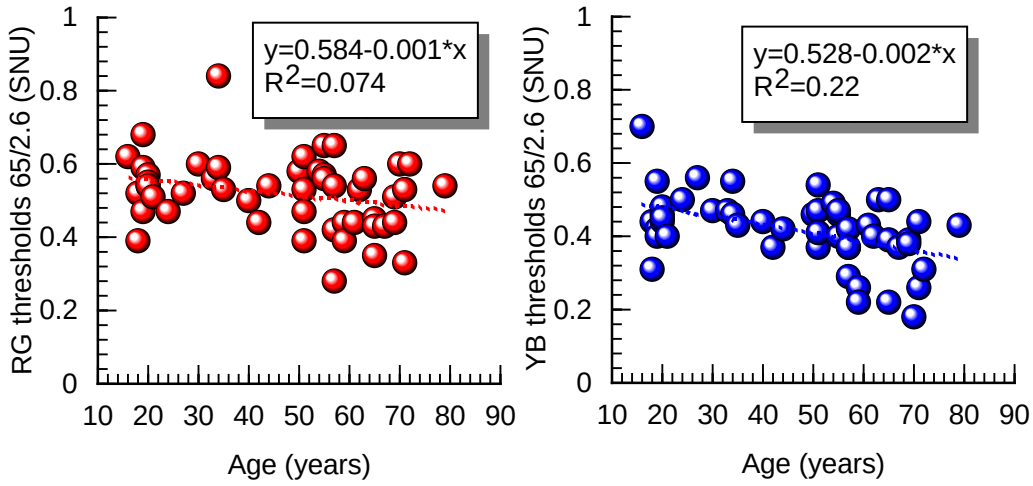

Figure 4-20: Effect of age on the ratio 65/2.6 cd·m^{-2} for RG (A) and YB (B) thresholds, without controlling for retinal illuminance (R^2=0.07 and R^2=0.02, p=0.06 and p=0.001, respectively) (n=51).

4.2 PROCESSING OF COLOUR SIGNALS IN CARRIERS OF COLOUR VISION DEFICIENCY

4.2.1 Subjects

A total of 62 participants were recruited to study the processing of colour signals in carriers of congenital colour vision deficiencies. The female carriers were divided into four groups depending on the deficiency carried: 16 carriers of deuteranomaly (cDA), six carriers of protanomaly (cPA), seven carriers of deuteranopia (cD) and seven carriers of protanopia (cP). Classification of the female carriers followed a full colour vision assessment of their offspring at the City University Colour Vision Clinics, including the Ishihara and AO-HRR plates, the City University test, the D-15, the Nagel anomaloscope and the CAD test. Males were classified as dichromats based on their Rayleigh match and RG colour detection thresholds. All dichromats recruited in this study matched 0-73 on the Nagel anomaloscope and had significantly larger RG thresholds, as measured with the CAD test. The RG colour detection thresholds measured on the CAD test correlate well with genotype classification, with dichromats producing significantly larger detection thresholds than anomalous trichromats, reaching the limits of the phosphors of the CRT monitor (Barbur et al., 2008). The CAD test also provides a classification of the subject as a protan or deutan based on the dichromatic colour confusion lines (Rodriguez-Carmona, 2006). For three DA carriers no information was available on their sons' performance on the various colour vision tests. The control group consisted of 26 normal trichromatic males. All groups had comparable ages (all $p>0.05$). The demographic characteristics of the population are

shown in Table 4-8. The t-test and the non-parametric Mann-Whitney test were employed for the investigation of differences between each group of carriers and the male trichromats; the latter was employed when the data were not normally distributed (tested with Shapiro-Wilk test).

	n	Age (mean ± SD)	p
Male controls	26	51.15 ± 14.1	
cDA (carriers of deuteranomaly)	16	54.0 ± 14.9	0.9*
cD (carriers of deuteranopia)	7	54.7 ± 7.3	0.4*
cPA (carriers of protanomaly)	6	51.0 ± 8.7	0.8*
cP (carriers of protanopia)	7	49.1± 13.0	0.7*

Table 4-8: Population demographic data (n=62) (* individual t-tests compared each group of carriers to the male controls).

4.2.2 Chromatic sensitivity

The RG chromatic sensitivities of all groups for the 4 light levels tested are shown in Figure 4-21. Carriers of DA showed reduced RG chromatic sensitivity at 26 $cd \cdot m^{-2}$ compared to trichromatic males ($p=0.015$ for 26 $cd \cdot m^{-2}$, $p>0.05$ for all other light levels), whilst the retinal illuminances of the two groups were not significantly different for any of the light levels employed ($0.25 \leq p \leq 0.59$). Carriers of D showed reduced RG chromatic sensitivity compared to male controls at 2.6 $cd \cdot m^{-2}$ ($p=0.04$, $p>0.05$ for all other light levels), whilst the retinal illuminances of the two groups were comparable for all testing conditions (all $p>0.05$). Carriers of P and PA had similar RG chromatic sensitivity and similar retinal illuminances to male controls (all $p>0.05$). The chromatic sensitivity of carriers of PA at 26 $cd \cdot m^{-2}$ correlated significantly with the Rayleigh match midpoint of their offsprings ($R^2=0.9$, $p=0.004$), but not for carriers of DA ($R^2=0.08$,

p=0.34) (Figure 4-22). The YB chromatic sensitivities were similar for all groups of carriers and normal trichromatic males at all light levels investigated (all p>0.05).

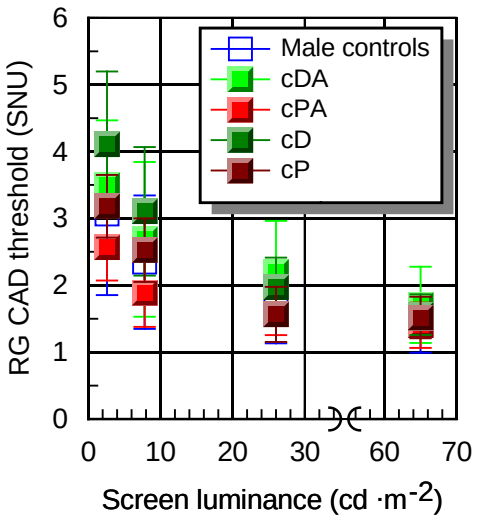

Figure 4-21: RG chromatic sensitivity of cP, cPA, cDA, cD and normal trichromatic males for the light levels investigated. Individual Mann-Whitney compared each group of carriers to the male trichromatic group. Carriers of DA had worse RG chromatic sensitivity than male trichromats at 26 cd·m^{-2} (p=0.015) and carriers of D had reduced RG chromatic sensitivity at 2.6 cd·m^{-2} (p=0.04). All groups had comparable retinal illuminances (p>0.5).

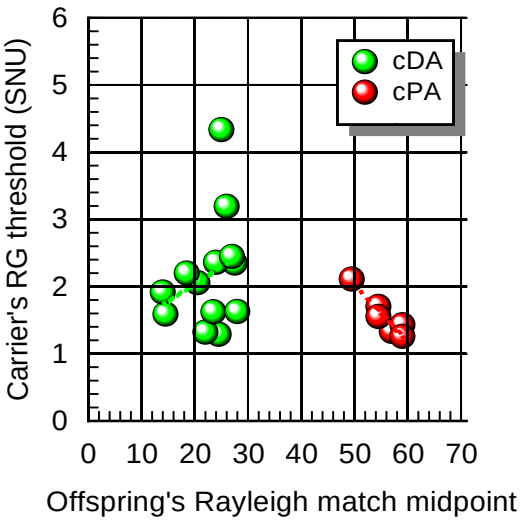

Figure 4-22: Linear correlation of RG chromatic sensitivity at 26 cd·m^{-2} for cDA (green symbols, R^2=0.08, p=0.34) and cPA (red symbols, R^2=0.9, p=0.004) with the offspring's Rayleigh match midpoint.

4.2.3 Rayleigh matches

Figure 4-23 and Table 4-9 show the Rayleigh match midpoints and matching ranges of all groups of carriers and for the male trichromats. The midpoint of the normal trichromatic group was 39.1 ± 1.4 (range 37.0 to 42.5) and the average range for the group was 3.5 (ranging from 1 to 6). The average midpoint of cDA was 38.3 ± 2.5 (ranging from 36.5 to 40.5) and was significantly different from the average midpoint of the normal trichromatic males ($p=0.04$). The Rayleigh matching ranges for cDA were not significantly different from normal trichromatic males (mean range=4.0, $p=0.41$). The average midpoint (39.1 ± 1.38; ranging from 37 to 41.5) and matching ranges (mean range=4.3, $p=0.34$) for cD were not significantly different from male controls ($p=0.77$ and $p=0.34$, respectively). The average midpoint for carriers of PA was 38.6 ± 2.5 (ranging from 36 to 43) and 37.9 ± 2.1 for cP (ranging from 34.5 to 40.0); these were not significantly different from the average midpoint of the control male group ($p=0.32$ and $p=0.36$, respectively). There was no significant difference between the matching ranges of cPA and cP and the normal trichromats (mean range=3.2 and 2.5, for cPA and cP, respectively; all $p>0.05$). No other correlations for any of the Rayleigh parameters between female carriers and their male offspring were significant for any of the groups ($p>0.05$).

	Male trichromats	cDA	cD	cPA	cP
Midpoint ± *SD*	39.1 ± 1.4	38.3 ± 2.5	39.1 ± 1.38	38.6 ± 2.5	37.9 ± 2.1
p		0.04	0.79	0.68	0.26
Range	37.0 to 42.5	36.5 to 40.5	37.0 to 41.5	36.0 to 43.0	34.5 to 40.0
p		0.41	0.21	0.75	0.25

Table 4-9: Mean Rayleigh match midpoints (± SD) and ranges of the male trichromats and each group of carriers. Individual t-tests compared each group of carriers to the male trichromatic group. Carriers of DA show significantly shifted midpoints compared to the male controls (p=0.04).

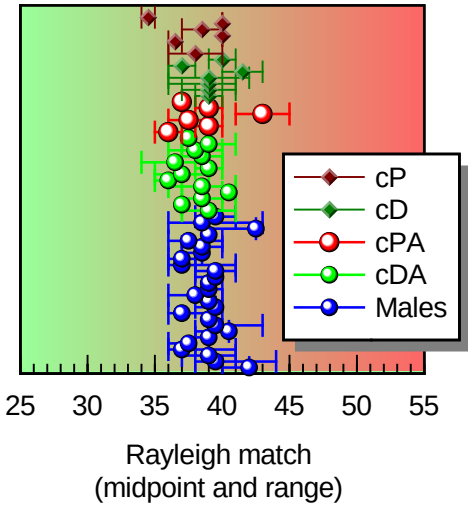

Figure 4-23: Rayleigh match-midpoints and ranges for males, cDA, cPA, cD and cP.

4.2.4 Pseudoisochromatic plates

Figure 4-24 shows the mean error scores for each group of female carriers and for normal trichromatic males. Figure 4-25 shows the percentage of subjects in each group that made at least one error on the AO-HRR and the Ishihara plates. Approximately 9% of the normal male trichromats made at least one error on the HRR

plates and 27% on the Ishihara plates. Normal trichromats made an average of 0.32 errors on the Ishihara plates, with only one subject making 2 errors. No significant differences were found between cPA and/or cP and normal trichromats for the AO-HRR ($p>0.05$) or the Ishihara plates ($p>0.05$, 33% of cPA and 16% of cP made an error). Carriers of DA performed worse than normal trichromats making significantly more errors both on the AO-HRR ($p=0.001$, mean=0.71 errors, ranging from 0 to 1) and on the Ishihara plates ($p=0.001$, mean=1.87 errors, ranging from 0 to 4) and up to 73% of cDA made errors on the pseudoisochromatic plates. Carriers of D performed significantly worse than normal trichromats on the Ishihara plates ($p=0.001$, mean= 1.29 errors, ranging from 1 to 2, 100% of cD made an error) but not on the AO-HRR plates ($p>0.05$). Approximately 50% of carriers of DA misread plate number 12 and 37.5% misread plates 9 and 17. More than 85% of the D carriers misread plate number 12 and approximately 29% misread plate 19.

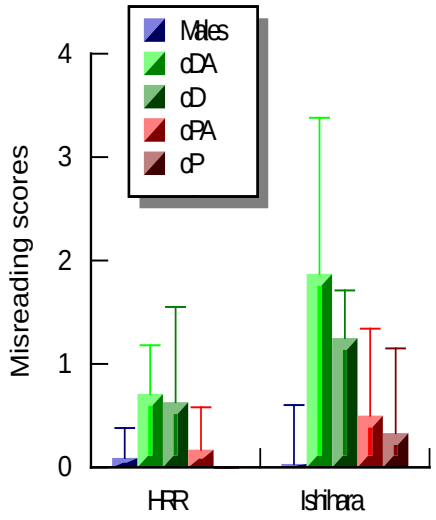

Figure 4-24: Mean error scores and SD on the HRR and Ishihara plates for each group. Individual Mann-Whitney tests compared each group of carriers to the male trichromatic group. Carriers of DA made more errors than normal controls on the Ishihara and AO-HRR plates (both p=0.001) and carriers of D performed worse than male controls on the Ishihara plates (p=0.001).

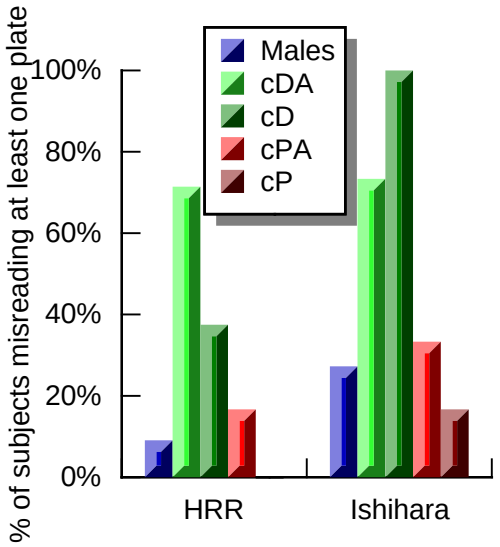

Figure 4-25: Percentage of subjects making errors on the HRR and Ishihara plates for each group.

4.2.5 Effects of retinal illuminance on chromatic sensitivity

Chromatic sensitivity was measured for each subject at 4 different background adaptation levels; the pupil diameter, the lens OD and MPOD were measured and allowed for an estimate of subject specific retinal illuminance (E) using Equation 3-6 and Equation 3-7. A non-linear function that described the increase in RG thresholds with decreasing retinal illuminance was fitted for each subject (Equation 4-1) (Figure 4-10).

Figure 4-26 shows how RG colour detection thresholds vary with retinal illuminance for normal trichromats, carriers of DA, D, PA and P. Figure 4-27 shows the mean % change in RG thresholds for each group of carriers with respect to male control group as a function of retinal illuminance. Positive changes indicate an increase in thresholds, i.e. lower chromatic sensitivity, whilst negative changes with respect to the male group indicate a decrease in colour detection thresholds and subsequently higher chromatic sensitivity. Carriers of D performed worse than males at all retinal illuminances; the effect was particularly large at lower light levels, with thresholds ~60% larger than normal males at 20 Td. Carriers of DA performed consistently worse than males for all light levels. Carriers of PA performed very similarly to normal trichromatic males, but at lower light levels carriers of PA outperformed normal trichromats with 28% lower thresholds. Carriers of P exhibited slightly larger thresholds than male trichromats over most of the range, except for the lowest retinal illuminances, when their thresholds became comparable to those measured in the male control group.

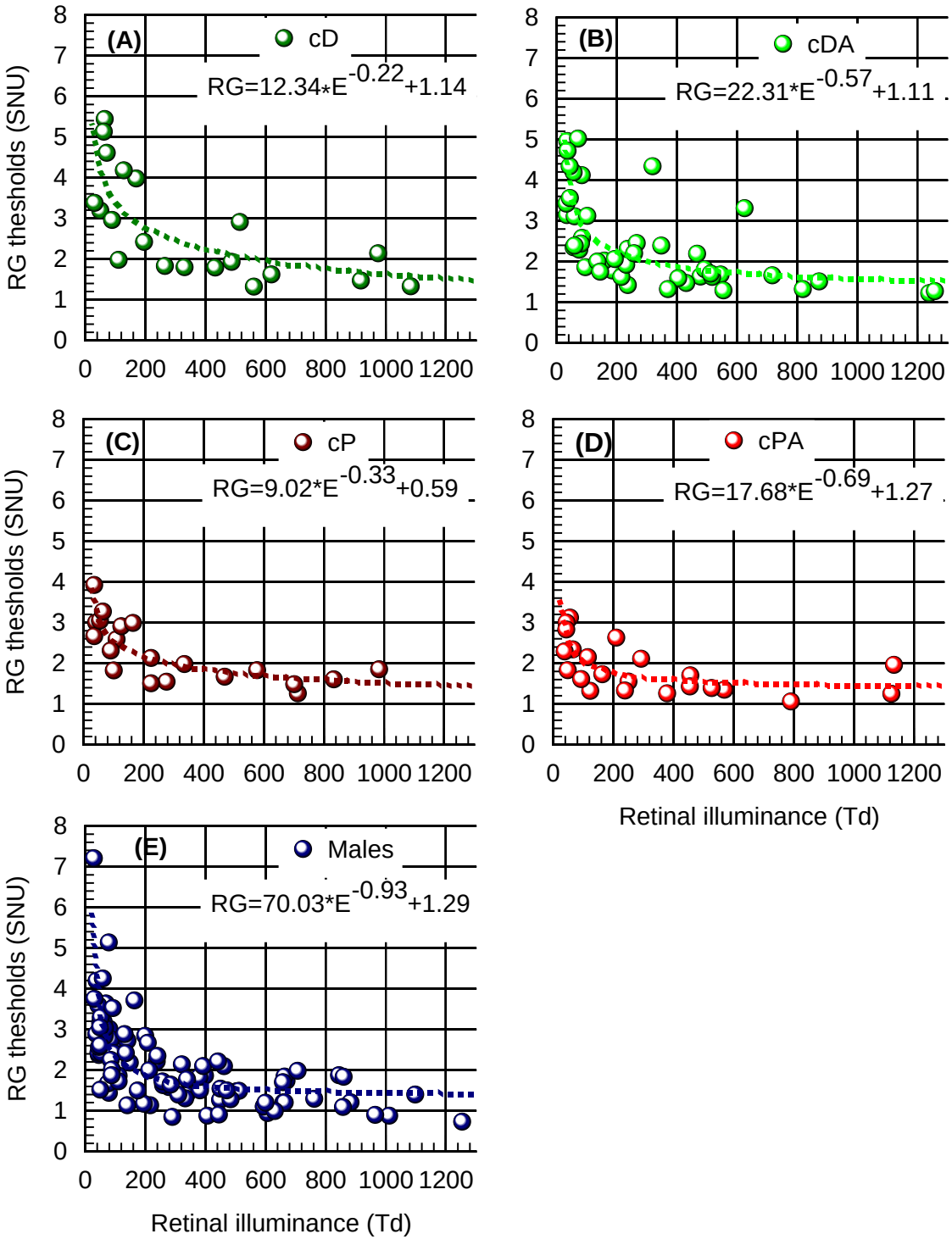

Figure 4-26: RG thresholds as a function of retinal illuminance and fitted models for cD (A), cDA (B), cP (C), cPA (D) and normal trichromatic males (E).

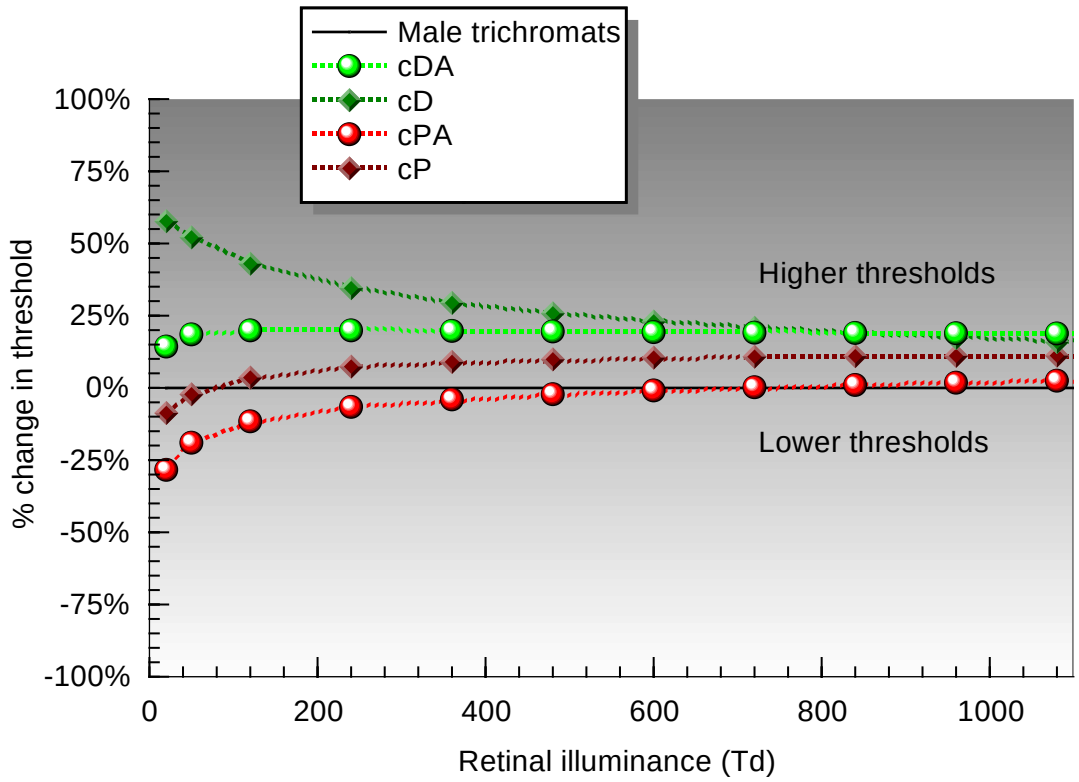

Figure 4-27: Mean % change in RG thresholds of cPA, cDA, cD and cP compared to normal trichromatic males for a range of retinal illuminances (fitted data).

5 DISCUSSION

5.1 THE EFFECTS OF AGEING ON CHROMATIC SENSITVITY

The main purpose of this study was to investigate the effects of age on chromatic sensitivity and to provide some answers to the long standing question regarding the role of pre-receptoral factors in the reduction of chromatic sensitivity with age. An important aspect of this study was to account for the key factors that affect retinal illuminance, i.e. the crystalline lens, the MP and the reduction in pupil diameter. After controlling for optical factors it was possible to assess the effects changes in receptoral and/or post-receptoral processing mechanisms have on colour vision in a population that spanned more than 6 decades.

Estimating retinal illuminance required careful measurements of pre-receptoral filters using the MAP test. The MAP test is a HFP technique that achieves measurement of the OD of the crystalline lens by utilising SW light absorption at eccentric locations, where the absorption by the MP is negligible. The MAP test does not measure the absolute absorption of the lens, but the relative change in lens OD with respect to young subjects. The use of the eccentric locations has been shown to be a valid index for lens OD (Wooten et al., 2007; Ciulla et al., 2001) and the MAP test has been shown to successfully describe the increase in lens OD with age (Barbur et al., 2010).

When measuring lens OD with broadband light the outcome depends on the spectral composition of the light used; this becomes more important when studying the effects of age on the absorption of the crystalline lens. Unless monochromatic lights are used the measured OD represents the weighted absorption of the lens for the spectral

radiance of the beam used, throughout all represented wavelengths. In the case of the MAP test the blue beam has peak radiance at 450 nm with a half maximum spectral width of ± 28 nm. The lens OD values derived from the MAP test are, therefore, indicative of the absorption of the lens for this range of wavelengths and this radiance. This may explain the noticeable differences in OD values between other studies and the estimates of the MAP test (Sample et al., 1988; Weale, 1988; Savage et al., 1993; Xu et al., 1997; Savage et al., 2001; Wooten et al., 2007). Additionally, the fact that the MAP test references the lens OD of each subject to the average young observer could lead to lower lens OD values compared to techniques that attempt a measurement of the absolute absorption by the crystalline lens.

It is of interest to compare the lens OD measures using the MAP test to previously reported measures using similar techniques. It is, however, difficult to reproduce the conditions of most of the aforementioned studies, which tended to employ monochromatic light. Apart from experimental studies, a model has been developed to predict the effects of age on the mean optical density of the ocular media (van de Kraats and van Norren, 2007). The results of the present study show a good correlation with predictions based on the van de Kraats and van Norren model (R^2=0.99, p<0.001), when the spectral transmittance functions predicted by the model are used to calculate the effective optical density of the lens for the SW beam used in the MAP test (see Figure 3-9 and Figure 4-2).

A number of different patterns of age related changes in the lens have been reported; age has been suggested to affect lens OD in a linear (Savage et al., 1993), exponential (Weale, 1988) and a bilinear manner (Pokorny et al., 1987; Hardy et al., 2005). The results presented in this study yield a non-linear increase of lens OD with age, with acceleration beyond the age of 50-60 years. It is unusual for a subject older

than 50 years of age to have a lens that is clearer than that of a younger subject. This study, however, reveals a 62-year-old phakic female, whose crystalline lens absorbs less SW light than that of the average young observer (see Figure 4-1). It is conceivable that occasionally subjects have unusually well preserved characteristics for their age. A significant increase in variability with age is evident in the lens OD estimates, illustrating that average age-adjusted lens OD estimates cannot be used for every subject (Sample et al., 1988; Hardy et al., 2005).

The optical density of the MP, an additional pre-receptoral filter absorbing SW light, was measured using the MAP test. The MAP test has some advantages over conventional optical HFP methods; the test offers variable geometry for line profile and two-dimensional measurements, sinusoidal, counter-phase modulation of the test and reference beams, a constant small modulation depth for the reference beam, background light adaptation for improved flicker sensitivity and estimates of the flicker-null point from both increments and decrements in stimulus modulation.

The average MPOD of the population investigated in this study was 0.5, similar to what has been reported before for the MAP test (Barbur et al., 2010). This average value exceeds slightly the range that has been reported by some studies (0.21 to 0.47) (Werner et al., 1987; Hammond and Caruso-Avery, 2000; Werner et al., 2000; Beatty et al., 2001; Ciulla and Hammond, 2004; Nolan et al., 2007; van der Veen et al., 2009), but is very similar to others (Hammond et al., 1997). A number of sample-related factors may have contributed to the higher mean MPOD in this study; smoking may have a damaging effect on the levels of MP (Hammond et al., 1996b), as well as race and iris colour of the subjects (Hammond et al., 1996a; Wolf-Schnurrbusch et al., 2007). The correction for peak MPOD employed in the MAP test might partly explain the aforementioned differences. In addition, the use of 4^{o} as the reference point by

some studies may underestimated the MPOD at the fixation point (Hammond and Caruso-Avery, 2000).

The findings on the dependence of MPOD on age were unexpected, as previous work with the MAP test has shown no significant effect of age from 18 to 61 years (Barbur et al., 2010). In this study the age range was extended to 79 years and the number of subjects was significantly increased, changes that undoubtedly improve the validity of the current findings. The effect, however, that age seems to have on MPOD remains of very low clinical significance given the current ambiguous role of the MP on ocular health. A similar rate of decline of the peak MPOD with age (0.01-0.02 per decade) has been considered in the past (Hammond and Caruso-Avery, 2000; Beatty et al., 2001; Ciulla and Hammond, 2004), but faster rates have been reported infrequently (Nolan et al., 2007). A decrease in the photoreceptor density with increasing age might provide some explanation for the age-related decrease of MP (Panda-Jonas et al., 1995), as the MP is located in the photoreceptor axons. The general indication is that the MPOD might undergo a small and very slow decrease with increasing age, which might explain why some studies have not reported a significant decrease (Werner et al., 1987; Hammond et al., 1997; Hammond et al., 1998; Chen et al., 2001; Barbur et al., 2010).

The average MPOD over the central 2.8^{o} remained unaffected by age. The MP is located in the layer of the fibres of Henle (Snodderly et al., 1984b) and in the inner and outer plexiform layers, where additional axons with MP are located (Trieschmann et al., 2008). The MP maximum density has been located in the fovea, but there have been interesting reports regarding the parafoveal locations and the concentration of MP. The relative sparing of foveal sensitivity in ARM could be a result of a protective role of the dense MP in the fovea and might explain why visual field defects occur

more often in the parafovea, where MP declines (Swann and Lovie-Kitchin, 1991); the topographical patterns of geographic atrophy in AMD suggest that parafoveal regions are particularly vulnerable to damage (Sarks et al., 1988). Adding to the emerging importance of the parafoveal MP levels, Chen et al. (2001) have reported a 'migration' of MP with age towards parafoveal locations. The results of this study do not suggest an increase in parafoveal MPOD, as the average MPOD at 0.8°, 1.8° and 2.8° eccentricity remained unaffected by age (all $p>0.05$) (Figure 5-1).

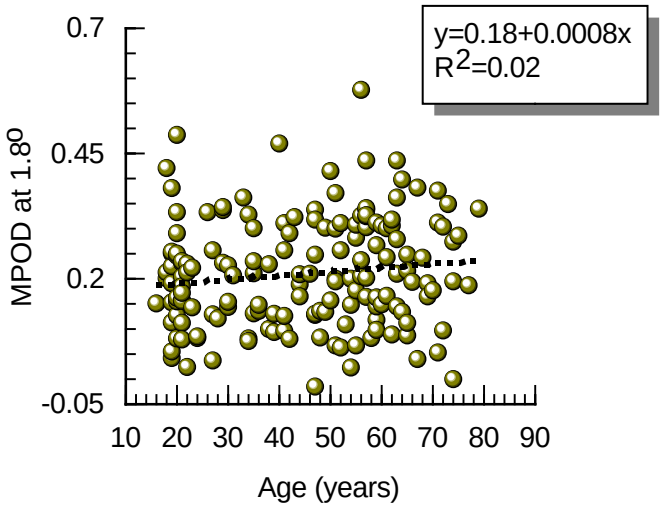

Figure 5-1: The effect of age on the MPOD at 1.8° (R^2=0.02, p=0.12).

The retinal illuminance was calculated for each subject, knowing the average absorption of SW light by the crystalline lens and the MP over the central 2.8° and the pupil diameter. The lens OD was not taken into account for the calculation of retinal illuminance in relation to RG chromatic sensitivity. The crystalline lens shows a small absorption of LW light that, like the SW absorption, increases with age (Gaillard et al., 2000; van de Kraats and van Norren, 2007). The absorption of LW light by the lens may also have a small effect when measuring cone spectral sensitivities (Werner and

Steele, 1988). Not accounting for lens OD in relation to RG chromatic sensitivity could have led to an overestimation of the retinal illuminance for the population of this study and particularly for older subjects. Given the restricted range of the SW beam used in the MAP test, which does not extend to LW light, taking the absorption of the lens into account for LW was not possible. In addition, retinal illuminance calculated in relation to YB chromatic sensitivity might have been underestimated, as the calculated retinal illuminances were specific to the light level available at SW. Retinal illuminance might have been underestimated, as more light would probably be available for somewhat longer wavelengths; although this is an obvious limitation, the S-cone responsivity function is very similar to the radiance of the SW beam of the MAP test (Figure 5-2). Since YB detection thresholds rely on S-cone signal changes, the approach adopted here is an acceptable compromise given the methodological limitations. These limitations may affect the HR index approach and will be discussed later.

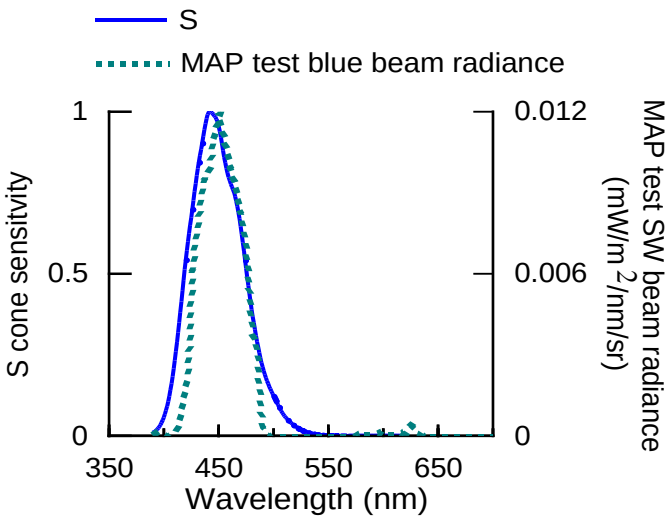

Figure 5-2: S-cone responsivity function and radiance of the SW beam of the MAP test.

After calculating retinal illuminance a model was fitted to describe the rate of change of colour detection thresholds with decreasing retinal illuminance. An empirical non-linear model was chosen, predicting the asymptotic decrease in colour detection thresholds as the retinal illuminance increases. The asymptote reflects the optimum threshold that is expected at brighter light levels. The fitted function made it possible to calculate the area under the curve, as an indication of the subject's threshold over a range of retinal illuminances. In order to assess RG and YB performance the corresponding areas under the fitted curves were calculated for the same range of retinal illuminance, i.e. 25-900 Td. This range of retinal illuminance was chosen since it represents the typical range for the population. Figure 4-8 reveals that a number of primarily young subjects had retinal illuminances beyond 900 Td in relation to RG chromatic sensitivity, but nearly no subject had retinal illuminances beyond 900 Td for YB chromatic sensitivity. On the contrary, the lowest retinal illuminance of only a few subjects was lower than 25 Td in relation to YB chromatic sensitivity.

The choice of the low integration limit was constrained by the need to have an accurate prediction of the subjects' threshold at the lowest effective retinal illuminance measured, with several values in the range 20 and 30 Td. Extending the range to e.g. 5 Td may disadvantage younger subjects, as the model would be required to predict the threshold below the measured retinal illuminance. The upper integration limit was selected as 900 Td because the rate of decrease in thresholds above this limit is very small. By excluding the highest light levels the effect is insignificant, as these measurements tend to represent the asymptotic region of the curve. The purpose of the model was to describe the rate of change in colour detection thresholds within the range of measured retinal illuminances. A higher value for the upper integration limit would over-represent the contribution of parameter T_o to the area under the subject's

curve and this in turn would reduce the relative significance of the higher thresholds measured at lower retinal illuminances. An examination of Figure 4-8 supports this approach, as above ~300 Td the data show relatively small inter-subject variability, but thresholds increase rapidly at lower retinal illuminances, with very large variability below ~125 Td.

The areas under the curves for the SNO are of particular interest. The possibility of overestimating the retinal illuminances with respect to RG chromatic sensitivity and underestimating the illuminance with respect to YB chromatic sensitivity was discussed earlier in this chapter. The final $A_{SNO\text{-}RG}$ was 1511 and the final $A_{SNO\text{-}YB}$ was 1257 (both recalculated after the exclusion of 5 outliers). Accounting for the pre-receptoral optical factors should lead to similar areas under the curve for the population. The reduced area under the curve for YB detection thresholds compared to RG may be a result of the methodological limitations in estimating the retinal illuminance. This should not, however, affect the calculation of the HR indices, as it would apply uniformly to all subjects and hence the SNO.

Having calculated the area under the curve every subject was compared to the SNO for the same range of retinal illuminances and the fractional change between two given curves was taken as the HR index. A negative HR index indicated worse performance than the SNO. In order to establish the statistical limits of the HR indices the best probability distribution function was fitted to the data. The distribution of the HR indices (RG and YB) did not fit well by any of the most commonly used statistical distributions. A non-parametric function was then fitted to describe the population specific distribution of HR indices, revealing some immediate outliers.

Other studies have shown that a number of factors can cause a spread in colour detection thresholds. The RG detection thresholds of normal trichromats and

congenitally colour deficient subjects form distinct, non-overlapping distributions (Rodriguez-Carmona, 2006). Retinal disease can also significantly affect colour detection thresholds as measured with the CAD test and subjects suffering from diabetes or AMD show noticeably larger thresholds than healthy individuals (O'Neill-Biba et al., 2010). Retinal disease, like glaucoma, can develop sub-clinically for some time before being clinically visible (Quigley and Addicks, 1982; Harwerth et al., 1999; Kerrigan-Baumrind et al., 2000) and data from our lab suggest that colour detection thresholds can be significantly affected before the clinical demonstration of retinal diseases (Figure 5-3). Defining an outlier can be a subjective approach that has to be made on an individual basis, taking into account the nature of the specific type of measurements.

The subjects that fell outside the 95% limits for the HR indices were excluded; these subjects lay far from the main body of the distribution (see Figure 4-12 and Figure 4-13) and it was considered probable that these outliers belonged to a different, unknown distribution. After excluding 5 outliers the SNO and the HR indices were recalculated and the 95% limits were reset, identifying 2 additional outliers. Observation of Figure 4-14 reveals that these subjects form the extreme ends of a continuous distribution, depicting the reduced probability of such extreme values. The exclusion process was, therefore, not taken any further.

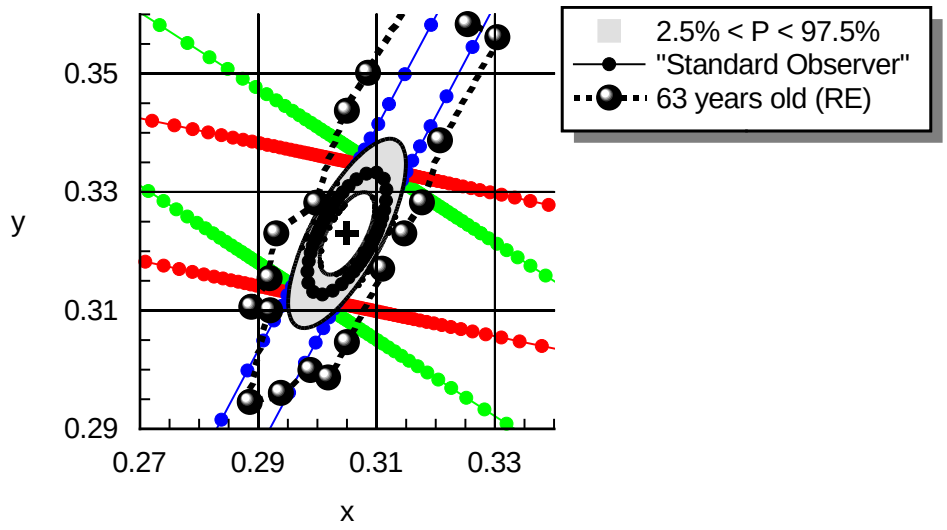

Figure 5-3: Colour detection thresholds for the right eye of a 63-year-old subject with no clinically visible retinal abnormalities. The subject developed AMD 4 years after the colour vision assessment.

The final RG and YB HR index limits are -0.51 to 0.48 and -0.59 to 0.44, respectively (Table 4-6). The limits seem to be symmetrical for the higher and lower ends for both RG and YB HR indices, with the YB HR indices shifted to slightly lower values for both the higher and lower limits. One interesting observation is related to the shape of the statistical distributions of the RG HR indices (see Figure 4-14); the distribution of the RG indices exhibits signs of bimodality, an observation which remains to be tested statistically (Silverman, 1981).

There are two possible explanations for this finding. Certain types of congenital colour vision deficiency cause significantly increased RG detection thresholds when carried by heterozygote females (section 4.2.2). If the female population happened to include carriers that were not aware of carrying such a gene it could have shifted the results towards lower RG HR index values. In this study we made every effort to exclude female carriers of colour vision deficiency; there is, however, always the possibility that carriers were part of this population. Another possible explanation is related to the

health of the participants. Approximately 20% of our subjects were taking medication to control high blood pressure and high cholesterol levels; this is lower than what has been reported for the UK population (see section 3.1). Every effort was made not to include subjects that were taking medication proven to affect colour vision (Lawrenson et al., 2002), but it is possible that some drugs may affect RG detection thresholds. It is also possible that high blood pressure and/or cholesterol levels affect RG colour detection thresholds, but conclusions cannot be drawn from this study. Given the fact that the population of this study reflects a random sample of the current ageing population in the UK, hence of the incidence of these two conditions, the specific patterns of the RG HR indices might have to be accepted in this form. A larger sample size would provide more information and would also be more indicative of subgroups within the population.

The symmetry between RG and YB HR indices reveals that RG and YB chromatic sensitivities are affected in a similar way by age. This is also supported by Figure 4-16, where, after excluding the 7 outliers, age seems to have a similar effect on the HR indices for RG and YB chromatic sensitivity. Further support is provided by the correlation of the RG and YB HR indices for the 53 normal subjects. The limits of the HR index reveal a 3 fold change in sensitivity between the lower and higher limits for RG and a 3.6 fold change for YB chromatic sensitivity. This is higher than what has been reported for the CAD test for single light level binocular measurements for a younger population (Rodriguez-Carmona, 2006). The monocular measurements, the extension of the age range and the addition of lower light levels might explain this difference. As an overall measure of chromatic sensitivity over a range of light levels in the high mesopic and the photopic range, the computed variation in chromatic sensitivity is relatively small.

The RG and YB colour processing channels were not always assumed to age simultaneously, with the YB channel believed to age faster. Results on various colour vision tests have shown generalised worsening of colour vision with increasing age (Verriest et al., 1982; Knoblauch et al., 1987; Shinomori et al., 2001), but losses along the tritan axis have been larger, occurred earlier in life and progressed faster compared to other chromatic axes (Verriest, 1963; Knoblauch et al., 1987; Haegerstrom-Portnoy, 1988; Shinomori et al., 2001). The preferential ageing apparent for the tritan axis has been attributed to the crystalline lens, its progressive yellowing with increasing age and the subsequent selective filtering of SW light by some studies (Knoblauch et al., 1987; Nguyen-Tri et al., 2003) but not by others (Beirne et al., 2008). The methods employed to measure RG and YB chromatic sensitivity may have affected the outcome.

The discrepancy between studies regarding the ascription of colour vision loss with age to the yellowing of the crystalline lens supports that a neural mechanism may also be involved. Studies on the efficiency of the human trichromatic system reveal that neural mechanisms also change with age. Senile photoreceptor changes have been reported in relation to cone density (Keunen et al., 1987; Panda-Jonas et al., 1995), cone quantal catch (Schefrin et al., 1992), photopigment density (Kilbride et al., 1986; Elsner et al., 1988; Elsner et al., 1998) and the morphology of the cone outer segments (Marshall, 1978). Approximately 40% of the S cones' sensitivity loss has been ascribed to light losses within the ocular media, with only the remaining loss attributable to receptoral and/or post-receptoral changes (Werner and Steele, 1988). On a retinal level the sensitivities the S cones go through continuous deterioration with increasing age, pointing to receptoral and/or post-receptoral factors (Haegerstrom-Portnoy, 1988; Johnson et al., 1988; Schefrin et al., 1992; Werner et al., 2000). At the

retinal level the sensitivities of the M and L cones also seem to decrease with age (Johnson et al., 1988; Werner and Steele, 1988; Werner et al., 2000).

This study demonstrates that after controlling for the variation in retinal illuminance by measuring lens OD, MPOD and pupil diameter, age has a small effect on the retinal and/or post-retinal neural mechanisms, as assessed by the HR index. A 75-year-old subject can, therefore, match the colour vision performance of a 20-year-old subject, provided retinal illuminance is adjusted for pupil size and additionally for pre-receptoral absorption of light by the lens and the MP in the case of YB chromatic sensitivity. The results of this study suggest that only ~20% of the variation can be explained by age for both RG and YB HR indices (see Figure 4-16). Previous studies attributed ~30% of the measured variation to age (Haegerstrom-Portnoy, 1988; Johnson et al., 1988; Werner and Steele, 1988; Schefrin et al., 1992; Werner et al., 2000).

The pupil diameter and the MP have not been accounted for in some of the aforementioned studies. Pupil diameter has been regarded less significant, as in sufficiently high luminances a smaller pupil will affect the test and the background equally and hence the same sensitivity will be obtained regardless of pupil size (Adams et al., 1987). Equally, since MP may not change throughout lifespan (Bone et al., 1988), it has not been regarded as an age dependant factor. Both of these factors, however, reduce the amount of light reaching the retina. Observation of Figure 4-8 reveals that the reduction of retinal illuminance might not be affecting chromatic sensitivity significantly at high light levels, but further reduction of low retinal illuminances can cause significant increases in colour detection thresholds.

The HR index can also be applied to congenitally colour deficient observers. The correlation between RG and YB detection thresholds for normal trichromatic observers allows the estimation of the RG thresholds of any observer (see Appendix F). This is

only possible if the YB HR index falls within normal limits, i.e. if the subject shows no signs of acquired YB colour vision deficiency. The difference between the modelled RG thresholds at the highest light levels tested, i.e. 65 $cd \cdot m^{-2}$, and the measured threshold at the same light level for a colour deficient subject can be ascribed to the congenital deficiency and can be subtracted from the subject's thresholds. The HR index can be calculated if one assumes that the subject can achieve the computed RG threshold, if his cone pigments were 'normal'. Figure 5-4 shows how the correction for colour vision deficiency is applied to the HR index. This 28-year-old subject shows the same pattern of colour vision loss with decreasing retinal illuminance as normal trichromats, but his asymptotic threshold is significantly higher, as a result of mild deuteranomaly. When the difference of the asymptotic thresholds is corrected and the deficiency is taken into account the subject has an HR index that falls within normal limits (HR index = -0.1).

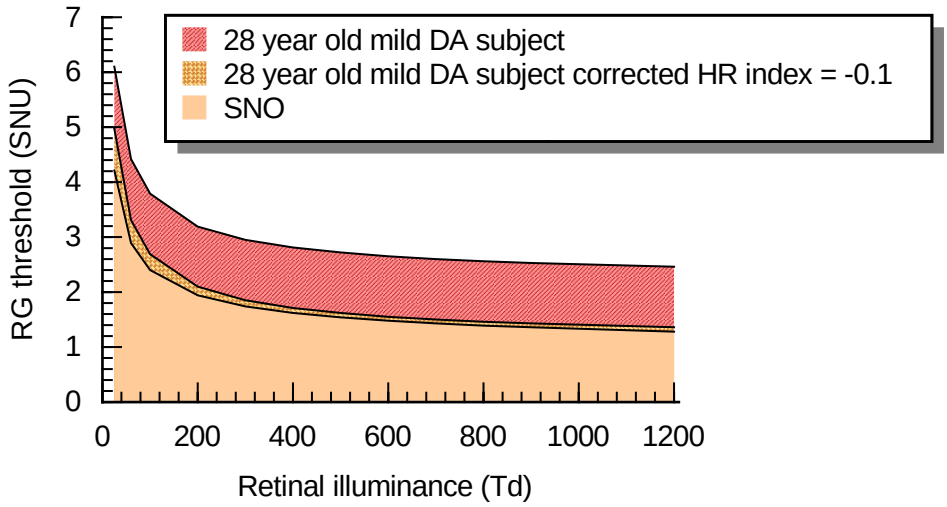

Figure 5-4: Calculation of the HR index of a mild DA subject. Provided that the YB HR index is within normal limits the RG asymptotic threshold can be adjusted based on the correlation between RG and YB detection thresholds for the 'normal' population. The difference (in this case 1.10 SNU) is then subtracted from the detection thresholds for each light level (see also Appendix F).

The HR index improves until approximately 35 years of age, decreasing subsequently in older ages. Non-linear effects on chromatic sensitivity have been reported previously; Knobblauch et al. (2001) have reported that chromatic sensitivity is likely to improve as one gets older until approximately adolescence and then deteriorate beyond adulthood, but that the age for best chromatic sensitivity (or in this case the highest HR index) can vary depending on the fitted function. In this study the HR indices for RG and YB peak between 30-40 years of age, which is somewhat higher than what has been previously reported (Knoblauch et al., 2001). This is in agreement with the smallest individual detection thresholds for individual light levels (see Figure 4-7). A number of non physiological factors may affect the age range for peak sensitivity. This study confirms that age does not affect chromatic sensitivity in a linear way.

This study supports the view that the major causes of reduction of chromatic sensitivity with age are the pre-receptoral factors. Often, a subject's retinal illuminance can mask the true retinal function. Figure 5-5 shows an example of a subject that would normally be considered to have borderline YB chromatic sensitivity. The YB threshold at 26 $cd \cdot m^{-2}$ is the highest for the group of 53 normal subjects, but the HR index is well within the normal limits. Similarly, Figure 5-6 shows a 65-year-old subject, where, although the threshold at 26 $cd \cdot m^{-2}$ is the 3rd highest of the group, the HR index is only 0.02, i.e. better than some younger subjects. In contrast, the 36-year-old subject shown in Figure 5-7 has only a threshold difference of 0.42 SNU when compared to the 65-year-old subject mentioned above, but has an abnormal HR index. This is because the reduction in retinal illuminance was not sufficient to account for the increase of the YB detection thresholds.

Such a detailed interpretation of chromatic sensitivity data would not have been possible without the information about retinal illuminance. Information about retinal illuminance on a single light level is, however, still not adequate for classification. Figure 5-8 shows a 70 year old subject with a profound increase in YB thresholds at the lowest light level tested, i.e. at 2.6 $cd \cdot m^{-2}$. An examination of the subject's HR index reveals a negative value, but within normal limits. Assessment of that subject at only one light level would not allow a classification, as the YB threshold at 65 $cd \cdot m^{-2}$ is well within the expected range, irrespectively of the subject's age.

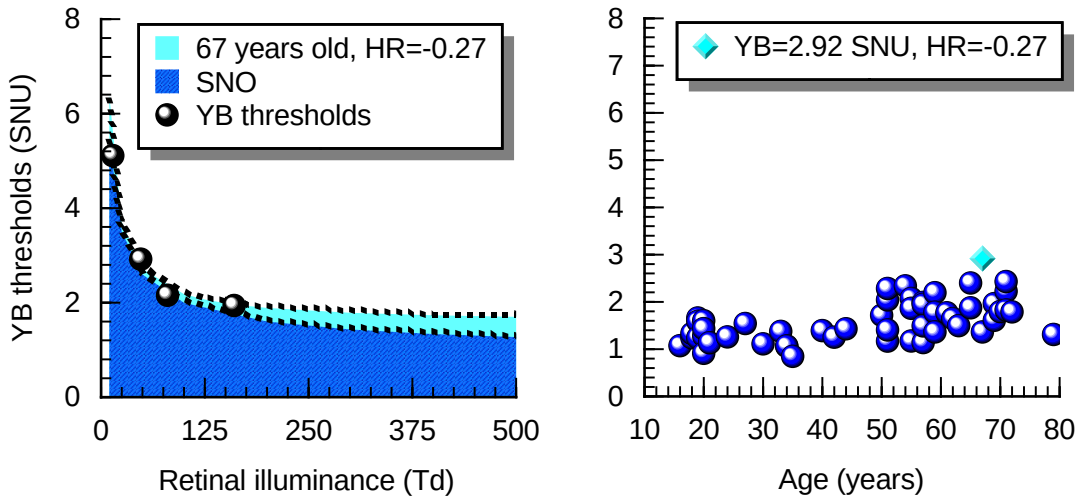

Figure 5-5: A 67-year-old subject with the highest YB threshold at 26 cd·m^{-2}, but an HR index within normal limits.

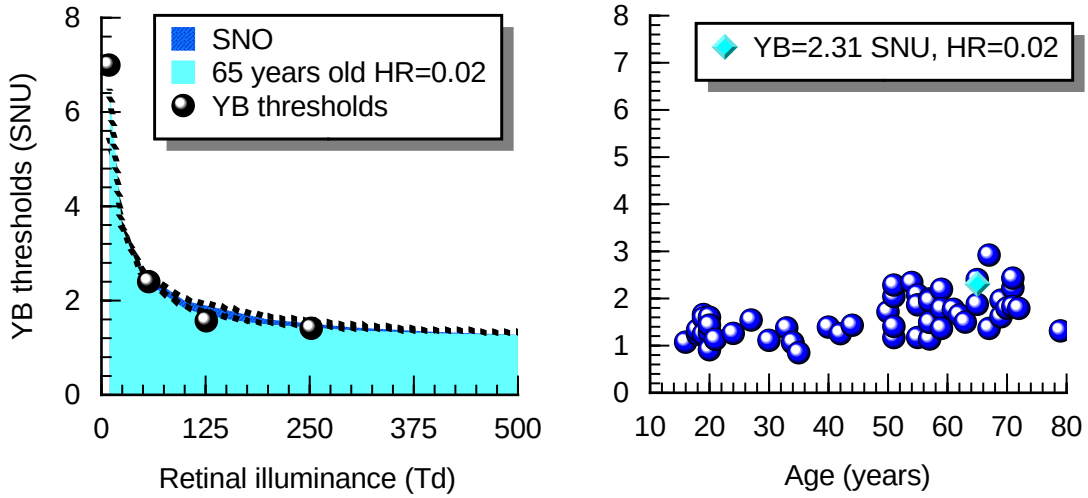

Figure 5-6: A 65-year-old subject with the 3rd highest YB threshold at 26 cd·m^{-2} and a normal HR index.

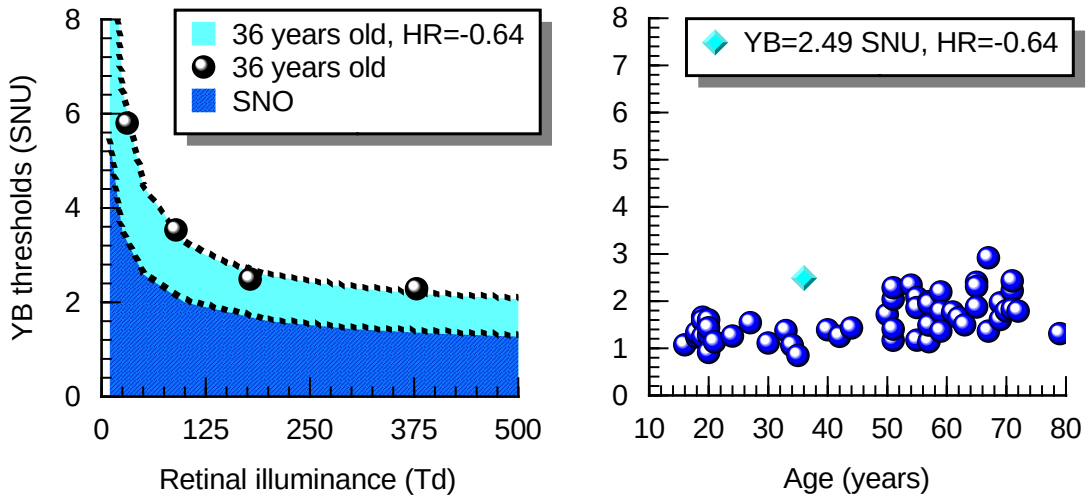

Figure 5-7: A 36-year-old subject with an abnormal HR index.

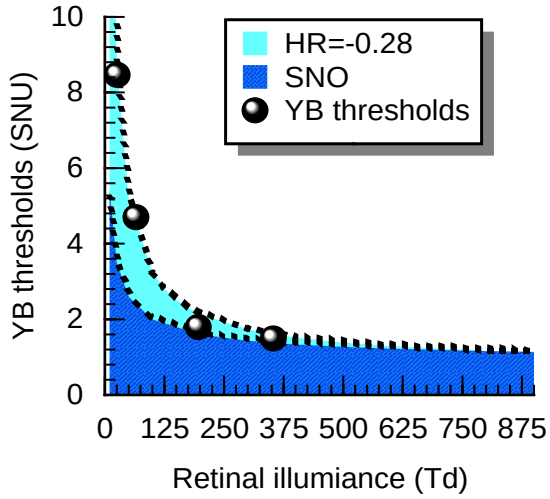

Figure 5-8: A 70-year-old subject with a YB HR index within normal limits, but an acceleration of the rate of change of colour detection thresholds with decreasing retinal illuminance.

Worsening of colour vision in older subjects has also been shown to be dependent on light level. Differences in visual performance between young and old observers are greatest at lower light levels (Knoblauch et al., 1987; Schefrin et al., 1992; Schefrin et al., 1995; Kraft and Werner, 1999) or, conversely, considerably smaller at higher light

levels. The results reported in this study suggest that age does not normally cause a preferential loss in chromatic sensitivity at lower retinal illuminances. When retinal illuminance is, however, not corrected for age-dependent factors, colour detection thresholds at 2.6 $cd \cdot m^{-2}$ seem to increase at a faster rate compared to detection thresholds measured at 65 $cd \cdot m^{-2}$. This is an artefact, as the effective retinal illuminance in older subjects is much lower when measured at 2.6 $cd \cdot m^{-2}$ compared to young subjects. At 65 $cd \cdot m^{-2}$ the pupil size tends to be smaller even in young subjects and the measured thresholds are less dependent on age, as the effective retinal illuminance is sufficient for most subjects to reach the asymptotic threshold.

It is known that early stages of retinal disease demonstrate a reduced visual function at lower light levels (Owsley et al., 2000; Owsley et al., 2001) and it is generally accepted that colour vision is a sensitive indicator of retinal disease. Diseases of the retina have been shown to affect chromatic sensitivity (Pacheco-Cutillas et al., 1999; Feitosa-Santana et al., 2010; O'Neill-Biba et al., 2010) and colour vision loss may precede visual acuity loss in ARM (Applegate et al., 1987). Additionally, subjects suffering from diabetes (either type I or type II) show reduced chromatic sensitivity in the absence of retinopathy (Hardy et al., 1992; Feitosa-Santana et al., 2010). The rapid increase of the YB thresholds of the 70-year-old subject with reduced light level (Figure 5-8) is of interest. It is possible that similar patterns of colour vision loss with reducing retinal illuminance might be linked to the earliest demonstration of the development of sub-clinical retinal disease, although no definite conclusions can be drawn from this study. Lower light levels impose higher metabolic demands on photoreceptors and the inability of the cones or rods to meet these metabolic expectations might be linked to the development of disease (Barbur and Connolly, 2011; Feigl et al., 2011). One can speculate that as the potential retinal disease

progresses the detection thresholds may be affected over a wider range of retinal illuminances, leading to an abnormal HR index.

Of the 60 subjects initially recruited, 11.7% (7 subjects) fell outside the normal limits; 3 subjects had abnormal HR indices for both RG and YB, whilst 2 subjects showed preferential loss for RG and 2 subjects for YB chromatic sensitivity. Surprisingly, a 36-year-old male was also identified as an outlier for YB chromatic sensitivity. For these subjects RG and YB HR indices did not show a strong correlation. This observation could in principle be related to developing disease that affects primarily either RG or YB chromatic mechanisms. It has been reported that various retinal pathologies have different effects on colour vision, depending on the retinal site affected. Traditionally, RG acquired defects have been associated with cone dystrophies and toxic neuropathy, among other pathologies, and YB defects are considered more common in peripheral retinal lesions or macular disorders (Birch, 2001). Assessment of chromatic sensitivity has revealed that AMD might preferentially affect YB detection thresholds in contrast to type II diabetes; the latter seems to affect RG and YB thresholds similarly (O'Neill-Biba et al., 2010). The existing findings cannot be used to determine whether the lack of correlation is linked to the development of disease. It is, however, suggested that the simultaneous ageing of the RG and YB colour processing channels is the expected effect of senescence on normal individuals and that any deviations from this pattern warrant further investigation.

Other visual functions could also be used as potential indicators of retinal disease. Mesopic flicker sensitivity is reduced in subjects carrying high-risk phenotypes for the development of AMD (Feigl et al., 2011) in the absence of clinical signs of the disease. Up to 69% of the middle aged population might carry high risk phenotypes for the development of AMD. This percentage is significantly higher than the 11% of the

outliers with reduced chromatic sensitivity identified in this study. The fact that carriers of high risk phenotypes show preferential reduction in mesopic visual function illustrates the potential advantage of being able to detect pre-clinical signs of developing retinal diseases. The minority of subjects that show loss of visual function in the absence of clinical abnormalities might be worth further longitudinal investigation.

5.2 PROCESSING OF COLOUR SIGNALS IN CARRIERS OF COLOUR VISION DEFICIENCY

This study investigated the chromatic sensitivity of female carriers of RG colour vision deficiency. Female carriers were divided into four groups depending on the deficiency involved and were compared to normal trichromatic male controls. The classification of the female carriers was not based on sequencing, but followed a full colour vision assessment of their offspring, including the CAD test and the Nagel anomaloscope. Although a more detailed classification would be provided by genotyping, the Rayleigh match has been frequently used to distinguish anomalous trichromats form dichromats (Franceschetti, 1928; Neitz et al., 1996), as well as a classification tool for carriers of colour vision deficiency (Jordan and Mollon, 1993; Hood et al., 2006). Female subjects were not included in the normal control group to avoid contamination by undetected heterozygous carriers. All groups had comparable age ranges and any differences in chromatic sensitivity cannot be attributed to ageing effects.

Cone pigments can exhibit large variability in the wavelength of peak spectral responsivity, with a large number of L and M pigment variants amongst normal

trichromats (Neitz et al., 1993). These variants may cause only minimal changes in RG Rayleigh matches (Neitz et al., 1991; Nathans et al., 1992). The normal male retina can often have more than two X-linked cone pigments, with two variant L pigments being the most common outcome (Neitz and Neitz, 1995). Most commonly the serine-containing L-cone pigment is red-shifted by ~ 2.7 nm with respect to the alanine-containing one (Sharpe et al., 1999). It has been shown that ~10 nm separations in deutan colour deficient subjects can yield RG detection thresholds that are, under optimum conditions, only twice as large as the standard normal threshold (Neitz et al., 1996; Rodriguez-Carmona et al., 2008). A measure of RG chromatic sensitivity based on the Nagel anomaloscope matching range can yield almost 90% of the normal RG chromatic sensitivity for the same 10 nm separation (Barbur et al., 2008). Normal cone pigment variations are therefore unlikely to produce measurable differences in RG colour discrimination among normal trichromats and may only affect the measured variability of normal trichromatic colour vision (Rodriguez-Carmona et al., 2005).

Many female non carriers could also express two variant L pigments. The expression of more than two X linked cone pigments in female subjects is unlikely to have a significant effect on the interpretation of the results of this study. The expression of more than two pigments in non carrier females has not resulted in any measurable colour vision differences between males and females in a number of previous studies (Pickford, 1947; Costa et al., 2006; Hood et al., 2006). Significant differences were found between the RG chromatic sensitivity of male and female subjects, without excluding female carriers (Rodriguez-Carmona et al., 2008). This study has shown that after excluding possible heterozygous female carriers any differences became insignificant. It is therefore extremely unlikely that normal variability in cone pigments, as expressed in random populations assessed in earlier studies (Pickford, 1947; Costa

et al., 2006; Hood et al., 2006; Rodriguez-Carmona et al., 2008) and possibly also present in our male and/or female populations, can have a significant effect on the current findings.

Carriers of DA and D performed significantly worse than males on the Ishihara plates, with a greater number of carriers making more errors; carriers of DA also performed worse on the AO-HRR plates. These findings confirm earlier reports on the inferior performance of deutan carriers on pseudoisochromatic plates (Waaler, 1927; Crone, 1959; Jordan and Mollon, 1993). The error scores reported here are similar to those reported before (Jordan and Mollon, 1993), but none of the carriers of this study made more than 4 errors on the Ishihara plates, despite the monocular administration of the tests. Carriers of DA and D showed different patterns of errors on the Ishihara plates. Nearly 44% of the DA carriers misread plate number 12 as ‘87’ and 37.5% misread plate number 9 as either ‘71’ or ‘21’, a finding that has also been reported in previous studies (Jordan and Mollon, 1993); 85% of carriers of D misread plate number 12 as ‘87’. These observations may reveal the underlying differences in the processing of the colour signals between carriers of DA and D, which will be examined further. The poorest performance of the deutan carriers in the pseudoisochromatic plates is also reflected in their significantly larger RG CAD thresholds, although RG detection thresholds and Ishihara error scores exhibit very poor correlation (Rodriguez-Carmona et al., 2011).

Carriers of PA and P did not show any significant differences in RG chromatic sensitivity when compared to normal trichromatic males, a finding that is consistent with reports from other studies (Verriest, 1972; Hood et al., 2006). The good performance of protan carriers cannot be attributed to the use of luminance cues (Verriest, 1972), since the CAD test makes use of achromatic dynamic luminance

contrast noise to mask the use of luminance signals, even in the most severe colour deficient subjects (Rodriguez-Carmona et al., 2005). The carriers of P and PA produced RG thresholds that were very similar to male controls under all lighting conditions (2.6, 7.8, 26 and 65 $cd \cdot m^{-2}$), even for the lowest light level employed where the signal-to-noise ratio is reduced significantly (Walkey et al., 2001).

Carriers of DA had significantly higher RG thresholds at normal photopic light levels (26 $cd \cdot m^{-2}$) when compared to the male control group, with no significant difference in retinal illuminance. Carriers of D exhibited RG thresholds that were comparable to the male group at 26 $cd \cdot m^{-2}$, but significantly lower RG chromatic sensitivity at the lowest light level tested (2.6 $cd \cdot m^{-2}$), in spite of similar retinal illuminances. Given the similar retinal illuminances between all groups, any observed differences are likely to reflect the variations in the receptoral and/or post-receptoral processing of colour signals.

The poorer chromatic sensitivity observed in deutan carriers has been attributed to the more extreme L:M ratios of these females (Hood et al., 2006). Subsequently, the good performance of protan carriers (carriers of P and PA combined) was attributed to the more equal relative numbers of L and M cones. According to X-inactivation the retinas of carriers of DA have four cone pigments expressed (Nagy et al., 1981), as shown schematically in Figure 5-9B (L' is a variant L photopigment expressed in DA carriers). In contrast, carriers of D would have only three photopigments expressed (S, M and L), but their M cone spatial density would be reduced significantly. The poor performance of all deutan carriers could be attributed to more extreme L:M ratios, but this explanation implies that all signals originating from L' cones in DA carriers are 'recognised' and hence pooled with normal L cone signals; similarly, signals originating from variant M' cones in PA carriers should be pooled with normal M cone signals. The

findings from this study are, however, not consistent with this hypothesis and require a fundamentally different interpretation.

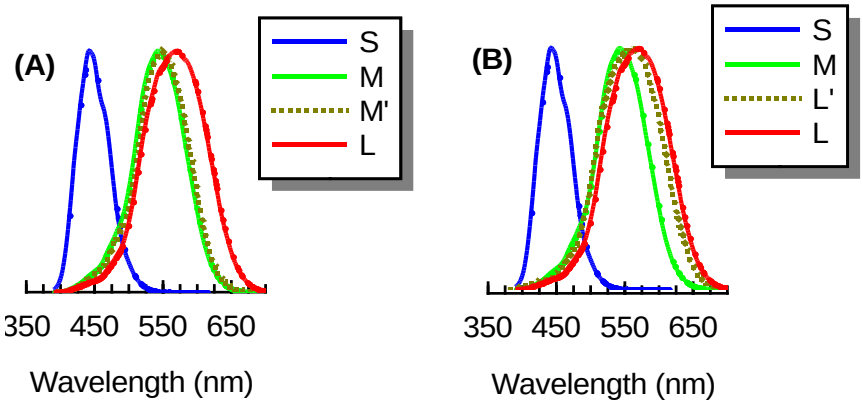

Figure 5-9: Schematic representation of the fourth pigments expressed in carriers of PA (A) and DA (B). M' is the hybrid pigment expressed in carriers of PA and L' is the hybrid pigment expressed in carriers of DA.

The RG colour detection thresholds measured in PA carriers correlate well with the Rayleigh match midpoint of their offsprings (see Figure 4-22). The principal parameter that causes an increase in the Rayleigh match midpoint in PA is the decrease in wavelength separation (dλ) between the normal M and the variant M' pigments (Barbur et al., 2008). Protanomalous subjects with a large separation between M and M' cones are therefore likely to exhibit lower match midpoints; the higher the match midpoint of protanomalous trichromats the smaller the expected separation (dλ) between M and M' (Figure 5-10, red symbols). The results of Figure 4-22 show that the RG thresholds in carriers of protanomaly decrease significantly with decreasing dλ values. This observation is consistent with pooling of M' and M cones in carriers of PA, as the closer the two pigments (M and M') the smaller the spectral broadening of the pooled

response and hence the better the sensitivity of the resulting RG mechanism of the PA carrier.

Carriers of PA showed a small but insignificant deutan shift in their Rayleigh matches. Of the 6 PA carriers 5 required less 670 nm light than normal trichromats in their Rayleigh match (see Figure 4-23). This finding is not consistent with some earlier observations (Schmidt, 1955), but a number of other studies have either found no significant shift from the normal position in the midpoints set by carriers of PA (Waaler, 1927; Jordan et al., 2010), or have even suggested a small deutan shift (Wieland, 1933). On the assumption that M' pools with M and the resulting combined spectral responsivity function shifts towards L, the Rayleigh match midpoint of the PA carriers would be expected to show a deutan shift (Figure 5-10, green data points), which is in agreement with the current findings. The deutan shift in the match midpoint caused by the hypothetical pooling of M' with M has also been predicted by other Nagel models (Sun and Shevell, 2008).

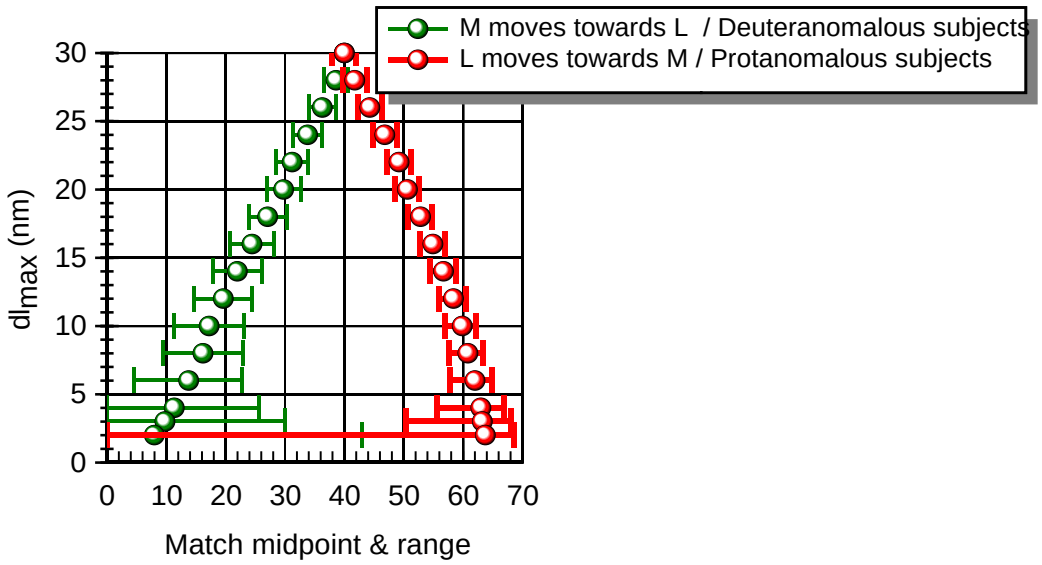

Figure 5-10: Model output showing how the match parameters change with the spectral separation between the two cone pigments. All other model parameters, such as cone pigment optical densities, remain unchanged. Red symbols show how the Rayleigh match parameters change in protanomalous subjects or when L is shifted towards M. Green symbols show how the Rayleigh match parameters change in deuteranomalous subjects or when M is shifted towards L (OD_L=OD_M=0.5) (Barbur et al., 2008).

Another way of broadening the spectral responsivity function of M cones is to increase the amount of pigment in the cones (Barbur et al., 2008). Figure 5-11 shows that the increased OD of M cones causes a deutan-like shift in match midpoint. It is therefore likely that a broadening of the spectral responsivity function of M cones, either by increasing the OD or by pooling M and M' cones, results in an overall deutan-like shift in Rayleigh match midpoint.

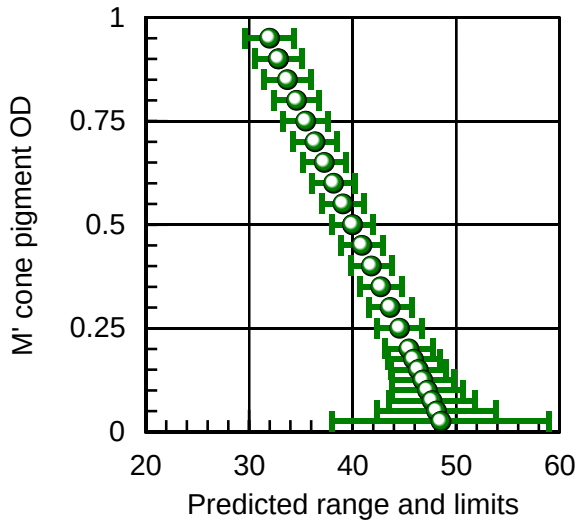

Figure 5-11: Model output showing how changes in the OD of M' can affect the match midpoint and matching range in protanomalous subjects. All other parameters remain unchanged (OD varies from ~ 1 to ~ 0) (Barbur et al., 2008).

A correlation of the carriers' RG threshold with the Rayleigh match midpoint of their offspring was not found in carriers of DA (see Figure 4-22). Assuming that L' was pooled with L, one would expect a similar correlation to that seen in carriers of PA. The absence of a definite correlation suggests that L' is not pooled selectively with L. Moreover, if L' pooled with L the Rayleigh match midpoints of DA carriers should be protan-like and shifted to higher than normal values, as shown in Figure 5-10 (Barbur et al., 2008; Sun and Shevell, 2008). Carriers of DA exhibited a significant deutan shift in their match midpoint compared to normal trichromats, a finding that has been reported in previous studies (Waaler, 1927; Jordan et al., 2010).

The current findings do not exclude the possibility that L' is pooled with M, but this would have detectable consequences. Deuteranomalous subjects rely on L-cone pigments separated by a maximum of 12 nm (Neitz et al., 1996). The wavelength separation between L' and M pigments in DA carriers could vary from ~16 nm to ~27 nm. If L' pooled exclusively with M the large broadening of the resulting spectral

responsivity function would alter the carriers' chromatic sensitivity significantly and this would be detected by currently used colour vision tests. The combined pooling of L' with either L or M, depending on the hybrid pigment's spectral tuning, would cause only a moderate loss of RG sensitivity compared to normal trichromatic males. The findings suggest that L' pools with either L or M cones, causing the small loss of chromatic sensitivity in DA carriers, as demonstrated in various colour vision tests. This form of processing of the signals generated in hybrid photopigments that are expressed in carriers of anomalous trichromacies does not require a specific cone arrangement (Sun and Shevell, 2008), as the hybrid photopigments may pool preferentially with the spectrally closest 'normal' pigments (M' might pool with M and L' can potentially pool with either L or M).

The results obtained in carriers of dichromacy require a different explanation. Carriers of P exhibit RG detection thresholds comparable to normal trichromatic males at all light levels, but carriers of D perform worse than male controls. This is particularly obvious at the lowest light levels tested. The disadvantage demonstrated in D carriers at low light levels may relate to the smaller number of M cones in the retina and hence the greatly skewed L:M ratio. The greater rate of increase in RG thresholds with reducing retinal illuminance in D carriers with respect to normal male controls may well reflect changes in rod-cone interaction effects, as a result of the significant reduction in M cone numbers.

As the light level is decreased cone signals become weaker and the responses of many ganglion cells that would normally depend on cone inputs become dominated by rod signals (Stabell and Stabell, 1996; Lee et al., 1997; Stabell and Stabell, 1998). The major advantage of rod mediated vision is the much higher sensitivity to light, which is achieved largely at the expense of spatial and temporal resolution (Barbur and

Stockman, 2010). The efficiency of the rod-cone interaction effects that minimise the use of rod signals in the mesopic range depends largely on the strength and number of cone signals available at any given light level. The effectiveness of rod signals at lower light levels may depend on the number of M cones, which overlap significantly in spectral sensitivity with rods. The increased dependence on rod signals in the mesopic range is accompanied by a selective loss of S cone sensitivity, with vision being mediated primarily through the use of rod and L cone signals (Pokorny et al., 2006). Carriers of D have a reduced number of M cones, leading to a higher than average L:M ratio (Konstantakopoulou et al., 2012). It is therefore possible that in carriers of D rod signals become effective sooner than would be expected for normal trichromats as the light level decreases, leading to a measurable reduction in RG chromatic sensitivity (see Figure 4-21 and Figure 4-27).

For carriers of P who might have a more balanced L:M ratio, i.e. fewer L cones, chromatic sensitivity shows a small relative improvement and approaches 'normal' levels at 50 Td. This observation suggests stronger chromatically opponent RG mechanisms and reduced intrusion of rod signals. Interestingly, RG thresholds in carriers of PA decrease by 28% at low light levels. This observation supports the proposed pooling of M' and M cones, which results in a broadening of spectral responsivity and enhanced signals. Carriers of PA could use this outcome to suppress more effectively rod signals at lower light levels. Rod intrusion may not, however, affect significantly the chromatic sensitivity in carriers of DA, who exhibit a consistent and unaltered disadvantage to normal trichromats throughout the 1000 Td range. This observation supports the combined pooling hypothesis of L' with both L and M, since this outcome is likely to reduce chromatic sensitivity for the group of DA carriers, independent of light level.

The noticeable differences amongst the four groups of carriers require an interpretation that does not compromise the significance of any findings. The mediation of the pooling of L' and M' by spectral similarities to the normal M and L satisfies the requirements for an explanation consistent with the findings for all carrier groups. This explanation does not require any specific cone arrangements and is consistent for carriers of DA and PA. The lack of obvious trends in carriers of DA suggests that L' might pool with M in some carriers and L in others, thus preventing a group trend from being revealed. The involvement of rods can explain the performance of D carriers and provides further support for spectrally mediated pooling of the hybrid pigments in carriers of anomalous trichromacies. Carriers of PA may not appear significantly different from male trichromats in conventional colour vision tests, but they reveal a potential for superior RG chromatic sensitivity at low light levels, a finding that warrants further investigation.

6 CONCLUSIONS

Understanding the effects age has on vision is important in view of the rapidly increasing older population. Increased longevity and changes in lifestyle point towards an increase in the prevalence of age-related ocular diseases. The cost of sight loss for the NHS in 2008 was estimated at approximately £2.14 billion and this was only for AMD, glaucoma, diabetic retinopathy and cataract (Winyard and McLaughlan, 2008). While efforts and resources are being channelled in the treatment of age-related ocular diseases, little is known about the subclinical development, the underlying mechanisms and the detection of these diseases at the very onset. Current clinical guidelines to community Optometrists discourage the referral to hospital eye services of individuals with drusen, the earliest stage of AMD, as no treatment is available and possibly as a way to minimise costs. AMD has, however, known risk factors that are associated with lifestyle and diet. It is only after the clinical manifestations of drusen that lifestyle may change following professional advice, but by this stage there is irreversible retinal damage. Similarly, glaucoma is only detected in the presence of visual field loss, optic nerve damage or high IOP, all of which can start developing years before they result in anatomical and functional changes.

For a number of years ageing has been associated with impaired colour vision. The factors that can affect chromatic sensitivity in older individuals are, however, numerous and if not taken into account can mask unexplained, clinically significant colour vision loss. Recently, Cynthia Owsley (2011) proposed that there might be “age-related psychophysical deficits in certain aspects of visual function that are exacerbated in older adults who eventually develop serious eye diseases, e.g. AMD or glaucoma” and continued to point out that “vulnerabilities in visual function in late life can potentially

reveal breakdowns in the visual system that are early markers or signs that disease development is likely".

This study was designed to reveal the signs that can identify individuals at high risk for developing ocular diseases, by attempting to separate age-related colour vision loss from potential pre-clinical indications of ocular disease. The HR index reveals that older normal subjects lose little chromatic sensitivity with age and these individuals are, therefore, considered to age healthily. A small percentage of subjects, primarily over 50 years of age, showed significant worsening of colour vision, an effect that may be attributed to early changes in retinal function. There is currently insufficient scientific evidence to justify the classification of these individuals as a high risk category, since current knowledge as to how psychophysical deficits develop and progress to the stage of visual impairment is inadequate. According to this study, approximately 11% of a randomly selected healthy population falls below the statistical limits for normal colour vision, indicating impaired retinal and/or post-retinal visual function for their age.

This finding may have clinical importance, as it has the potential of providing information about the functional status of the retina that cannot be identified with currently established clinical tests. For example, high contrast visual acuity is not sensitive enough to detect small changes in the retinal function and remains largely unaffected by early stages of AMD, glaucoma and diabetic retinopathy. Future studies should involve long-term monitoring of individuals with normal and abnormal HR indices, in order to establish the percentage of subjects and the time course of the developing retinal disease, following the early detection of colour vision loss. The time frame for the development of disease could provide useful additional information about the pathophysiology and the development of various diseases and, if studied in detail,

may reveal an optimum intervention window for each developing disease. The rapidly ageing population and the increased costs of treatment necessary for age-related ocular diseases justify the early identification of disease, with the ultimate aim that prevention will extend normal functional vision.

The study on carriers of congenital RG deficiency reveals new information relevant not only to chromatic processing, but also to the plasticity of the human visual system. The processing of signals from the hybrid pigment in carriers of anomalous trichromacy has been explained either through the tetrachromatic theory, or through the integration of the hybrid pigment signals into the existing colour processing channels. This study suggested that the processing of the hybrid pigment may be pre-programmed for carriers of PA, but not for carriers of DA and further explains the underlying aetiology; the pre-programmed pooling of M' with M may be dictated by the spectral proximity of the pigments, whilst the apparent randomness of the pooling of L' in carriers of DA may reflect the more equal spectral separations between the three pigments involved.

The human visual system does not seem to have enough plasticity to develop a separate channel for the processing of signals from the hybrid pigments (Wachtler et al., 2007). Indeed, the advantages of a separate channel remain to be analysed. At the same time our visual system seems to be able to utilise its components to change the dynamics of photoreceptor interaction and optimise visual performance under challenging conditions; the presence of an increased number of M-like cones in carriers of PA may weaken the rod involvement in light levels unusually low for normal trichromats, whilst the reduced absolute numbers of M cones in carriers of D may promote the dynamic involvement of the rods and impair chromatic sensitivity.

The rod-cone interaction effects may reveal more information in studies extending from normal trichromats to congenitally colour deficient subjects, particularly when

accompanied by detailed genetic analysis of cone pigments. Combination of genetics and psychophysical studies will help establish how these females make use of their unique cone mosaics. Finally, the results of this study reveal a potentially new technique for identification of female carriers of congenital RG deficiency via non-invasive, simple colour vision testing. The characteristic performance of female carriers in the various colour vision tests could provide an indication about the possibility of being a carrier of a specific type of colour vision deficiency.

The two principal studies reported in this thesis reveal the extensive variability that exists in ‘normal’ colour vision and the need to understand the causal aetiologies, with direct benefits to clinical practice.

APPENDIX A. MAP TEST STIMULUS GEOMETRY

The stimulus geometry designed for the measurement of the MP employs a disc stimulus of 0.36^{o} diameter at the fovea and a sector annulus that changes in width and angular subtense, as shown in Figure A-1. The small foveal stimulus ensures adequate spatial sampling accuracy, without the need to involve spatial averaging. The stimulus increases systematically in area with eccentricity (e) as the sector of an annulus of width, W, and angular subtense α, to make the measurements easier to carry out and to ensure optimum flicker detection.

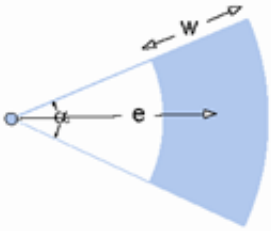

W (rad) = (3.1415+42*ABS(e) +175*2^1.5)/860
alpha (rad) = 2.2*EXP(-12*e^0.8)+0.64

Eccentricity e(deg)	Sector width W(deg)	Sector angle alpha (deg)
0	disc (0.36 deg)	360
0.8	0.26	121.70
1.8	0.32	96.02
2.8	0.39	79.80
3.8	0.45	68.72
6.8	0.64	50.90
7.8	0.71	47.72

Figure A-1: Definition of the spatial dimensions of the stimulus employed in the MAP test.

APPENDIX B. PHOTOMETRIC MODEL FOR COMPUTATION OF PEAK MPOD

Definitions:

V(λ) – CIE 1932 spectral responsivity function, with the MP for the standard observer removed. The peak absorption optical density for the MP of the standard observer was taken to be 0.352.

S(λ) – Relative spectral radiance distribution of the SW (test) beam

L(λ) – Relative spectral radiance distribution of the LW (reference) beam

T(λ) – Spectral transmittance function of the MP; $T(\lambda) = 10^{-OD_{peak} \cdot \varepsilon(\lambda)}$, where OD_{peak} is the peak optical density and ε(λ) is the spectral extinction function of the pigment.

OD_m - Measured optical pigment density using the MAP test; $OD_m = \log_{10} \cdot \left(\frac{SF}{SP}\right)$, where SF and SP is the ratio of measured test beam intensities at the fovea and the extreme periphery. Alternatively, $SF = SP \cdot 10^{OD_m}$

Far periphery:

Consider the flicker-null point in the far periphery where the light absorption of the MP is negligible. The signal generated by the SW beam must equal the signal generated by the LW beam:

$\sum L(\lambda) \cdot V(\lambda) d\lambda = c \sum S_P(\lambda) \cdot V(\lambda) d\lambda$, where c is a constant needed to ensure that the intensity of the SW beam produces a flicker-null point.

Let $LV = \sum L(\lambda) \cdot V(\lambda) d\lambda$ and $SV = \sum S_P(\lambda) \cdot V(\lambda) d\lambda$, hence c = LV/SV

Foveal measurement:

The intensity of the reference beam remains unchanged, but that of the test beam is increased by a factor 10^{OD_m}, to cancel out the absorption of blue light by the MP. Hence,

$$\sum L(\lambda)\cdot V(\lambda)\cdot 10^{-OD_{peak}\cdot\varepsilon(\lambda)}d\lambda = 10^{OD_m}\cdot c\sum S_P(\lambda)\cdot V(\lambda)\cdot 10^{-OD_{peak}\cdot\varepsilon(\lambda)}d\lambda$$

For simplicity, we define two new variables:

Let $SVT = \sum S_P(\lambda)\cdot V(\lambda)\cdot 10^{-OD_{peak}\cdot\varepsilon(\lambda)}d\lambda$ and $LVT = \sum L(\lambda)\cdot V(\lambda)\cdot 10^{-OD_{peak}\cdot\varepsilon(\lambda)}d\lambda$.

The condition for the flicker-null point at the fovea can now be expressed as:

$$10^{OD_m} SVT = \frac{SV}{LV}\cdot LVT.$$

Hence,

$10^{OD_m} = \frac{SV}{LV}\cdot\frac{LVT}{SVT}$, where any small effect of MP on the LW reference beam has also been taken into account.

Finally, the measured optical density, OD_m of the MP can be related directly to its peak optical density, OD_{peak}, by the following equation:

$$OD_m = \log_{10}\left(\frac{SV}{LV}\cdot\frac{LVT}{SVT}\right).$$

LVT, SVT, LV and SV are evaluated by numeric integration for any value of OD_{peak} and the corresponding value of OD_m computed. This process is repeated for discrete values of OD_m as shown in Figure 3-4D. The non-linear relationship is fitted with a 5^{th} order polynomial function, which provides an easy and accurate way of estimating the OD_{peak} for any measured value of OD_m.

APPENDIX C. MAP TEST SHORT-WAVELEGTH SENSITIVITY FOR YOUNG OBSERVERS

SW beam luminance for 34 subjects <22 years of age			
Median	SD	Minimum	Maximum
1.39 $cd \cdot m^{-2}$	0.19 $cd \cdot m^{-2}$	1.05 $cd \cdot m^{-2}$	1.70 $cd \cdot m^{-2}$

Table C-1: Median, SD and range of SW beam luminance values for 6.8^{o} and 7.8^{o} for 34 young subjects, serving as the reference group for estimating the lens OD.

APPENDIX D. ERRORS AND MISREADINGS ON THE ISHIHARA TEST PLATES

Table D-1 shows the most common errors and misreadings on the Ishihara test. These are not exhaustive, as an observer may make an error or a misreading that is less common and therefore not listed below.

Plate	Normal colour vision	Error by colour deficient observer	Misreading
1	12	12	12
2	8	3	
3	6	5	8
4	29	70	28
5	57	35	
6	5	2	8
7	3	5	8
8	15	17	18
9	74	21	
10	2	-	
11	6	-	8
12	97	-	87
13	45	-	46
14	5	-	
15	7	-	
16	16	-	18
17	73	-	75/78/15/13
18	-	Any number	
19	-	Any number	
20	-	Any number	
21	-	Any number	
22	26	Deutans see digit on the left / Protans see digit on the right	
23	42		
24	35		
25	96		

Table D-1: Ishihara errors and misreadings.

APPENDIX E. TUKEY'S BOX-PLOT FOR THE IDENTIFICATION OF OUTLIERS

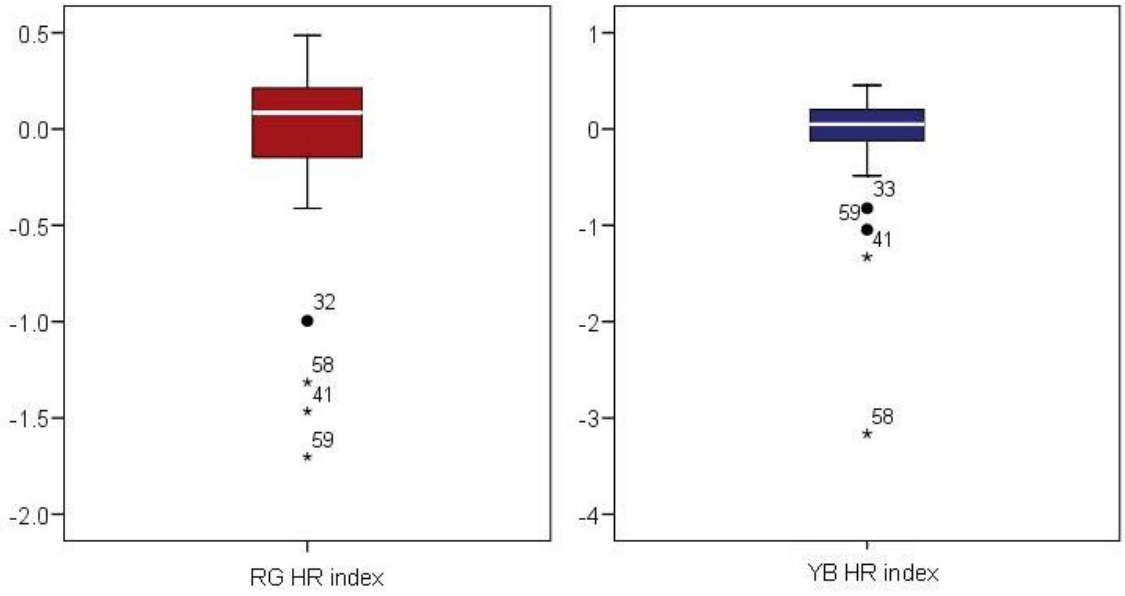

Figure E-1: Tukey's box-plots for RG and YB HR indices; 5 outliers are identified (numbers refer to the ID assigned to each subject). These outliers are the same subjects excluded following the step by step approach described in section 4.1.2.3.

APPENDIX F. THE HR INDEX IN CONGENITAL COLOUR VISION DEFICIENCY

The mild DA subject shown in Figure F-1 has a measured YB threshold at 65 cd·m^{-2} of 0.89 SNU. Given the regression equation of Figure F-3 the estimated RG threshold for 65 cd·m^{-2} would be 0.57·0.89+0.594=1.10 SNU. The difference between the measured RG threshold at 65 cd·m^{-2} (2.37 SNU) and the estimated threshold (1.10 SNU) is attributed to the L' that is shifted with respect to the 'normal' M pigment. This value is then subtracted from the RG detection threshold for each light level (Figure F-2). The HR index can be calculated using the corrected values.

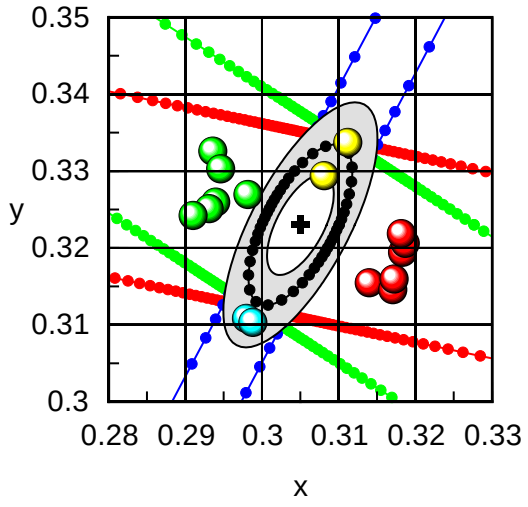

Figure F-1: CAD plot of a mild DA 28 year old subject (RG=2.87 at 26 cd·m^{-2}).

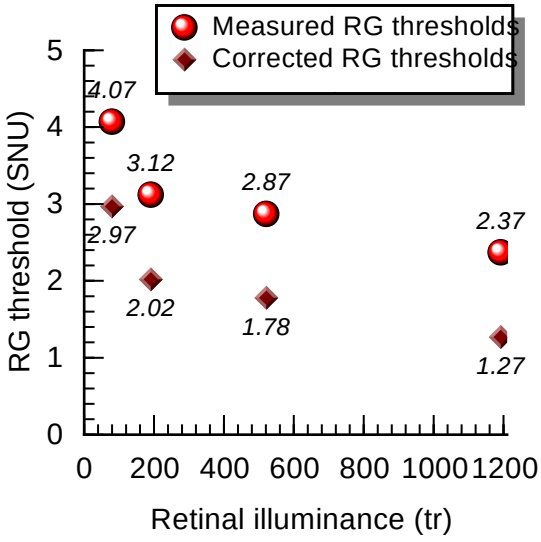

Figure F-2: Correction of the RG thresholds for a mild DA subject, after subtracting 1.10 SNU from each measured threshold. The data labels show the threshold values.

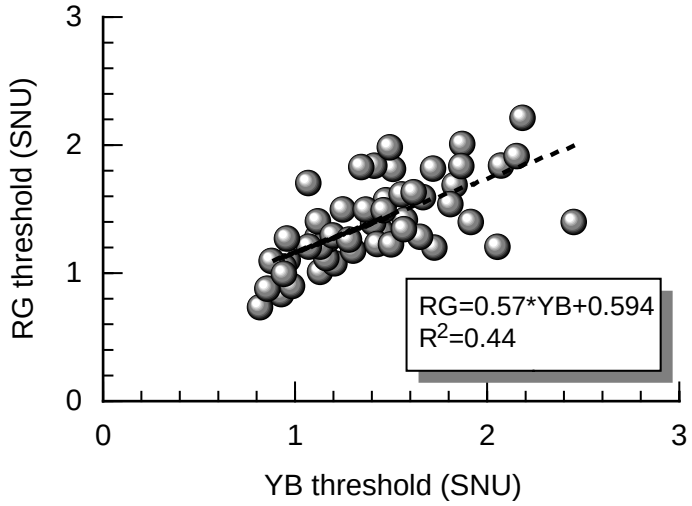

Figure F-3: Correlation of RG and YB detection thresholds for 65 cd·m^{-2} (R^2=0.44, p<0.001) (n=53).

REFERENCES

ADAMS, A. J., SCHEFRIN, B. & HUIE, K. 1987. New clinical color threshold test for eye disease. *Am J Optom Physiol Opt,* 64**,** 29-37.

AHMAD, A. & SPEAR, P. D. 1993. Effects of aging on the size, density, and number of rhesus monkey lateral geniculate neurons. *J Comp Neurol,* 334**,** 631-43.

ALEXANDRIDIS, E., LEENDERTZ, J. A. & BARBUR, J. L. 1991. Methods for studying the behaviour of the pupil. *Journal of Psychophysiology,* 5**,** 223-239.

AMOS-LANDGRAF, J. M., COTTLE, A., PLENGE, R. M., FRIEZ, M., SCHWARTZ, C. E., LONGSHORE, J. & WILLARD, H. F. 2006. X chromosome-inactivation patterns of 1,005 phenotypically unaffected females. *Am J Hum Genet,* 79**,** 493-9.

APPLEGATE, R. A., ADAMS, A. J., CAVENDER, J. C. & ZISMAN, F. 1987. Early color vision changes in age-related maculopathy. *Appl Opt,* 26**,** 1458-62.

ATTARCHI, M. S., LABBAFINEJAD, Y. & MOHAMMADI, S. 2010. Occupational exposure to different levels of mixed organic solvents and colour vision impairment. *Neurotoxicol Teratol,* 32**,** 558-62.

BARAAS, R. C., CARROLL, J., GUNTHER, K. L., CHUNG, M., WILLIAMS, D. R., FOSTER, D. H. & NEITZ, M. 2007. Adaptive optics retinal imaging reveals S-cone dystrophy in tritan color-vision deficiency. *J Opt Soc Am A Opt Image Sci Vis,* 24**,** 1438-47.

BARBUR, J. L. 2004. 'Double-blindsight' revealed through the processing of color and luminance contrast defined motion signals. *Prog Brain Res,* 144**,** 243-59.

BARBUR, J. L. & CONNOLLY, D. M. 2011. Effects of hypoxia on color vision with emphasis on the mesopic range. *Expert Rev. Ophthalmol.,* 6**,** 409-420.

BARBUR, J. L., HARLOW, A. J. & PLANT, G. T. 1994. Insights into the different exploits of colour in the visual cortex. *Proc Biol Sci,* 258**,** 327-34.

BARBUR, J. L., HOLLIDAY, I. E. & RUDDOCK, K. H. 1981. The spatial and temporal organisation of motion perception units in human vision. *Acta Psychol (Amst),* 48**,** 35-47.

BARBUR, J. L., KONSTANTAKOPOULOU, E., RODRIGUEZ-CARMONA, M., HARLOW, J. A., ROBSON, A. G. & MORELAND, J. D. 2010. The Macular Assessment Profile test - a new VDU-based technique for measuring the spatial distribution of the macular pigment, lens density and rapid flicker sensitivity. *Ophthalmic Physiol Opt,* 30**,** 470-83.

BARBUR, J. L., RODRIGUEZ-CARMONA, M. & HARLOW, A. J. Establishing the statistical limits of "normal" chromatic sensitivity CIE Proceedings; 75 Years of the Standard Colorimetric Observer, May 2006 2006 Ottawa, Ontario.

BARBUR, J. L., RODRIGUEZ-CARMONA, M., HARLOW, J. A., MANCUSO, K., NEITZ, J. & NEITZ, M. 2008. A study of unusual Rayleigh matches in deutan deficiency. *Vis Neurosci,* 25**,** 507-16.

BARBUR, J. L. & RUDDOCK, K. H. 1980. Spatial characteristics of movement detection mechanisms in human vision. I. Achromatic vision. *Biol Cybern,* 37**,** 77-92.

BARBUR, J. L. & STOCKMAN, A. 2010. Photopic, Mesopic and Scotopic Vision and Changes in Visual Performance. *In:* DARTT, D., BESHARSE, J. C. & DANA, R. (eds.) *Encyclopedia of the eye.* Oxford: Elsevier Ltd.

BARBUR, J. L., THOMSON, W. & FORSYTH, P. 1987. A New System for the Simultaneous Measurement of Pupil Size and Two-Dimensional Eye Movements. *Clin. Vis. Sci.,* 2**,** 131-142.

BARNSTABLE, C. F. 2004. Molecular Regulation of Vertebrate Retinal Development. *In:* CHALUPA, L. M. & WERNER, J. S. (eds.) *The Visual Neurosciences.* Cambridge MA: MIT Press

BEATTY, S., MURRAY, I. J., HENSON, D. B., CARDEN, D., KOH, H. & BOULTON, M. E. 2001. Macular pigment and risk for age-related macular degeneration in subjects from a Northern European population. *Invest Ophthalmol Vis Sci,* 42**,** 439-46.

BEEMS, E. M. & VAN BEST, J. A. 1990. Light transmission of the cornea in whole human eyes. *Exp Eye Res,* 50**,** 393-5.

BEIRNE, R. O., MCILREAVY, L. & ZLATKOVA, M. B. 2008. The effect of age-related lens yellowing on Farnsworth-Munsell 100 hue error score. *Ophthalmic Physiol Opt,* 28**,** 448-56.

BERENDSCHOT, T. T., BROEKMANS, W. M., KLOPPING-KETELAARS, I. A., KARDINAAL, A. F., VAN POPPEL, G. & VAN NORREN, D. 2002. Lens aging in relation to nutritional determinants and possible risk factors for age-related cataract. *Arch Ophthalmol,* 120**,** 1732-7.

BERENDSCHOT, T. T. & VAN NORREN, D. 2006. Macular pigment shows ringlike structures. *Invest Ophthalmol Vis Sci,* 47**,** 709-14.

BERNSTEIN, P. S., YOSHIDA, M. D., KATZ, N. B., MCCLANE, R. W. & GELLERMANN, W. 1998. Raman detection of macular carotenoid pigments in intact human retina. *Invest Ophthalmol Vis Sci,* 39**,** 2003-11.

BERSON, D. M., DUNN, F. A. & TAKAO, M. 2002. Phototransduction by retinal ganglion cells that set the circadian clock. *Science,* 295**,** 1070-3.

BIRCH, J. 2001. *Diagnosis of defective colour vision,* Oxfrord, Butterworth-Heinemann.

BIRCH, J. & MCKEEVER, L. M. 1993. Survey of the accuracy of new pseudoisochromatic plates. *Ophthalmic Physiol Opt,* 13**,** 35-40.

BIRD, A. C. 1992. Bruch's membrane change with age. *Br J Ophthalmol,* 76**,** 166-8.

BITTEL, D. C., THEODORO, M. F., KIBIRYEVA, N., FISCHER, W., TALEBIZADEH, Z. & BUTLER, M. G. 2008. Comparison of X-chromosome inactivation patterns in multiple tissues from human females. *J Med Genet,* 45**,** 309-13.

BOETTNER, E. A. & WOLTER, J. 1962. Transmission of the ocular media. *Invest Ophthalmol Vis Sci,* 1**,** 776-783.

BOLLINGER, K., BIALOZYNSKI, C., NEITZ, J. & NEITZ, M. 2001. The importance of deleterious mutations of M pigment genes as a cause of color vision defects. *Color Research & Application,* 26**,** S100-S105.

BONE, R. A., LANDRUM, J. T. & CAINS, A. 1992. Optical density spectra of the macular pigment in vivo and in vitro. *Vision Res,* 32**,** 105-10.

BONE, R. A., LANDRUM, J. T., FERNANDEZ, L. & TARSIS, S. L. 1988. Analysis of the macular pigment by HPLC: retinal distribution and age study. *Invest Ophthalmol Vis Sci,* 29**,** 843-9.

BONE, R. A., LANDRUM, J. T. & TARSIS, S. L. 1985. Preliminary identification of the human macular pigment. *Vision Res,* 25**,** 1531-5.

BORN, G., GRUTZNER, P. & HEMMINGER, H. 1976. [Evidence for reduced colour vision in carriers of congenital colour vision deficiencies (author's transl)]. *Hum Genet,* 32**,** 189-96.

BOWMAKER, J. K. & DARTNALL, H. J. 1980. Visual pigments of rods and cones in a human retina. *J Physiol,* 298**,** 501-11.

BRAINARD, D. H., ROORDA, A., YAMAUCHI, Y., CALDERONE, J. B., METHA, A., NEITZ, M., NEITZ, J., WILLIAMS, D. R. & JACOBS, G. H. 2000. Functional consequences of the relative numbers of L and M cones. *J Opt Soc Am A Opt Image Sci Vis,* 17**,** 607-14.

BRODMANN, K. 1909. *Vergleichende Lokalisationslehre der Grosshirnrinde,* Leipzig: Barth.

BROWN, C. J. 1999. Skewed X-chromosome inactivation: cause or consequence? *J Natl Cancer Inst,* 91**,** 304-5.

BUCK, S. L. 2004. Rod-Cone Interactions in Human Vision. *In:* CHALUPA, L. M. & WERNER, J. S. (eds.) *The Visual Neurosciences.* Cambridge MA: MIT Press

BUMSTED, K. & HENDRICKSON, A. 1999. Distribution and development of short-wavelength cones differ between Macaca monkey and human fovea. *J Comp Neurol,* 403**,** 502-16.

BURNS, M. E. & LAMB, T. D. 2004. Visual Transduction by Rod and Cone Photoreceptors. *In:* CHALUPA, L. M. & WERNER, J. S. (eds.) *The Visual Neurosciences.* Cambridge MA: MIT Press

BUSQUE, L., MIO, R., MATTIOLI, J., BRAIS, E., BLAIS, N., LALONDE, Y., MARAGH, M. & GILLILAND, D. G. 1996. Nonrandom X-inactivation patterns in normal females: lyonization ratios vary with age. *Blood,* 88**,** 59-65.

CARROLL, J., BARAAS, R. C., WAGNER-SCHUMAN, M., RHA, J., SIEBE, C. A., SLOAN, C., TAIT, D. M., THOMPSON, S., MORGAN, J. I., NEITZ, J., WILLIAMS, D. R., FOSTER, D. H. & NEITZ, M. 2009. Cone photoreceptor

mosaic disruption associated with Cys203Arg mutation in the M-cone opsin. *Proc Natl Acad Sci U S A,* 106**,** 20948-53.

CARROLL, J., MCMAHON, C., NEITZ, M. & NEITZ, J. 2000. Flicker-photometric electroretinogram estimates of L:M cone photoreceptor ratio in men with photopigment spectra derived from genetics. *J Opt Soc Am A Opt Image Sci Vis,* 17**,** 499-509.

CARROLL, J., NEITZ, J. & NEITZ, M. 2002. Estimates of L:M cone ratio from ERG flicker photometry and genetics. *J Vis* [Online], 2. Available: http://journalofvision.org/2/8/1/.

CARROLL, J., NEITZ, M., HOFER, H., NEITZ, J. & WILLIAMS, D. R. 2004. Functional photoreceptor loss revealed with adaptive optics: an alternate cause of color blindness. *Proc Natl Acad Sci U S A,* 101**,** 8461-6.

CHARMAN, N. W. 2009. Forming an optical image: the optical elements of the eye. *In:* ROSENFIELD, M. & LOGAN, N. (eds.) *Optometry: Science, Techniques and Clinical Management.* Elsevier Ltd.

CHEN, S. F., CHANG, Y. & WU, J. C. 2001. The spatial distribution of macular pigment in humans. *Curr Eye Res,* 23**,** 422-34.

CICERONE, C. M. & NERGER, J. L. 1989. The relative numbers of long-wavelength-sensitive to middle-wavelength-sensitive cones in the human fovea centralis. *Vision Res,* 29**,** 115-28.

CIULLA, T. A. & HAMMOND, B. R., JR. 2004. Macular pigment density and aging, assessed in the normal elderly and those with cataracts and age-related macular degeneration. *Am J Ophthalmol,* 138**,** 582-7.

CIULLA, T. A., HAMMOND, B. R., JR., YUNG, C. W. & PRATT, L. M. 2001. Macular pigment optical density before and after cataract extraction. *Invest Ophthalmol Vis Sci,* 42**,** 1338-41.

COHN, S. A., EMMERICH, D. S. & CARLSON, E. A. 1989. Differences in the responses of heterozygous carriers of colorblindness and normal controls to briefly presented stimuli. *Vision Res,* 29**,** 255-62.

COSTA, M. F., VENTURA, D. F., PERAZZOLO, F., MURAKOSHI, M. & SILVEIRA, L. C. 2006. Absence of binocular summation, eye dominance, and learning effects in color discrimination. *Vis Neurosci,* 23**,** 461-9.

COTTER, P. D., MAY, A., FITZSIMONS, E. J., HOUSTON, T., WOODCOCK, B. E., AL-SABAH, A. I., WONG, L. & BISHOP, D. F. 1995. Late-onset X-linked sideroblastic anemia. Missense mutations in the erythroid delta-aminolevulinate synthase (ALAS2) gene in two pyridoxine-responsive patients initially diagnosed with acquired refractory anemia and ringed sideroblasts. *J Clin Invest,* 96**,** 2090-6.

CRONE, R. A. 1959. Spectral sensitivity in color-defective subjects and heterozygous carriers. *Am J Ophthalmol,* 48**,** 231-8.

CURCIO, C. A., ALLEN, K. A., SLOAN, K. R., LEREA, C. L., HURLEY, J. B., KLOCK, I. B. & MILAM, A. H. 1991. Distribution and morphology of human cone photoreceptors stained with anti-blue opsin. *J Comp Neurol,* 312**,** 610-24.

CURCIO, C. A. & DRUCKER, D. N. 1993. Retinal ganglion cells in Alzheimer's disease and aging. *Ann Neurol,* 33**,** 248-57.

CURCIO, C. A., MILLICAN, C. L., ALLEN, K. A. & KALINA, R. E. 1993. Aging of the human photoreceptor mosaic: evidence for selective vulnerability of rods in central retina. *Invest Ophthalmol Vis Sci,* 34**,** 3278-96.

CURCIO, C. A., MILLICAN, C. L., BAILEY, T. & KRUTH, H. S. 2001. Accumulation of cholesterol with age in human Bruch's membrane. *Invest Ophthalmol Vis Sci,* 42**,** 265-74.

CURCIO, C. A., OWSLEY, C. & JACKSON, G. R. 2000. Spare the rods, save the cones in aging and age-related maculopathy. *Invest Ophthalmol Vis Sci,* 41**,** 2015-8.

CURCIO, C. A., SLOAN, K. R., KALINA, R. E. & HENDRICKSON, A. E. 1990. Human photoreceptor topography. *J Comp Neurol,* 292**,** 497-523.

DACEY, D. M. 1996. Circuitry for color coding in the primate retina. *Proc Natl Acad Sci U S A,* 93**,** 582-8.

DACEY, D. M. & LEE, B. B. 1994. The 'blue-on' opponent pathway in primate retina originates from a distinct bistratified ganglion cell type. *Nature,* 367**,** 731-5.

DAIN, S. J., RAMMOHAN, K. W., BENES, S. C. & KING-SMITH, P. E. 1990. Chromatic, spatial, and temporal losses of sensitivity in multiple sclerosis. *Invest Ophthalmol Vis Sci,* 31**,** 548-58.

DAVISON, P., AKKALI, M., LOUGHMAN, J., SCANLON, G., NOLAN, J. & BEATTY, S. 2011. Macular pigment: its associations with color discrimination and matching. *Optom Vis Sci,* 88**,** 816-22.

DELORI, F. C. & BURNS, S. A. 1996. Fundus reflectance and the measurement of crystalline lens density. *J Opt Soc Am A Opt Image Sci Vis,* 13**,** 215-26.

DILLON, J., ZHENG, L., MERRIAM, J. C. & GAILLARD, E. R. 2004. Transmission of light to the aging human retina: possible implications for age related macular degeneration. *Exp Eye Res,* 79**,** 753-9.

DOUGHTY, M. J. & ZAMAN, M. L. 2000. Human corneal thickness and its impact on intraocular pressure measures: a review and meta-analysis approach. *Surv Ophthalmol,* 44**,** 367-408.

DUBBELMAN, M. & VAN DER HEIJDE, G. L. 2001. The shape of the aging human lens: curvature, equivalent refractive index and the lens paradox. *Vision Res,* 41**,** 1867-77.

DUBBELMAN, M., VAN DER HEIJDE, G. L. & WEEBER, H. A. 2001. The thickness of the aging human lens obtained from corrected Scheimpflug images. *Optom Vis Sci,* 78**,** 411-6.

EGAN, C. A., ROBSON, A. G. & MORELAND, J. D. 2009. Comparison of Motion Photometry and 2-Wavelength Fundus Autofluorescence Assessments of Macular Pigment Spatial Profiles in Healthy Subjects. *Invest Ophthalmol Vis Sci,* 50 (E-abstract 1714).

EL KASSAR, N., HETET, G., BRIERE, J. & GRANDCHAMP, B. 1998. X-chromosome inactivation in healthy females: incidence of excessive lyonization with age and comparison of assays involving DNA methylation and transcript polymorphisms. *Clin Chem,* 44**,** 61-7.

ELSNER, A. E., BERK, L., BURNS, S. A. & ROSENBERG, P. R. 1988. Aging and human cone photopigments. *J Opt Soc Am A,* 5**,** 2106-12.

ELSNER, A. E., BURNS, S. A., BEAUSENCOURT, E. & WEITER, J. J. 1998. Foveal cone photopigment distribution: small alterations associated with macular pigment distribution. *Invest Ophthalmol Vis Sci,* 39**,** 2394-404.

FEIGL, B., CAO, D., MORRIS, C. P. & ZELE, A. J. 2011. Persons with age-related maculopathy risk genotypes and clinically normal eyes have reduced mesopic vision. *Invest Ophthalmol Vis Sci,* 52**,** 1145-50.

FEITOSA-SANTANA, C., PARAMEI, G. V., NISHI, M., GUALTIERI, M., COSTA, M. F. & VENTURA, D. F. 2010. Color vision impairment in type 2 diabetes assessed by the D-15d test and the Cambridge Colour Test. *Ophthalmic Physiol Opt,* 30**,** 717-23.

FRANCESCHETTI, A. 1928. Die Bedeutung der Einstellungsbreite am Anomaloskop für die Diagnose der einzelnen Typen der Farbensinnstörungen, nebst Bemerkungenüber ihren Vererbungsmodus. *Schweizerische Medizinische Wochenschrift,* 52**,** 1273–1279.

GAILLARD, E. R., ZHENG, L., MERRIAM, J. C. & DILLON, J. 2000. Age-related changes in the absorption characteristics of the primate lens. *Invest Ophthalmol Vis Sci,* 41**,** 1454-9.

GAO, H. & HOLLYFIELD, J. G. 1992. Aging of the human retina. Differential loss of neurons and retinal pigment epithelial cells. *Invest Ophthalmol Vis Sci,* 33**,** 1-17.

GUNTHER, K. L. & DOBKINS, K. R. 2002. Individual differences in chromatic (red/green) contrast sensitivity are constrained by the relative number of L-versus M-cones in the eye. *Vision Res,* 42**,** 1367-78.

GUPTA, N., GREENBERG, G., DE TILLY, L. N., GRAY, B., POLEMIDIOTIS, M. & YUCEL, Y. H. 2009. Atrophy of the lateral geniculate nucleus in human glaucoma detected by magnetic resonance imaging. *Br J Ophthalmol,* 93**,** 56-60.

HAEGERSTROM-PORTNOY, G. 1988. Short-wavelength-sensitive-cone sensitivity loss with aging: a protective role for macular pigment? *J Opt Soc Am A,* 5**,** 2140-4.

HAMMOND, B. R., JR. & CARUSO-AVERY, M. 2000. Macular pigment optical density in a Southwestern sample. *Invest Ophthalmol Vis Sci,* 41**,** 1492-7.

HAMMOND, B. R., JR., FULD, K. & SNODDERLY, D. M. 1996a. Iris color and macular pigment optical density. *Exp.Eye Res.,* 62**,** 293-297.

HAMMOND, B. R., JR., WOOTEN, B. R. & SNODDERLY, D. M. 1996b. Cigarette smoking and retinal carotenoids: implications for age-related macular degeneration. *Vision Res.,* 36**,** 3003-3009.

HAMMOND, B. R., JR., WOOTEN, B. R. & SNODDERLY, D. M. 1997. Individual variations in the spatial profile of human macular pigment. *J Opt Soc Am A Opt Image Sci Vis,* 14**,** 1187-96.

HAMMOND, B. R., JR., WOOTEN, B. R. & SNODDERLY, D. M. 1998. Preservation of visual sensitivity of older subjects: association with macular pigment density. *Invest Ophthalmol Vis Sci,* 39**,** 397-406.

HANDELMAN, G. J., DRATZ, E. A., REAY, C. C. & VAN KUIJK, J. G. 1988. Carotenoids in the human macula and whole retina. *Invest Ophthalmol Vis Sci,* 29**,** 850-5.

HARDY, J. L., FREDERICK, C. M., KAY, P. & WERNER, J. S. 2005. Color naming, lens aging, and grue: what the optics of the aging eye can teach us about color language. *Psychol Sci,* 16**,** 321-7.

HARDY, K. J., LIPTON, J., SCASE, M. O., FOSTER, D. H. & SCARPELLO, J. H. 1992. Detection of colour vision abnormalities in uncomplicated type 1 diabetic patients with angiographically normal retinas. *Br J Ophthalmol,* 76**,** 461-4.

HARDY, L. H., RAND, G. & RITTLER, M. C. 1954. The H-R-R polychromatic plates. I. A. test for the detection, classification, and estimation of the degree of defective color vision. *AMA Arch Ophthalmol,* 51**,** 216-28.

HARWERTH, R. S., CARTER-DAWSON, L., SHEN, F., SMITH, E. L., 3RD & CRAWFORD, M. L. 1999. Ganglion cell losses underlying visual field defects from experimental glaucoma. *Invest Ophthalmol Vis Sci,* 40**,** 2242-50.

HERING, E. (ed.) 1964. *Outlines of a theory of the light sense (translated by Leo M Hurvich and Dorothea Jameson),* Cambridge (MA): Harvard University Press.

HOFER, H., CARROLL, J., NEITZ, J., NEITZ, M. & WILLIAMS, D. R. 2005. Organization of the human trichromatic cone mosaic. *J Neurosci,* 25**,** 9669-79.

HOOD, S. M., MOLLON, J. D., PURVES, L. & JORDAN, G. 2006. Color discrimination in carriers of color deficiency. *Vision Res,* 46**,** 2894-900.

HTTP://WEBVISION.MED.UTAH.EDU/. [Accessed 7th September 2011].

HTTP://WWW.CVRL.ORG/. [Accessed 7th September 2011].

JAGLA, W. M., JAGLE, H., HAYASHI, T., SHARPE, L. T. & DEEB, S. S. 2002. The molecular basis of dichromatic color vision in males with multiple red and green visual pigment genes. *Hum Mol Genet,* 11**,** 23-32.

JENNINGS, B. J. & BARBUR, J. L. 2010. Colour detection thresholds as a function of chromatic adaptation and light level. *Ophthalmic Physiol Opt,* 30**,** 560-7.

JOHNSON, C. A., ADAMS, A. J., TWELKER, J. D. & QUIGG, J. M. 1988. Age-related changes in the central visual field for short-wavelength-sensitive pathways. *J Opt Soc Am A,* 5**,** 2131-9.

JOHNSON, C. A. & MARSHALL, D., JR. 1995. Aging effects for opponent mechanisms in the central visual field. *Optom Vis Sci,* 72**,** 75-82.

JORDAN, G., DEEB, S. S., BOSTEN, J. M. & MOLLON, J. D. 2010. The dimensionality of color vision in carriers of anomalous trichromacy. *J Vis* [Online], 10. Available: http://www.journalofvision.org/content/10/8/12.

JORDAN, G. & MOLLON, J. D. 1993. A study of women heterozygous for colour deficiencies. *Vision Res,* 33**,** 1495-508.

JORGENSEN, A. L., PHILIP, J., RASKIND, W. H., MATSUSHITA, M., CHRISTENSEN, B., DREYER, V. & MOTULSKY, A. G. 1992. Different patterns of X inactivation in MZ twins discordant for red-green color-vision deficiency. *Am J Hum Genet,* 51**,** 291-8.

KAAS, J. H., HUERTA, M. F., WEBER, J. T. & HARTING, J. K. 1978. Patterns of retinal terminations and laminar organization of the lateral geniculate nucleus of primates. *J Comp Neurol,* 182**,** 517-53.

KERRIGAN-BAUMRIND, L. A., QUIGLEY, H. A., PEASE, M. E., KERRIGAN, D. F. & MITCHELL, R. S. 2000. Number of ganglion cells in glaucoma eyes compared with threshold visual field tests in the same persons. *Invest Ophthalmol Vis Sci,* 41**,** 741-8.

KEUNEN, J. E., VAN NORREN, D. & VAN MEEL, G. J. 1987. Density of foveal cone pigments at older age. *Invest Ophthalmol Vis Sci,* 28**,** 985-91.

KILBRIDE, P. E., HUTMAN, L. P., FISHMAN, M. & READ, J. S. 1986. Foveal cone pigment density difference in the aging human eye. *Vision Res,* 26**,** 321-5.

KINNEAR, P. R. & SAHRAIE, A. 2002. New Farnsworth-Munsell 100 hue test norms of normal observers for each year of age 5-22 and for age decades 30-70. *Br J Ophthalmol,* 86**,** 1408-11.

KLUG, K., HERR, S., NGO, I. T., STERLING, P. & SCHEIN, S. 2003. Macaque retina contains an S-cone OFF midget pathway. *J Neurosci,* 23**,** 9881-7.

KNOBLAUCH, K., NEITZ, M. & NEITZ, J. 2006. An urn model of the development of L/M cone ratios in human and macaque retinas. *Vis Neurosci,* 23**,** 387-94.

KNOBLAUCH, K., SAUNDERS, F., KUSUDA, M., HYNES, R., PODGOR, M., HIGGINS, K. E. & DE MONASTERIO, F. M. 1987. Age and illuminance effects in the Farnsworth-Munsell 100-hue test. *Appl Opt,* 26**,** 1441-1448.

KNOBLAUCH, K., VITAL-DURAND, F. & BARBUR, J. L. 2001. Variation of chromatic sensitivity across the life span. *Vision Res,* 41**,** 23-36.

KÖLLNER, H. 1912. Die Störungen des Farbensinners. Ihre klinische Bedeutung und ihre Diagnose. Berlin: Karger.

KÖNIG, A. & DIETERICI, C. 1893. Die Grundempfindungen in normalen und anomalen Farbensystemen und ihre Intensitätsverteilung im Spektrum. *Z. Psychol. Physiol. Sinnesorg,* 4**,** 241-347.

KONSTANTAKOPOULOU, E., RODRIGUEZ-CARMONA, M. & BARBUR, J. L. 2012. Processing of color signals in female carriers of color vision deficiency. *J Vis,* 12.

KORCZYN, A. D., LAOR, N. & NEMET, P. 1976. Sympathetic pupillary tone in old age. *Arch Ophthalmol,* 94**,** 1905-6.

KRAFT, J. M. & WERNER, J. S. 1999. Aging and the saturation of colors. 1. Colorimetric purity discrimination. *J Opt Soc Am A Opt Image Sci Vis,* 16**,** 223-30.

KREMERS, J., SCHOLL, H. P., KNAU, H., BERENDSCHOT, T. T., USUI, T. & SHARPE, L. T. 2000. L/M cone ratios in human trichromats assessed by psychophysics, electroretinography, and retinal densitometry. *J Opt Soc Am A Opt Image Sci Vis,* 17**,** 517-26.

KRILL, A. E. & SCHNEIDERMAN, A. 1964. A Hue Discrimination Defect in So-Called Normal Carriers of Color Vision Defects. *Invest Ophthalmol,* 3**,** 445-50.

LAKOWSKI, R. 1962. Is the deterioration of colour discrimination with age due to lens or retinal changes? *Die Farbe,* 11**,** 69-86.

LANG, A. & GOOD, G. W. 2001. Color discrimination in heterozygous deutan carriers. *Optom Vis Sci,* 78**,** 584-8.

LAWRENSON, J. G., KELLY, C., LAWRENSON, A. L. & BIRCH, J. 2002. Acquired colour vision deficiency in patients receiving digoxin maintenance therapy. *Br J Ophthalmol,* 86**,** 1259-61.

LEE, B. B. 2004. Paths to colour in the retina. *Clin Exp Optom,* 87**,** 239-48.

LEE, B. B., SMITH, V. C., POKORNY, J. & KREMERS, J. 1997. Rod inputs to macaque ganglion cells. *Vision Res,* 37**,** 2813-28.

LERMAN, S. 1984. Biophysical aspects of corneal and lenticular transparency. *Curr Eye Res* 3**,** 3-14.

LEVENTHAL, A. G., RODIECK, R. W. & DREHER, B. 1981. Retinal ganglion cell classes in the Old World monkey: morphology and central projections. *Science,* 213**,** 1139-42.

LYON, M. F. 1961. Gene action in the X-chromosome of the mouse (Mus musculus L.). *Nature,* 190**,** 372-3.

LYON, M. F. 1972. X-chromosome inactivation and developmental patterns in mammals. *Biol Rev Camb Philos Soc,* 47**,** 1-35.

LYON, M. F. 2002. X-chromosome inactivation and human genetic disease. *Acta Paediatr Suppl,* 91**,** 107-12.

MANTYJARVI, M. I. 1990. Color vision defect as first symptom of progressive cone-rod dystrophy. *J Clin Neuroophthalmol,* 10**,** 266-70.

MARSHALL, J. Ageing changes in human cones. Proceedings of the 23rd international congress of ophthalmology, 1978 Kyoto. 375-378.

MIYAHARA, E., POKORNY, J., SMITH, V. C., BARON, R. & BARON, E. 1998. Color vision in two observers with highly biased LWS/MWS cone ratios. *Vision Res,* 38**,** 601-12.

MORELAND, J. D. 2004. Macular pigment assessment by motion photometry. *Arch Biochem Biophys,* 430**,** 143-8.

MORELAND, J. D. & DAIN, S. L. 1995. Macular pigment contributes to variance in 100-hue tests. *Doc. Ophthalmol. Proc. Ser.,* 57**,** 517-522.

MORELAND, J. D., ROBSON, A. G. & KULIKOWSKI, J. J. 2001. Macular pigment assessment using a colour monitor. *Colour Research and Application,* 26**,** S261-S263.

NAGY, A. L., MACLEOD, D. I., HEYNEMAN, N. E. & EISNER, A. 1981. Four cone pigments in women heterozygous for color deficiency. *J Opt Soc Am,* 71**,** 719-22.

NATHANS, J., MERBS, S. L., SUNG, C. H., WEITZ, C. J. & WANG, Y. 1992. Molecular genetics of human visual pigments. *Annu Rev Genet,* 26**,** 403-24.

NATHANS, J., PIANTANIDA, T. P., EDDY, R. L., SHOWS, T. B. & HOGNESS, D. S. 1986. Molecular genetics of inherited variation in human color vision. *Science,* 232**,** 203-10.

NATIONAL CENTRE FOR SOCIAL RESEARCH & UNIVERSITY COLLEGE LONDON DEPARTMENT OF EPIDEMIOLOGY AND PUBLIC HEALTH 2008. Health Survey for England 2008. Physical activity and fitness. Colchester, Essex.

NATIONAL CENTRE FOR SOCIAL RESEARCH & UNIVERSITY COLLEGE LONDON DEPARTMENT OF EPIDEMIOLOGY AND PUBLIC HEALTH 2011. Health Survey for England. Colchester, Essex.

NEITZ, J. & JACOBS, G. H. 1986. Polymorphism of the long-wavelength cone in normal human colour vision. *Nature,* 323**,** 623-5.

NEITZ, J. & JACOBS, G. H. 1990. Polymorphism in normal human color vision and its mechanism. *Vision Res,* 30**,** 621-36.

NEITZ, J. & NEITZ, M. 2011. The genetics of normal and defective color vision. *Vision Res,* 51**,** 633-51.

NEITZ, J., NEITZ, M., HE, J. C. & SHEVELL, S. K. 1999. Trichromatic color vision with only two spectrally distinct photopigments. *Nat Neurosci,* 2**,** 884-8.

NEITZ, J., NEITZ, M. & JACOBS, G. H. 1993. More than three different cone pigments among people with normal color vision. *Vision Res,* 33**,** 117-22.

NEITZ, J., NEITZ, M. & KAINZ, P. M. 1996. Visual pigment gene structure and the severity of color vision defects. *Science,* 274**,** 801-4.

NEITZ, M. & NEITZ, J. 1995. Numbers and ratios of visual pigment genes for normal red-green color vision. *Science,* 267**,** 1013-6.

NEITZ, M., NEITZ, J. & GRISHOK, A. 1995a. Polymorphism in the number of genes encoding long-wavelength-sensitive cone pigments among males with normal color vision. *Vision Res,* 35**,** 2395-407.

NEITZ, M., NEITZ, J. & JACOBS, G. H. 1991. Spectral tuning of pigments underlying red-green color vision. *Science,* 252**,** 971-4.

NEITZ, M., NEITZ, J. & JACOBS, G. H. 1995b. Genetic basis of photopigment variations in human dichromats. *Vision Res,* 35**,** 2095-103.

NGUYEN-TRI, D., OVERBURY, O. & FAUBERT, J. 2003. The role of lenticular senescence in age-related color vision changes. *Invest Ophthalmol Vis Sci,* 44**,** 3698-704.

NOLAN, J. M., STACK, J., O, O. D., LOANE, E. & BEATTY, S. 2007. Risk factors for age-related maculopathy are associated with a relative lack of macular pigment. *Exp Eye Res,* 84**,** 61-74.

O'NEILL-BIBA, M., SIVAPRASAD, S., RODRIGUEZ-CARMONA, M., WOLF, J. E. & BARBUR, J. L. 2010. Loss of chromatic sensitivity in AMD and diabetes: a comparative study. *Ophthalmic Physiol Opt,* 30**,** 705-16.

OSTERBERG, G. 1935. Topography of the layer of rods and cones in the human retina. *Acta Ophthalmol,* 13**,** 1-103.

OWSLEY, C. 2011. Aging and vision. *Vision Res,* 51**,** 1610-22.

OWSLEY, C., JACKSON, G. R., CIDECIYAN, A. V., HUANG, Y., FINE, S. L., HO, A. C., MAGUIRE, M. G., LOLLEY, V. & JACOBSON, S. G. 2000. Psychophysical evidence for rod vulnerability in age-related macular degeneration. *Invest Ophthalmol Vis Sci,* 41**,** 267-73.

OWSLEY, C., JACKSON, G. R., WHITE, M., FEIST, R. & EDWARDS, D. 2001. Delays in rod-mediated dark adaptation in early age-related maculopathy. *Ophthalmology,* 108**,** 1196-202.

OYSTER, C. W. 1999. *The Human Eye - Structure and Function,* Sunderland, Massachusetts, Sineaur Associates Inc.

PACHECO-CUTILLAS, M., EDGAR, D. F. & SAHRAIE, A. 1999. Acquired colour vision defects in glaucoma-their detection and clinical significance. *Br J Ophthalmol,* 83**,** 1396-402.

PANDA-JONAS, S., JONAS, J. B. & JAKOBCZYK-ZMIJA, M. 1995. Retinal photoreceptor density decreases with age. *Ophthalmology,* 102**,** 1853-9.

PICKFORD, R. W. 1947. Sex differences in colour vision. *Nature,* 159**,** 606.

PICKFORD, R. W. 1949. Colour vision of heterozygotes for sex-linked red-green defects. *Nature,* 163**,** 804.

POKORNY, J., LUTZE, M., CAO, D. & ZELE, A. J. 2006. The color of night: Surface color perception under dim illuminations. *Vis Neurosci,* 23**,** 525-30.

POKORNY, J., SMITH, V. C. & LUTZE, M. 1987. Aging of the human lens. *Appl. Opt.,* 26**,** 1437-1440.

QUIGLEY, H. A. & ADDICKS, E. M. 1982. Quantitative studies of retinal nerve fiber layer defects. *Arch Ophthalmol,* 100**,** 807-14.

ROBSON, A. G., HARDING, G., VAN KUIJK, F. J., PAULEIKHOFF, D., HOLDER, G. E., BIRD, A. C., FITZKE, F. W. & MORELAND, J. D. 2005. Comparison of fundus autofluorescence and minimum-motion measurements of macular pigment distribution profiles derived from identical retinal areas. *Perception,* 34**,** 1029-34.

ROBSON, A. G., MORELAND, J. D., PAULEIKHOFF, D., MORRISSEY, T., HOLDER, G. E., FITZKE, F. W., BIRD, A. C. & VAN KUIJK, F. J. 2003. Macular pigment density and distribution: comparison of fundus autofluorescence with minimum motion photometry. *Vision Res,* 43**,** 1765-75.

ROBSON, A. G. & PARRY, N. R. 2008. Measurement of macular pigment optical density and distribution using the steady-state visual evoked potential. *Vis Neurosci,* 25**,** 575-83.

RODRIGUEZ-CARMONA, M. 2006. *Variability of chromatic sensitivity: Fundamental studies and clinical applications.* PhD, City University.

RODRIGUEZ-CARMONA, M., HARLOW, A. J., WALKER, G. & BARBUR, J. L. The variability of normal trichromatic vision and the establishment of the normal

matching range. Proceedings of the 10th Congress of the Association Internationale de la Couleur (AIC), 2005 Granada, Spain. 979-982.

RODRIGUEZ-CARMONA, M., KVANSAKUL, J., HARLOW, J. A., KOPCKE, W., SCHALCH, W. & BARBUR, J. L. 2006. The effects of supplementation with lutein and/or zeaxanthin on human macular pigment density and colour vision. *Ophthalmic Physiol Opt,* 26**,** 137-47.

RODRIGUEZ-CARMONA, M., O'NEILL-BIBA, M. & BARBUR, J. L. 2011. Assessing the severity of color vision loss with implications for aviation and other occupational environments *Aviat Space Environ Med,* 83**,** 1-11.

RODRIGUEZ-CARMONA, M., O'NEILL-BIBA, M. & BARBUR, J. L. 2012. Assessing the severity of color vision loss with implications for aviation and other occupational environments *Aviat Space Environ Med,* 83**,** 19-29.

RODRIGUEZ-CARMONA, M., SHARPE, L. T., HARLOW, J. A. & BARBUR, J. L. 2008. Sex-related differences in chromatic sensitivity. *Vis Neurosci,* 25**,** 433-40.

ROORDA, A., METHA, A. B., LENNIE, P. & WILLIAMS, D. R. 2001. Packing arrangement of the three cone classes in primate retina. *Vision Res,* 41**,** 1291-306.

ROORDA, A. & WILLIAMS, D. R. 1999. The arrangement of the three cone classes in the living human eye. *Nature,* 397**,** 520-2.

RUSHTON, W. A. 1966. Densitometry of pigments in rods and cones of normal and color defective subjects. *Invest Ophthalmol,* 5**,** 233-41.

RUSHTON, W. A. 1972. Pigments and signals in colour vision. *J Physiol,* 220**,** 1P-P.

RUSSELL, M. H., MURRAY, I. J., METCALFE, R. A. & KULIKOWSKI, J. J. 1991. The visual defect in multiple sclerosis and optic neuritis. A combined

psychophysical and electrophysiological investigation. *Brain,* 114 (Pt 6)**,** 2419-35.

SAMPLE, P. A., ESTERSON, F. D., WEINREB, R. N. & BOYNTON, R. M. 1988. The aging lens: in vivo assessment of light absorption in 84 human eyes. *Invest Ophthalmol Vis Sci,* 29**,** 1306-11.

SARKS, J. P., SARKS, S. H. & KILLINGSWORTH, M. C. 1988. Evolution of geographic atrophy of the retinal pigment epithelium. *Eye (Lond),* 2 (Pt 5)**,** 552-77.

SAVAGE, G. L., HAEGERSTROM-PORTNOY, G., ADAMS, A. J. & HEWLETT, S. E. 1993. Age changes in the optical density of human ocular media. *Clin Vision Sci,* 8**,** 97-108.

SAVAGE, G. L., JOHNSON, C. A. & HOWARD, D. L. 2001. A comparison of noninvasive objective and subjective measurements of the optical density of human ocular media. *Optom Vis Sci,* 78**,** 386-95.

SCHAFER, W. D. & WEALE, R. A. 1970. The influence of age and retinal illumination on the pupillary near reflex. *Vision Res,* 10**,** 179-91.

SCHEFRIN, B. E., SHINOMORI, K. & WERNER, J. S. 1995. Contributions of neural pathways to age-related losses in chromatic discrimination. *J Opt Soc Am A Opt Image Sci Vis,* 12**,** 1233-41.

SCHEFRIN, B. E., WERNER, J. S., PLACH, M., UTLAUT, N. & SWITKES, E. 1992. Sites of age-related sensitivity loss in a short-wave cone pathway. *J Opt Soc Am A,* 9**,** 355-63.

SCHMIDT, I. 1955. A sign of manifest heterozygosity in carriers of color deficiency. *Am J Optom Arch Am Acad Optom,* 32**,** 404-8.

SHARP, A., ROBINSON, D. & JACOBS, P. 2000. Age- and tissue-specific variation of X chromosome inactivation ratios in normal women. *Hum Genet,* 107**,** 343-9.

SHARPE, L. T., STOCKMAN, A., JAGLE, H. & NATHANS, J. 1999. Opsin genes, cone photopigments, color vision, and color blindness. *In:* GEGENFURTNER, K. R. & SHARPE, L. T. (eds.) *Color Vision: From Genes to Perception.* Cambridge: Cambridge University Press.

SHINOMORI, K., SCHEFRIN, B. E. & WERNER, J. S. 2001. Age-related changes in wavelength discrimination. *J Opt Soc Am A Opt Image Sci Vis,* 18**,** 310-8.

SILVERMAN, B. W. 1981. Using Kernel Density Estimates to Investigate Multimodality. *J. Roy. Statist. Soc. Ser. B* 43**,** 97-99.

SJOBERG, S. A., NEITZ, M., BALDING, S. D. & NEITZ, J. 1998. L-cone pigment genes expressed in normal colour vision. *Vision Res,* 38**,** 3213-9.

SMITH, V. C. & POKORNY, J. 1975. Spectral sensitivity of the foveal cone photopigments between 400 and 500 nm. *Vision Res,* 15**,** 161-71.

SNODDERLY, D. M., AURAN, J. D. & DELORI, F. C. 1984a. The macular pigment. II. Spatial distribution in primate retinas. *Invest Ophthalmol Vis Sci,* 25**,** 674-85.

SNODDERLY, D. M., BROWN, P. K., DELORI, F. C. & AURAN, J. D. 1984b. The macular pigment. I. Absorbance spectra, localization, and discrimination from other yellow pigments in primate retinas. *Invest Ophthalmol Vis Sci,* 25**,** 660-73.

STABELL, B. & STABELL, U. 1996. Peripheral colour vision: effects of rod intrusion at different eccentricities. *Vision Res,* 36**,** 3407-14.

STABELL, B. & STABELL, U. 1998. Chromatic rod-cone interaction during dark adaptation. *J Opt Soc Am A Opt Image Sci Vis,* 15**,** 2809-15.

STARITA, C., HUSSAIN, A. A., PAGLIARINI, S. & MARSHALL, J. 1996. Hydrodynamics of ageing Bruch's membrane: implications for macular disease. *Exp Eye Res,* 62**,** 565-72.

STILES, W. S. & BURCH, J. M. 1959. NPL colour-matching investigation: Final report (1958). *Optica Acta,* 6**,** 1-26.

STOCKMAN, A. & SHARPE, L. T. 2000. The spectral sensitivities of the middle- and long-wavelength-sensitive cones derived from measurements in observers of known genotype. *Vision Res,* 40**,** 1711-37.

SUN, Y. & SHEVELL, S. K. 2008. Rayleigh matches in carriers of inherited color vision defects: the contribution from the third L/M photopigment. *Vis Neurosci,* 25**,** 455-62.

SWANN, P. G. & LOVIE-KITCHIN, J. E. 1991. Age-related maculopathy. II: The nature of the central visual field loss. *Ophthalmic Physiol Opt,* 11**,** 59-70.

TAIT, D. M. & CARROLL, J. 2009. Normality of colour vision in a compound heterozygous female carrying protan and deutan defects. *Clin Exp Optom,* 92**,** 356-61.

TRIESCHMANN, M., VAN KUIJK, F. J., ALEXANDER, R., HERMANS, P., LUTHERT, P., BIRD, A. C. & PAULEIKHOFF, D. 2008. Macular pigment in the human retina: histological evaluation of localization and distribution. *Eye,* 22**,** 132-7.

VAN DE KRAATS, J., BERENDSCHOT, T. T., VALEN, S. & VAN NORREN, D. 2006. Fast assessment of the central macular pigment density with natural pupil using the macular pigment reflectometer. *J Biomed Opt,* 11**,** 064031.

VAN DE KRAATS, J., KANIS, M. J., GENDERS, S. W. & VAN NORREN, D. 2008. Lutein and zeaxanthin measured separately in the living human retina with fundus reflectometry. *Invest Ophthalmol Vis Sci,* 49**,** 5568-73.

VAN DE KRAATS, J. & VAN NORREN, D. 2007. Optical density of the aging human ocular media in the visible and the UV. *J Opt Soc Am A Opt Image Sci Vis,* 24**,** 1842-57.

VAN DER VEEN, R. L., BERENDSCHOT, T. T., HENDRIKSE, F., CARDEN, D., MAKRIDAKI, M. & MURRAY, I. J. 2009. A new desktop instrument for measuring macular pigment optical density based on a novel technique for setting flicker thresholds. *Ophthalmic Physiol Opt,* 29**,** 127-37.

VAN NORREN, D. & VOS, J. J. 1974. Spectral transmission of the human ocular media *Vis. Res.,* 14**,** 1237-1244.

VERRIEST, G. 1963. Further studies on acquired deficiency of color discrimination. *J Opt Soc Am,* 53**,** 185-95.

VERRIEST, G. 1972. Chromaticity discrimination in protan and deutan heterozygotes. *Die Farbe,* 21**,** 7-16.

VERRIEST, G., VAN LAETHEM, J. & UVIJLS, A. 1982. A new assessment of the normal ranges of the Farnsworth-Munsell 100-hue test scores. *Am J Ophthalmol,* 93**,** 635-42.

VOS, J. J. & WALRAVEN, P. L. 1971. On the derivation of the foveal receptor primaries. *Vision Res,* 11**,** 799-818.

WAALER, G. H. M. 1927. Uber die Erblichkeitsverhältnisse der verschiedenen Arten von angeborener Rotgrünblindheit. *Zeirschrtft fir induktive Abstammungs und Vererbungslehre,* 45**,** 279-333.

WACHTLER, T., DOI, E., LEE, T. & SEJNOWSKI, T. J. 2007. Cone selectivity derived from the responses of the retinal cone mosaic to natural scenes. *J Vis* [Online], 7. Available: http://www.journalofvision.org/content/7/8/6.long.

WALKEY, H. C., BARBUR, J. L., HARLOW, A. J. & MAKOUS, W. 2001. Measurements of Chromatic Sensitivity in the Mesopic Range. *Colour Research and Application,* 26**,** S36-S42.

WEALE, R. A. 1988. Age and the transmittance of the human crystalline lens. *J Physiol,* 395**,** 577-87.

WENT, L. N. & PRONK, N. 1985. The genetics of tritan disturbances. *Hum Genet,* 69**,** 255-62.

WERNER, J. S. 1982. Development of scotopic sensitivity and the absorption spectrum of the human ocular media. *J Opt Soc Am,* 72**,** 247-58.

WERNER, J. S., BIEBER, M. L. & SCHEFRIN, B. E. 2000. Senescence of foveal and parafoveal cone sensitivities and their relations to macular pigment density. *J Opt Soc Am A Opt Image Sci Vis,* 17**,** 1918-32.

WERNER, J. S., DONNELLY, S. K. & KLIEGL, R. 1987. Aging and human macular pigment density. Appended with translations from the work of Max Schultze and Ewald Hering. *Vision Res,* 27**,** 257-68.

WERNER, J. S., PETERZELL, D. H. & SCHEETZ, A. J. 1990. Light, vision, and aging. *Optom Vis Sci,* 67**,** 214-29.

WERNER, J. S. & STEELE, V. G. 1988. Sensitivity of human foveal color mechanisms throughout the life span. *J Opt Soc Am A,* 5**,** 2122-30.

WIELAND, M. 1933. Untersuchungen über Farbenscwäche bei Konduktorinnen. *Archiv für Ophthalmology,* 30**,** 441-462.

WINDERICKX, J., BATTISTI, L., HIBIYA, Y., MOTULSKY, A. G. & DEEB, S. S. 1993. Haplotype diversity in the human red and green opsin genes: evidence for frequent sequence exchange in exon 3. *Hum Mol Genet,* 2**,** 1413-21.

WINDERICKX, J., BATTISTI, L., MOTULSKY, A. G. & DEEB, S. S. 1992. Selective expression of human X chromosome-linked green opsin genes. *Proc Natl Acad Sci U S A,* 89**,** 9710-4.

WINN, B., WHITAKER, D., ELLIOTT, D. B. & PHILLIPS, N. J. 1994. Factors affecting light-adapted pupil size in normal human subjects. *Invest Ophthalmol Vis Sci,* 35**,** 1132-7.

WINYARD, S. & MCLAUGHLAN, B. 2008. Cost oversight? : www.rnib.org.uk.

WOLF-SCHNURRBUSCH, U. E., ROOSLI, N., WEYERMANN, E., HELDNER, M. R., HOHNE, K. & WOLF, S. 2007. Ethnic differences in macular pigment density and distribution. *Invest Ophthalmol Vis Sci,* 48**,** 3783-7.

WOOTEN, B. R., HAMMOND, B. R. & RENZI, L. M. 2007. Using scotopic and photopic flicker to measure lens optical density. *Ophthalmic Physiol Opt,* 27**,** 321-8.

WRIGHT, W. D. 1952. The characteristics of tritanopia. *J Opt Soc Am,* 42**,** 509-21.

WUSTEMEYER, H., MOESSNER, A., JAHN, C. & WOLF, S. 2003. Macular pigment density in healthy subjects quantified with a modified confocal scanning laser ophthalmoscope. *Graefes Arch Clin Exp Ophthalmol,* 241**,** 647-51.

WYSZECKI, G. & STILES, W. S. 1982. *Color Science: Concepts and Methods, Quantitative Data and Formulae,* New York, Wiley.

XU, J., POKORNY, J. & SMITH, V. C. 1997. Optical density of the human lens. *J Opt Soc Am A Opt Image Sci Vis,* 14**,** 953-60.

YASUMA, T., TOKUDA, H. & ICHIKAWA, H. 1984. Abnormalities of cone photopigments in genetic carriers of protanomaly. *Arch Ophthalmol,* 102**,** 897-900.